Devic mouse: a spontaneous double-transgenic mouse model of human opticospinal multiple sclerosis and autoimmune T- B cell cooperation

Dissertation

**zur Erlangung des Doktorgrades
der Naturwissenschaften (Dr. rer. nat.)
der Fakultät für Biologie
der Ludwig-Maximilians-Universität München**

**vorgelegt von
Gurumoorthy Krishnamoorthy
India**

Munich, June 2006

Hiermit erkläre ich, dass ich die vorliegende Dissertation mit Ausnahme der Immunhistochemie selbständig und ohne unerlaubte Hilfe habe.

Ich habe weder anderweitig versucht, eine Dissertation oder Teile einer Dissertation einzureichen beziehungsweise einer Prüfungskommission vorzulegen, noch eine Doktorprüfung durchzuführen.

Munich, June 2006

Dissertation eingereicht: 12-06-06

Tag der mündlichen Prüfung:

24-01-2007

Erstgutachter: Prof. Dr. Elisabeth Weiß

Zweitgutachter: PD Dr. Christine Falk

TABLE OF CONTENTS

1. Summary

Multiple sclerosis (MS) is an autoimmune inflammatory disease of the central nervous system (CNS). Myelin antigen(s) specific T cells, B cells, and antibodies are thought to play a role in the pathogenesis of MS. While the influence of autoantigen specific CD4$^+$ T cells has been extensively studied in animal models, the relevance of autoantigen specific B cells and their interactions with pathogenic T cells are largely unknown.

The original aim of the present study was to create a new mouse model with which to investigate the interaction of myelin autoantigen specific B and T cells and their role in MS pathogenesis. The study was further expanded to analyze the nature and triggers of spontaneous disease and similarity of the mouse lesion pattern to that in human disease.

The double-transgenic mouse ("Devic mouse") strain presented here contains myelin oligodendrocyte glycoprotein (MOG)-specific T as well as B cells. A significant proportion (>50%) of these mice showed spontaneous experimental autoimmune encephalomyelitis (EAE)-like disease at a young age. In contrast, all single transgenic littermates were free of clinical disease. Spontaneous EAE requires both MOG-specific T and B cells, since the breeding of MOG-specific Ig heavy chain knock-in mice with ovalbumin specific T cell receptor (TCR) transgenic mice did not develop any disease.

Histological analysis of the CNS of affected mice revealed restricted localization of lesions in the spinal cord and optic nerves as well as severe demyelination and axonal damage that spared brain and cerebellum. The inflammatory infiltrates were predominantly composed of macrophages and CD4$^+$ T cells, but occasionally also eosinophils. This peculiar localization of the demyelinating lesions and infiltration profile differ from classic EAE and is reminiscent of Devic's neuromyelitis optica, a variant of classic MS in humans.

It is not well understood what triggers the initiation of spontaneous EAE. The microbial environment does not significantly affect the clinical disease. Stimulation of the innate immune system with toll-like receptor (TLR) ligands or depletion of

putative regulatory cells did not significantly affect EAE development. The (re-) activation of lymphocytes in sick Devic mice mainly occurs in the CNS without evidence of priming in the peripheral lymphoid organs.

MOG-specific B and T cells cooperate by means of several mechanisms. MOG-specific B cells, which bind MOG but not the immunodominant peptide MOG 35-55 via their surface immunoglobulin (Ig), efficiently presented even high dilutions of MOG to T cells. This resulted in the enhanced proliferation of T and B cells as well as rapid activation. Stimulated T, but not B cells, secreted large amounts of Th1 cytokines IFNγ and IL-2 along with small amounts of Th2 cytokine IL-5. In addition, MOG-stimulated T and B cells expressed a set of co-stimulatory molecules, which further help to modulate the proliferation and activation. Surprisingly, the double-transgenic Devic mice, but not their single transgenic littermates, had high titers of MOG-specific IgG1 antibodies in the serum, which indicates a previous encounter with antigen *in vivo*. However, similar MOG-specific serum IgG1 titers were present irrespective of the clinical status. The transfer of EAE by Devic splenocytes in immunodeficient mice or by bone marrow reconstitution in wild-type mice further supported the *in vivo* cooperation of MOG-specific T and B cells to induce spontaneous EAE.

In summary, Devic mice show several salient features that are important for study of the pathogenic mechanisms of CNS autoimmunity. As a model of spontaneous autoimmunity, they may allow us to study the triggering factors of autoimmunity as well as the factors that determine restricted infiltration of immune cells into the CNS. In addition, the model may be useful for validating novel therapies for autoimmune CNS diseases.

2. Introduction

The immune system normally eliminates threats from invading pathogens, but at times it directs its potent reactivity against the body's self-constituents, causing autoimmunity. Autoimmune diseases represent a group of diseases that often involve distinct anatomical regions. They are estimated to affect approximately 5% of the world population (Davidson and Diamond, 2001; Jacobson et al., 1997), causing morbidity and mortality on an immense scale. Although the pathogenic mechanisms of many autoimmune diseases have not been clearly defined, it is widely believed that they are caused by a combination of several factors such as genetic susceptibility and environmental triggers. Epidemiological studies strongly suggest that allergic and autoimmune diseases are clearly on the rise in the developed countries.

Infectious agents are involved in a complex relationship with autoimmunity. While the absence of infection favors autoimmunity, its presence can also precipitate autoimmunity (Bach, 2002; Christen and von Herrath, 2005). Clinically, autoimmune diseases are broadly classified as systemic and organ-specific autoimmune diseases. An example of systemic disease is systemic lupus erythematosus; organ-specific autoimmune diseases include multiple sclerosis, type I diabetes, and rheumatoid arthritis.

2.1 Multiple sclerosis (MS)

2.1.1 Definition

Multiple sclerosis is the major chronic inflammatory disease of the central nervous system (CNS); it affects more than 1 million people, mainly in Western societies. MS is more prevalent in females than males (~1.6: 1), often develops during young adulthood, and is generally present throughout life. Typical disabilities caused by MS include paralysis, lack of co-ordination, sensory disturbances, and impaired vision and cognitive function (Sospedra and Martin, 2005). It is believed to be an autoimmune-mediated disorder in which autoreactive cells directed against

components of the myelin sheath attack and destroy the myelin (Noseworthy et al., 2000).

2.1.2 Clinical course

MS occurs in various clinical forms and can be distinguished by its clinical course. These forms include primary-progressive (PP)-, secondary-progressive (SP)-, relapsing-remitting (RR)-MS, and progressive-relapsing (PR)-MS (Figure 2.1). Most commonly, MS patients develop an RR course, during which episodes of acute worsening of the disease alternate with periods of recovery, and between relapses the course of the disease is stable. Relapses or "attacks" typically occur with symptoms that develop over hours to several days, persist for several days or weeks, and then gradually dissipate. The traffic of activated, myelin-reactive T cells within the CNS causes acute inflammation associated with edema, which may explain the periodicity of the relapses. However, in a minority of patients, disease progresses steadily from the onset, without acute attacks and involving a gradual neurologic deterioration (PP-MS).
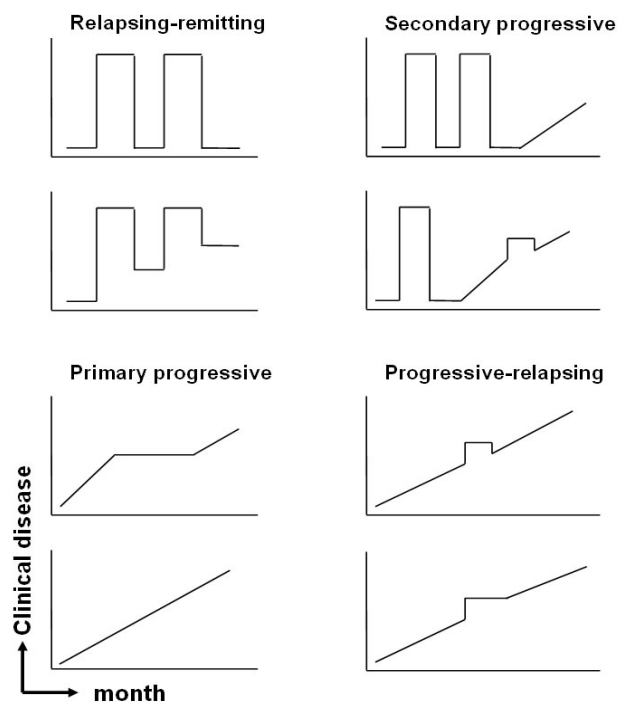
Figure 2.1

Schematic depiction of clinical course of multiple sclerosis (modified from Kieseier and Hartung, 2003).

SP-MS is characterized by gradual neurologic deterioration with or without further acute relapses in patients who previously had RR-MS. PR-MS typically shows disease progress from the onset, acute relapses with or without full recovery, and periods of continuous progression between relapses (Sospedra and Martin, 2005; Kieseier and Hartung, 2003).

2.1.3 Pathology

Chronic MS brain tissue has sharply demarcated demyelinated plaques throughout the CNS white matter. It exhibits a certain predilection for the optic nerves, periventricular regions, brainstem, cerebellum, and spinal cord (Lassmann et al., 2001). Some patients develop a so-called clinically isolated syndrome, for example, optic neuritis, brainstem dysfunction, or incomplete transverse myelitis as their first event. There is also substantial axonal injury with axonal transactions throughout the MS lesions. The inflammatory lesions are dominated by inflammatory infiltrates in the perivascular area with extensive demyelination. Perivascular infiltrates are composed of oligoclonal T cells consisting of CD4$^+$, CD8$^+$, $\gamma\delta$ T cells, macrophages with occasional B cells and plasma cells (Hafler, 2004; Hauser et al., 1986; Traugott et al., 1983). Activated macrophages in the center of the plaques contain myelin debris, and the number of oligodendrocytes is reduced.

In a recent pathological study of a large series of actively demyelinating MS lesions, four histopathological patterns were defined on the basis of myelin loss, the geography and extension of plaques, the pattern of oligodendrocyte destruction, and the evidence of complement activation. All actively demyelinating lesions had inflammatory infiltrates composed mainly of T cells and macrophages. Pattern I (macrophage-associated demyelination) lesions contained toxic products of activated macrophages and microglia associated with degenerating myelin. This suggests that T cell-mediated inflammation is involved with macrophage/microglia activation. Most of the mouse models of autoimmune encephalomyelitis show a close resemblance to this pattern of myelin destruction. Pattern II (antibody-mediated demyelination) lesions contain immunoglobulin and activated complement deposited at sites of active myelin destruction together with activated

macrophages/microglia. These lesions are very similar to the experimental autoimmune encephalomyelitis (EAE) models that are induced by sensitization with myelin oligodendrocyte glycoprotein (MOG). In pattern III (distal oligodendrogliopathy-associated demyelination) lesions, a rim of myelin is frequently preserved around inflamed blood vessels within the demyelinated plaque. The striking feature of these lesions is a preferential loss of myelin-associated glycoprotein (MAG), whereas other myelin proteins (proteolipid protein (PLP), myelin basic protein (MBP), and 2',3'-cyclic nucleotide 3'-phosphodiesterase (CNPase)) are still present within the partly damaged myelin sheaths. The degeneration of distal oligodendrocyte processes, followed by oligodendrocyte apoptosis and demyelination, are commonly observed in virus-induced white matter diseases as well as in white matter strokes. This suggests that the possible mechanism is secondary ischemic damage of the white matter. Pattern IV (primary oligodendrocyte degeneration) lesions are very infrequent in MS. In this pattern, demyelination is associated with oligodendrocyte death in a small rim of periplaque white matter, adjacent to the zone of active myelin destruction (Lucchinetti et al., 2000; Lassmann et al., 2001). Although this is true for classic MS, some variants of the disease, e.g., Devic's disease (see below), exhibit lesions restricted to the optic nerves and spinal cord (Cree et al., 2002).

2.2 Devic's neuromyelitis optica (NMO): a variant of classic MS

In contrast to the classic MS subtypes, patients with neuromyelitis optica, also termed Devic's disease, develop both bilateral or unilateral optic neuritis and myelitis without any involvement of the brain. It is still being debated, whether Devic's disease is a variant of MS or a distinct neurological disorder (Minagar et al., 2002). Interestingly, this kind of opticospinal MS is a common inflammatory demyelinating disease in Asia. In Japan, for example, it accounts for 15-40% of MS cases (Kira, 2003). The majority of Devic's patients develop optic neuritis and later acquire myelitis. The intervals between both manifestations vary. Monophasic and relapsing variants of Devic's disease have been described. Recurrent attacks are associated

with female sex, older age at onset, longer intervals between neuritis and myelitis, and the presence of systemic autoimmune disorders (Wingerchuk et al., 1999).

In Devic's disease, acute spinal cord lesions develop with diffuse swelling and softening extending over multiple spinal segments. Occasionally they may involve the entire spinal cord, showing a patchy or continuous distribution. As in MS, extensive macrophage infiltration is associated with myelin and axonal loss that occurs with necrosis of both gray and white matter (Mandler et al., 1993). A detailed pathological analysis of 80 NMO lesions recently revealed that demyelinating lesions are associated with perivascular deposition of Ig, local activation of complement, and marked eosinophilic infiltration (Lucchinetti et al., 2002). The factors that determine this selective attack on only the optic nerve and spinal cord are not known. Are the structure and stability of the blood-brain barrier (BBB) responsible or are there regional differences in the ability of the CNS to process and present antigen to the T cells?

There is no selective diagnostic marker, and no disease autoantigen has been clearly associated with Devic's disease. An NMO-specific IgG autoantibody, which is not present in other inflammatory diseases of the CNS including classic MS, was recently identified in some Devic's patients. These NMO-IgGs seem to specifically localize in the BBB (Lennon et al., 2004). Interestingly, these NMO-IgGs have been shown to cross-react with mouse aquaporin-4 (AQP4) present in the CNS, kidney, and gut tissues. On the basis of these findings it has been suggested that AQP4 could be a potential target autoantigen (Lennon et al., 2005). AQP4 is an integral membrane protein that is present on astrocytic end-feet of the CNS, and is associated with the dystrophin-associated proteins. It is the predominant water channel in the CNS and has been implicated in pathophysiological conditions such as brain edema after intoxication (Vajda et al., 2002) and focal cerebral ischemia (Saadoun et al., 2002; Agre and Kozono, 2003). However, the widespread expression of AQP4 in the CNS and periphery does not explain the restricted lesion distribution in NMO patients (Badaut et al., 2002).

On the basis of animal experiments and the presence of MOG-specific antibodies in NMO patients, the myelin oligodendrocyte glycoprotein (MOG) has also been

suggested to be a potential target autoantigen. Brown Norway (BN) rats immunized with MOG reproduce several features of NMO. Lesions are spread around the optic nerve, and there is fulminant EAE in the spinal cord with widespread demyelination and axonal injury. Importantly, demyelination is also associated with large numbers of eosinophils and deposition of complement, both of which are strikingly similar to human NMO (Stefferl et al., 1999; Storch et al., 1998).

2.3 Disease etiology

The etiology of MS remains unclear, but evidence for the contribution of genetic factors is unequivocal. MS may also require additional environmental triggers.

2.3.1 Genetic factors

The role of genetic factors in a person's susceptibility to MS remains complex and poorly understood. The highest prevalence of MS is found in northern Europe and North America. Its low prevalence in Asia and Africa suggests that genetic factors, ethnic background, and environmental factors contribute to susceptibility to the disease. Population, family, and twin studies show that the prevalence is substantially increased in family members of MS patients. For example, the risk to develop MS and the concordance rate in monozygotic twins are much higher than among dizygotic twins (Dyment et al., 2004). Although no clear disease-causing genes have been identified, whole genome screens in multiple families of MS indicate that a considerable number of genes confer susceptibility to MS; the strongest linkage is to human leukocyte antigen (HLA) class II (Dyment et al., 2004; Sawcer et al., 1997). Genetic linkage studies showed that there is a significant association of HLA class II alleles HLA-DRB1*1501 and HLA-DQB1*0601 with MS (Olerup and Hillert, 1991). HLA class II genes may confer a risk of MS by several mechanisms. Disease-associated HLA molecules can preferentially present myelin peptides. In addition, several reports showed an association of genes such as T-cell receptor (TCR) beta, CTLA4 (Cytotoxic T-lymphocyte-associated protein 4), ICAM1, CCR5, and CD45 with MS (Dyment et al., 2004).

The difference in the disease incidence between males and females (~1.6: 1) also suggests that hormonal variables are risk factors. This view is supported by several observations: the lower relapse rates during pregnancy; the rebound after postpartum; the worsening of MS during menstruation; the correlation of high estradiol and low progesterone with increased magnetic resonance imaging (MRI) disease activity; the gender differences in EAE, an animal model of MS; the protective effect of testosterone; and the therapeutic effects of estriol in RR-MS. The precise mechanisms by which sex hormones influence MS susceptibility are not known, but the stimulatory effects of estrogens on proinflammatory cytokine secretion and the opposite effects of androgens are probably represent one mechanism (reviewed in Sospedra and Martin, 2005).

2.3.2 Environmental factors

Among putative environmental factors, both infectious (virus and bacteria) agents and lifestyle influences have been proposed to induce or contribute to disease expression (Coo and Aronson, 2004). Many studies have suggested an association between episodes of MS exacerbation and concomitant viral or microbial infections. Suitable candidates among the viruses are herpesviruses or retroviruses, which induce persistent infection; they have been widely studied in MS (Gilden, 2005).

Herpesviruses are neurotropic and of particular interest in MS studies. Human herpesvirus 6 (HHV-6) and Epstein-Barr virus (EBV) are the leading candidates. Human herpesviruses (HHV-6 and HHV-8) have been reported to be present in active MS plaques (Soldan et al., 1997). The seroprevalence for both is high, i.e., >80% for HHV-6 and 90% for EBV. Recently, the probing of cerebrospinal fluid (CSF) and serum IgG antibodies from MS patients revealed cross-reactivity to two EBV proteins, BRRF2 and EBNA-1 (Cepok et al., 2005). In addition, the reactivation of latent EBV infections correlated with MS relapses (Wandinger et al., 2000).

Infectious agents could induce MS by several mechanisms, including molecular mimicry and bystander activation. Molecular mimicry is the term coined for the activation of autoreactive cells by cross-reactivity between self-antigens and foreign agents (Oldstone, 2005). It involves the potential reactivity of T and B cells with

epitopes shared by infectious agents and self-antigens. During thymic selection, the recognition of self-antigens by T cells at intermediate affinity leads to positive selection. These T cells are exported to the periphery. Self-reactive T cells, which recognize the antigenic epitopes shared by self and infectious agents, could be activated during infection and then migrate across the BBB to infiltrate CNS and damage the brain tissue, leading to the development of autoimmune disease. Although examples of such stringent homology have been reported for MBP, a myelin antigen, and viruses (Fujinami and Oldstone, 1985), the occurrence of such complete matching is a rare event. In addition, protein cleavage is required to generate such a perfect matching epitope (Figure 2.2). Wucherpfennig & Strominger showed, however, that the MBP-specific T cell clones (TCC) derived from MS patients could be activated by viral and bacterial peptides that shared a major histocompatibility complex (MHC) binding motif with MBP. They confirmed the prediction that complete sequence homology was not required for cross-recognition (Figure 2.2; Wucherpfennig and Strominger, 1995). Further, data on crystal structure showed that a T cell receptor (TCR) from an MS patient recognized both MBP and EBV-derived peptide (Lang et al., 2002). Although these findings demonstrate that molecular mimicry could explain the link between infection and MS, evidence for this phenomenon in human autoimmune diseases is still scarce.

Sequence homology

TTH **YGSLPQ** K   MBP (66-75)
ICG **YGSLPQ** E   HBV-P (589-598)

MHC and TCR contact motifs

VVHFFKNIVTPR   MBP (86-97)
LVHFVRDFAQLL   HSV Terminase

Figure 2.2

Evolution of molecular mimicry. Sequence homology between MBP and cross-reactive foreign antigens, hepatitis B virus polymerase (HBV-P), and herpes simplex virus (HSV) terminase.

Bystander activation assumes that autoreactive cells are activated due to non-specific inflammatory events that occur during infections. Toll-like receptors (TLR), which recognize molecular patterns of infectious agents, superantigens that bind TCR outside the peptide binding groove, and inflammatory cytokines released during infection can also induce potent TCR-independent bystander activation of autoreactive T cells. The second category involves the unveiling of host antigens and the adjuvant effect of infectious agents on antigen-presenting cells (APCs). Indeed, activation of APCs by TLR9 or TLR4 ligands in PLP 139-151 TCR transgenic mice with a genetically resistant B10.S background resulted in the development of autoimmunity (Waldner et al., 2004).

2.4 Target autoantigens in MS and EAE

Pathological observations made in MS clearly indicate that the disease process is mainly concentrated in myelinated areas of the brain and spinal cord. Seminal observations from Rivers, who showed that injection of spinal cord or brain homogenates into healthy primates caused a disease similar to MS, also further supported the view that the target antigens are primarily located in the myelin sheaths of the CNS white matter. Many decades later many investigators showed that immunization of susceptible animals with purified and defined components of myelin sheath induced the disease (Wekerle et al., 1994). Several candidate autoantigens are present in the CNS white matter, and many of them have been shown to induce EAE, an experimental model of MS (Figure 2.3).
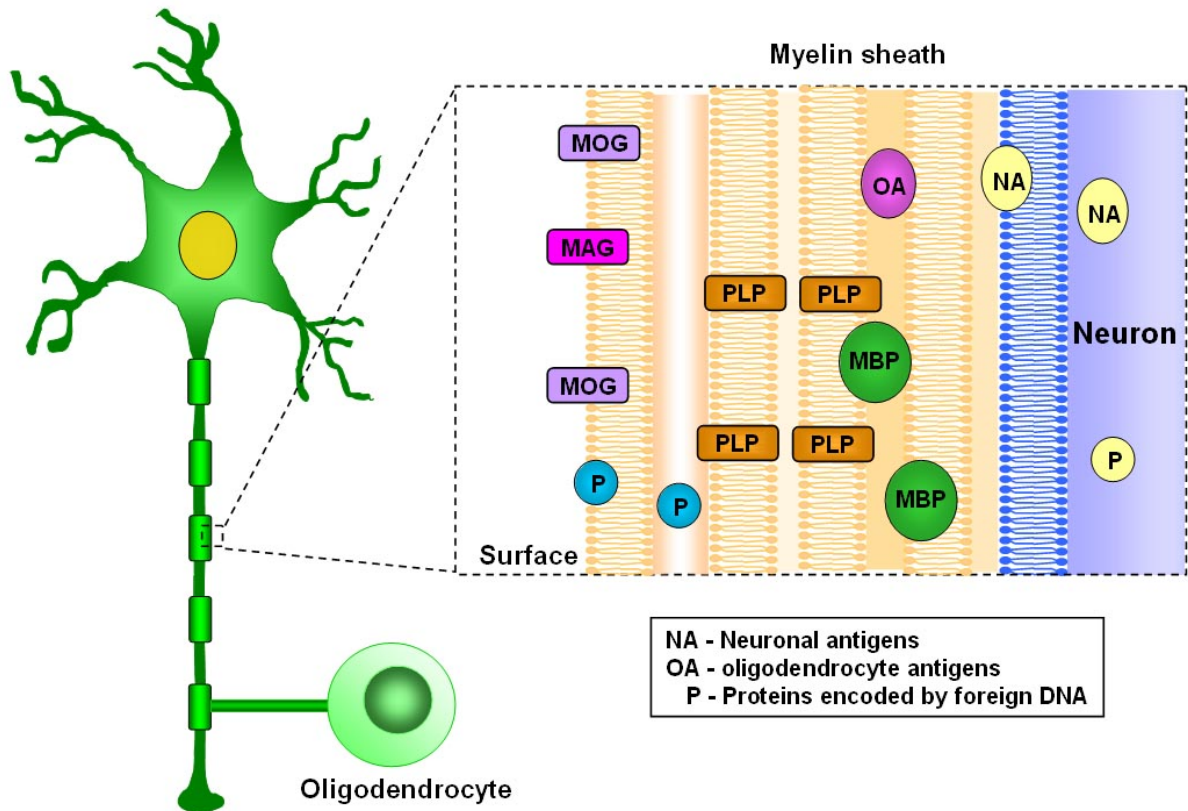
Figure 2.3

MS and EAE auto-antigens in CNS white matter (modified from Hemmer et al., 2002). MBP, myelin basic protein; MOG, myelin oligodendrocyte glycoprotein; MAG, myelin associated glycoprotein; PLP, proteolipid protein; OA, oligodendrocyte antigens; NA, neuronal antigens.

2.4.1 Myelin basic protein (MBP)

MBP is one of the most abundant myelin proteins (approximately 30%–40%) and is probably the best-studied one in MS owing to its water solubility and ease of purification. It is found in both the central and the peripheral myelin sheath. MBP transcripts have also been demonstrated in peripheral lymphoid organs (Bruno et al., 2002). Mammals have five MBP isoforms with an approximate molecular weight of 14.0–21.5 KDa. These isoforms are produced by alternative splicing of 11 exons within the Golli-MBP locus (Seamons et al., 2003). MBP is positioned at the intracellular surface of myelin membranes, the so-called major dense line, which interacts with acidic lipid moieties to maintain the structure of compact myelin. MBP has been used extensively in MS as well as in EAE studies. Several mouse, rat

strains, guinea pigs, and nonhuman primates developed EAE after immunization with MBP-derived peptides (Wekerle et al., 1994). In humans, a large body of evidence suggests that MBP is one of the main target autoantigens. Several immunodominant epitopes have been described together with MS-associated class II alleles. Moreover, TCR transgenic mice have been generated for the immunodominant MBP, and they also developed spontaneous EAE at various frequencies (see below; Goverman et al., 1993; Lafaille et al., 1994).

2.4.2 Proteolipid protein (PLP)

The membrane protein PLP is the most abundant CNS myelin protein (about 50% of all myelin proteins). It is highly hydrophobic and highly conserved across all species. Two main transcripts have been described in mice: one encodes for the full-length 276 amino acid (aa) isoform, the other for the DM-20 isoform lacking 35 amino acids (Baumann and Pham-Dinh, 2001). The brain and spinal cord mainly express full-length PLP, whereas peripheral lymphoid organs express predominantly the DM-20 isoform (Bruno et al., 2002; Klein et al., 2000). This differential peripheral expression is relevant for one major encephalitogenic and immunodominant PLP 139−154 peptide that is present in full-length PLP, but is absent in the DM-20 isoform, and therefore is not available for thymic negative selection. Consequently, high frequencies of PLP 139−154-specific T cells have been observed even in naive unprimed animals (Kuchroo et al., 2002). Furthermore, PLP-specific TCR transgenic mice with a SJL/J genetic background spontaneously developed severe EAE (Waldner et al., 2000).

2.4.3 Myelin oligodendrocyte glycoprotein (MOG)

MOG was originally identified to be a target of antibody-mediated demyelination in a guinea pig model of EAE (Linington and Lassmann, 1987; Lebar et al., 1986). It is a 218 aa glycosylated transmembrane protein and a member of the Ig superfamily. Quantitatively, it is a minor constituent of the CNS myelin sheath, where it accounts for approximately 0.05% of all myelin proteins. It is expressed only in the CNS and is highly conserved between different species (Johns and Bernard, 1999). MOG is

expressed late during the formation of the compact myelin sheath (Slavin et al., 1997). The function of MOG is still not known, since MOG knockout (KO) mice develop in a phenotypically normal way (Delarasse et al., 2003; Linares et al., 2003).

The topology of MOG indicates that it has two membrane-associated regions, where the C-terminal domain is associated with rather than spans the membrane. Recent structural investigation confirmed these observations (Breithaupt et al., 2003; Clements et al., 2003). Table 2.1 summarizes the biochemical properties of MOG.

Table 2.1

Properties of MOG (Johns and Bernard, 1999; von Budingen et al., 2001)

1. CNS myelin specific integral membrane glycoprotein present on the surface of oligodendrocytes and on the outer lamellae of the myelin sheath
2. Expression parallels with myelination
3. Surface marker of oligodendrocyte maturation
4. Molecular size of 28 kDa on SDS-PAGE
5. Glycosylated in native form and N-glycosylation at position 31
6. Highly conserved in different species
7. Maps to the MHC region in the mouse, rat, and human

MOG can be differentiated from other myelin autoantigens, since it is accessible to both T cell and antibody-mediated damage owing to its location on the outermost lamellae of the myelin sheath. Due to this accessibility, several lines of evidence suggest that MOG plays an important role in the pathogenesis of MS. Although it is a minor glycoprotein of the CNS myelin sheath, significant T cell responses and anti-MOG antibodies have been identified in MS patients. Furthermore, anti-MOG antibodies were detected in the CSF of some patients (Xiao et al., 1991), and they were specifically bound to the disintegrating myelin around axons in lesions of acute MS patients (Genain et al., 1999). Anti-MOG antibodies together with encephalitogenic T cells produce demyelination similar to MS in a marmoset model of EAE (Genain et al., 1995), and extensive demyelination was observed in

immunized rodents after injection of anti-MOG monoclonal antibody (Schluesener et al., 1987).

The mechanisms by which MOG-specific antibodies induce demyelination are not known. Obviously, the ability to fix complement is attributed to the demyelination induced by MOG/anti-MOG complex (Piddlesden et al., 1993). Other mechanisms including antibody-dependent cell cytotoxicity (ADCC) and the direct role of anti-MOG antibody-induced demyelination have also been proposed. Recently, it was shown that anti-MOG antibody-induced cross-linking of oligodendrocytes leads to the repartitioning of MOG into lipid rafts, specialized plasma membrane microdomains rich in cholesterol and glycosphingolipids. These rafts serve as a platform for the initiation of signal transduction by favoring specific protein-protein interactions. Further MOG antibody alters the phosphorylation states of specific proteins, increases Ca^{2+} influx, and activates MAPK, Akt pathways, resulting in dramatic changes in oligodendrocyte cell processes (Marta et al., 2005a; Marta et al., 2003). All these data clearly indicate that anti-MOG antibody plays a direct role in the induction of demyelination in addition to mediating damage to the immune complex. Moreover, pathogenic and non-pathogenic antibodies can be distinguished by their ability to bind conformational epitopes of MOG (Bourquin et al., 2003; Marta et al., 2005b).

2.4.4 Other myelin and non-myelin antigens

In addition to the antigens described above, several other myelin and non-myelin antigens have also been implicated in MS pathogenesis. These include MAG, CNPase, oligodendrocyte specific protein (OSP), myelin-associated oligodendrocytic basic protein (MOBP), α, β-crystallin, and s100β.

MAG is located at the inner surface of the myelin sheath opposite to the axon surface, while MOBP, like MBP, is located at the major dense line of compact myelin. Both MAG 596−612 and MAG 609−62 peptides (Andersson et al., 2002; Morris-Downes et al., 2002) as well as MOBP 37–60 peptide (Holz et al., 2000) have been found to induce EAE in animals. MAG and MOBP-specific antibodies have also been found in the CSF of MS patients.

OSP, the third most abundant myelin protein (7%), is expressed at the tight junctions of the CNS and testis. Several OSP peptides were shown to induce EAE in SJL/J mice. Occasionally, OSP-specific antibodies are also found in the CSF of RR-MS patients (Bronstein et al., 1997).

2.5 Immune responses in the pathogenesis of MS

MS is considered a Th1-mediated disease. This view is mainly based on the cellular composition of brain lesions and CSF as well as the data from EAE models. EAE can be induced either by injecting myelin components or by transferring Th1 cell lines specific for the myelin proteins into susceptible animals. The transfer of antibodies does not induce EAE. This concept may, however, be too simplistic to cover the complete spectrum of multiple sclerosis pathology. Recently, antibodies (Cross et al., 2001) and CD8+ T cells (Babbe et al., 2000; Friese and Fugger, 2005) have been implicated in the pathogenesis of MS. Figure 2.4 shows the current view on the pathogenesis of MS.

Irrespective of the causative agent, two critical steps are required for the autoreactive lymphocytes to damage the CNS. First, the myelin antigen-reactive lymphocytes must be activated in the periphery to enter through the BBB. This specific migratory pattern and functional changes of autoreactive T cells have been observed in an experimental model of the adoptive transfer of EAE. The model clearly indicates that the activation of T cells is required for migration across the BBB (Flugel et al., 2001). Second, the MHC class II and co-stimulatory molecules must be upregulated by the pro-inflammatory milieu in the CNS. Normally the CNS is an immune-privileged organ due to its low expression of MHC molecules and the absence of professional APCs. This is an important factor in the outcome of CNS damage, since local reactivation of the autoreactive T cells requires efficient antigen presentation by the APCs.

In a genetically susceptible individual, T (CD4$^+$ and CD8$^+$) and B cells might be primed in the peripheral lymphoid organs either by endogenous antigen released from the CNS or by cross-reactive antigen from microbes. Dendritic cells, macrophages, and antigen-specific B cells are potent APCs, which efficiently

stimulate T cell responses. Underlying defects in the immunoregulatory mechanisms such as decreased numbers of regulatory cells (Tregs) in some individuals allow further activation of the autoreactive cells. B cells could also be activated by the antigen. When enhanced by cytokines released by T cells, the activated B cells might eventually differentiate into antibody-producing plasma cells.
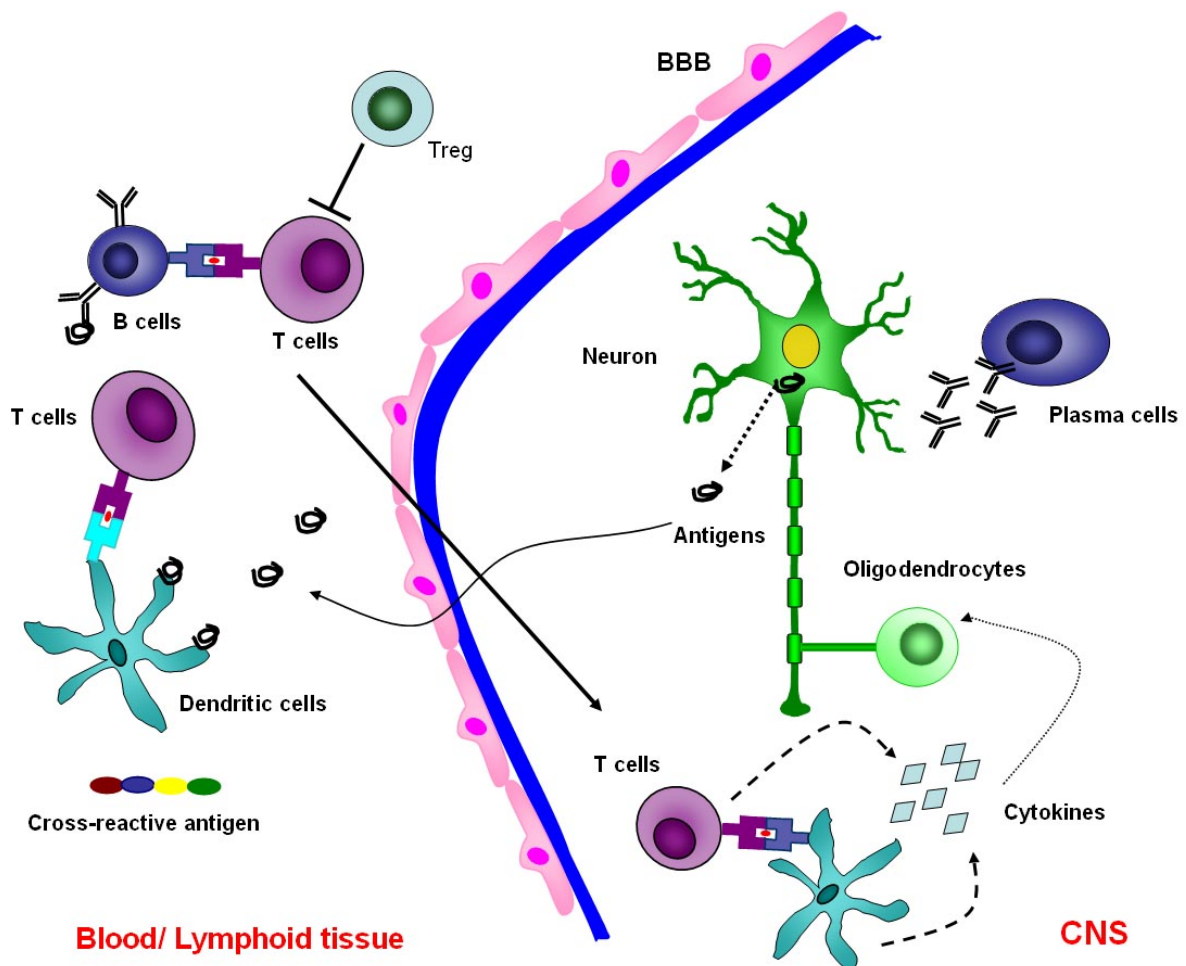
Figure 2.4

Current concepts of immunopathogenesis of MS. (For explanation please see the text)

After initial priming in the periphery, both activated T and B cells undergo clonal expansion and migrate across the BBB to reach the CNS. In the CNS, T cells are reactivated by the local antigen presenting cells such as activated microglia or CNS infiltrated macrophages. CD8$^+$ T cells recognize the myelin antigens presented by

MHC I molecules and can directly damage the cells expressing the antigens. Reactivation of autoreactive CD4$^+$ T cells by specific antigens leads to the secretion of proinflammatory cytokines, which further attract other immune cells like macrophages. Macrophages contribute to the inflammation by releasing several inflammatory mediators as well as by initiating phagocyotosis of the myelin sheath. CNS infiltrated B cells re-encounter the antigen, mature to antibody producing plasma cells, and secrete large amounts of antigen-specific Ig. These antibodies damage the myelin sheath either by complement-mediated damage or by direct activation of the downstream signaling mechanisms (Hemmer et al., 2002; Hafler, 2004).

2.6 Major players in MS

2.6.1 CD4$^+$ T Cells

Since Rivers showed that the injection of spinal cord or brain homogenates into healthy primates caused a disease similar to MS (Rivers et al., 1933), many animal models have been developed by immunization with purified myelin antigens together with adjuvant (Gold et al., 2000). In addition, the transfer of CD4$^+$ encephalitogenic T cell lines has also been shown to induce disease (Wekerle et al., 1994; Ben-Nun et al., 1981). These animal models showed that the CD4$^+$ T cells are the main players in EAE. This view, however, is probably oversimplified, as these models did not reproduce MS in all its clinical and structural aspects.

Nevertheless, MS favors CD4$^+$ autoreactive T cells as a central factor in the autoimmune pathogenesis. CD4$^+$ T cells are the major component in MS lesions and in CSF-infiltrating inflammatory cells in MS. Furthermore, linkage studies have shown that a substantial degree of genetic risk is conferred by HLA-DR and HLA-DQ molecules. Indeed, "humanized" transgenic mice expressing either MS associated HLA-DR or -DQ molecules are susceptible to EAE (Kawamura et al., 2000), and mice expressing both MS-associated HLA-DR molecules and MS patient–derived MBP-specific TCR develop spontaneous or induced EAE (Madsen et al., 1999). Many investigators have reported various frequencies of myelin antigen specific T

cells present in the peripheral blood mononuclear cells (PBMCs) of MS patients as well as healthy people (Sospedra and Martin, 2005).

2.6.2 CD8$^+$ T Cells

The role of CD8$^+$ T cells in the pathogenesis of MS was ignored for a long time. One reason for this was that the CNS was considered an immune-privileged organ and protected from T cell-mediated damage, partly by the reduced expression of MHC class I molecules. In addition, CD8$^+$ T cells are difficult to handle *in vitro*. However, several lines of evidence support the direct or indirect role of CD8$^+$ T cells in MS (Friese and Fugger, 2005). Pronounced oligoclonal expansions of CD8$^+$ memory T cells have been found in the CSF (Jacobsen et al., 2002), MS brain tissue and in blood (Babbe et al., 2000). In addition, many HLA class I–restricted myelin epitopes have been described for several myelin proteins. At least for some of them CD8$^+$ T cell clones have been isolated from the patients (Tsuchida et al., 1994). Further, MBP-specific CD8$^+$ T cell response has been shown to be increased in MS patients (Zang et al., 2004). Finally, MOG and MBP specific cytotoxic T cells are shown to induce EAE in animal models (Huseby et al., 2001a; Sun et al., 2001).

2.6.3 B cells and antibodies

There is much evidence to implicate B cells and antibodies in the pathogenesis of MS. The observation that oligoclonal Igs are present in the CSF of MS patients and are produced intrathecally, indirectly suggested a role for B cells and antibodies (Walsh and Tourtellotte, 1986; Walsh et al., 1985). However, no pathological role for CSF antibodies was demonstrated with certainty. Myelin-specific antibodies have been found in chronic MS plaques as well as in active MS lesions (Genain et al., 1999). Further, a recent pathological study has also shown that type II lesions are mainly antibody-mediated (Lucchinetti et al., 2000).

Many investigators have observed the presence of specific antibodies for MOG, MBP, PLP, MAG, CNPase, and several other myelin antigens in MS patients (Cross et al., 2001; Sospedra and Martin, 2005). Although it is unlikely that all these antibodies have a direct functional role in the pathogenesis in MS, MOG-specific (but

not anti-MBP or anti-PLP) antibodies were shown in experimental models to accelerate EAE (Genain et al., 1995; Schluesener et al., 1987; Storch et al., 1998). An MOG-specific antibody expressing transgenic mice developed EAE with earlier onset when immunized with myelin antigens (Litzenburger et al., 1998). In addition, resistance to recombinant MOG-induced EAE in B cell deficient mice compared to MOG 35-55-induced EAE suggested a critical role for B cells (Lyons et al., 1999).

In principle, both B cells and antibodies can contribute to MS disease pathogenesis in several ways. (a) B cells act as APCs to capture and present the autoantigen(s) to autoreactive T cells. (b) B cells might provide co-stimulation to autoreactive T cells. (c) They might recruit autoreactive T cells to the CNS by binding Igs. (d) B cells might also be responsible for the opsonization of myelin for phagocytosis and destruction of myelin within plaques. e) B cells can also secrete cytokines to create an inflammatory milieu.

2.7 Animal models of multiple sclerosis

Animal models have been used extensively in biomedical research. They are invaluable for investigating disease mechanisms. Prompted by the unexpected observation that immunization of humans against viral diseases such as rabies with CNS contaminated vaccines triggered paralytic CNS disease, Thomas Rivers injected brain extracts from rabbits into monkeys and showed a similar CNS disease (Rivers et al., 1933). Since then scientists have investigated the demyelinating potential of several myelin antigens together with adjuvants (MBP, PLP, MOG, and MAG; see Figure 2.3). These models are collectively called EAE.

EAE can be induced in several rodent strains as well as in primates, either by active immunization or passive transfer of T cells. The immunization of susceptible animals with complete Freund's adjuvant (CFA) containing heat-killed Mycobacterium tuberculosis was shown to produce encephalomyelitis and is known as active EAE (Gold et al., 2000; t Hart et al., 2004). Later, Paterson *et al.* showed that the adoptive transfer of lymphocytes obtained from sensitized animals caused clinical symptoms of EAE in naïve recipients (termed passive EAE induction; Paterson, 1960). The classic EAE induced by immunization with myelin antigens in

CFA or adoptive transfer of encephalitogenic T cells in the Lewis rat results in a characteristic ascending paralysis, which starts with a flaccid tail, hind-limb weakness, leading to paralysis of the hind limbs, and occasionally ending with complete hind and forelimb paralysis.

EAE models are heterogeneous in nature. Every model differs from all others by several aspects that include sensitivity, clinical course, and pathology. The sensitivity and clinical course of the disease depends on several factors such as age, sex, antigen, dose, route of administration, and species. Several species and strains including rats, mice, marmosets, and monkeys have been used to induce EAE. All differ in their clinical course as well as sensitivity to the antigen. The clinical course of EAE models is classified as acute, hyperacute, chronic-progressive, or relapsing–remitting. The differences between species and strains can partly be explained by the genetic variations in the MHC gene as well as other genes known to modulate the immune responses. For example, the response to a particular encephalitogenic epitope is dependent on the population of TCR and MHC class II molecules (Swanborg, 1995). Consequently, each animal species might offer an advantage for studying a particular aspect of the disease but the evaluation of novel therapies should be validated in several models (Steinman, 1999).

2.7.1 Mouse models

The mouse model offers several unique advantages over most other EAE models: the extensive knowledge accumulated in mouse genetics; the availability of molecular and immunological reagents; and the availability of transgenic and knockout strains, all of which make the mouse a first-choice model organism. Depending on the mouse strain analyzed, either a monophasic chronic-progressive or the relapsing–remitting form of MS can be observed. Clinical disease in mice is paralleled by histopathological changes of severe inflammation in the CNS; in some mouse models, this is accompanied by demyelination. However, the relative resistance of other mouse strains to EAE induction, the variability in disease incidence and kinetics, and the need for strong adjuvants, including mycobacteria

and pertussis toxin, make it difficult to study certain aspects of the pathogenesis. For example, adoptive transfer of EAE is more difficult in mice than in Lewis rats.

2.7.1.1 Induced models

Most of the active EAE induction protocols require CFA as an adjuvant. It facilitates the gradual and constant release of antigen into the draining lymph nodes, thus delaying the destruction of the antigen and increasing its dispersion. The mycobacteria in CFA amplify the immune response by stimulating the innate immune system. This causes a strong inflammatory response that leads to lymph node hyperplasia and augments the T cell responses. Pertussis toxin is often used to induce EAE in mice (Linthicum and Frelinger, 1982). It is thought to support the induction of EAE by breaking down T cell tolerance (Waldner et al., 2004), penetrating the BBB, and activating TLR4 (Racke et al., 2005).

Passive EAE induction by means of the transfer of encephalitogenic T cell clones or lines obtained from immunized animals and stimulated *in vitro* by the autoantigen offers the advantage of eliminating the use of additional adjuvant, which results in a strong artificial inflammatory condition. Under such conditions, EAE develops more quickly and is less variable, allowing study of the effector phase of the disease independently of the mechanisms involved in the induction phase (Wekerle et al., 1994).

However, induced models have several drawbacks. Not only are they artificial, but they also do not reflect the true pathogenic mechanisms of MS. While MS pathology (described in section 2.5) is complex and involves pronounced demyelination and cellular infiltration, induced mouse models are often too simple. Extensive demyelination and a topology of the lesions similar to that in human MS are often not reproduced in the experimental EAE models. Moreover, the potential role of antibodies and B cells might also be underestimated in the classic models of Th1-prone EAE. Finally, experimental difficulties in the induction and generation of T cell lines from some strains limit their usefulness for the study of pathogenic mechanisms.

2.7.1.2 Transgenic models

Transgenic models have been instrumental in the study of the pathogenesis of MS. They offer selective advantages over induced models for the study of pathogenic mechanisms and the evaluation of novel therapeutic compounds. HLA II transgenic mice, pathogenic TCR or BCR (B cell receptor) transgenic mice knock-in, and knock-out mice were developed and used in several studies. Human HLA class II or rodent MHC class II restricted TCR transgenic mice were derived from T cell clones isolated either from MS patients or from sensitized animals. This procedure is mainly based on the view that MS is mediated by Th1 cells.

HLA transgenics

HLA transgenic mice express the susceptible MHC II genes from patients and interact better with human TCR to mimic the human disease. Transgenic mice that express the DRB1*1501 allele, as well as an MS patient-derived TCR specific for the DRB1*1501-MBP (85–99) complex, and the human CD4 co-receptor have been generated. About 4% of these mice developed spontaneous EAE. The incidence was increased in recombinase-activating gene (RAG)-deficient background. After immunization, they developed relapsing-remitting EAE as in MS, thus supporting the involvement of the DRB1*1501-restricted MBP epitope in the pathogenesis of MS (Madsen et al., 1999). Several other HLA transgenic mice that express HLA-DRB1*0101 (recognizing MBP 139–154; Altmann et al., 1995), HLA-DRB1*0401 (recognizing MBP 87–106; Ito et al., 1996), and HLA-DRB1*1502 (recognizing PLP 95–116; Kawamura et al., 2000) have also been used.

TCR and BCR transgenic models

The earliest TCR transgenic models that recognize I-A^u restricted MBP Ac1-11 peptide were developed (Goverman et al., 1993; Lafaille et al., 1994). Like HLA II transgenic mice, TCR transgenic mice derived from human pathogenic T cell clones were also generated (Madsen et al., 1999; Ellmerich et al., 2004). They were used to

study disease-related epitope spreading and other aspects of pathogenesis. During the last decade, several TCR transgenic models have been created in different strains and for different myelin antigenic peptides (Table 2.2).

Studies of TCR transgenic mice have provided useful insights into the complex pathogenic mechanisms. For example, the contribution of environmental triggers to induce EAE was studied in MBP-specific TCR transgenic mice, approximately 14 - 44% of which developed spontaneous EAE under conventional housing conditions but not in specific pathogen-free (SPF) conditions (Goverman et al., 1993). These studies suggested possible environmental trigger(s) for EAE, but a definite candidate pathogen was not established.

Table 2.2 TCR transgenic models of multiple sclerosis (Modified from Lafaille, 2004).

Clone	Antigen	Restriction	TCRα	TCRβ	RAG	spontaneous EAE	Reference
172.10	MBPAc1-11	I-A^u	Vα2.3	Vβ8.2	RAG +/+	14-44%	Goverman et al., 1993
19	MBPAc1-11	I-A^u	Vα4	Vβ8.2	RAG -/-	100%	Lafaille et al., 1994
1934.4	MBPAc1-11	I-A^u	Vα4	Vβ8.2	RAG +/+	0%	Liu et al., 1995 Pearson et al., 1997
	MBP121-150	I-Au	Vα2	Vβ4	RAG +/+	0%	Huseby et al., 2001b
Ob.1A12	MBP84-102	HLA-DR2	Vα3	Vβ2.1	RAG -/-	100%	Madsen et al., 1999
4E3	PLP139-151	I-A^s	Vα11	Vβ16	RAG +/+	83%	Waldner et al., 2000
5B6	PLP139-151	I-A^s	Vα4	Vβ6	RAG +/+	45%	Waldner et al., 2000
2D2	MOG35-55	I-A^b	Vα3.2	Vβ11	RAG +/+	4%	Bettelli et al., 2003

In another model of MBP TCR mice, 100% of the transgenic mice developed EAE in a RAG-deficient background, in which all T cells bear the pathogenic TCR, since rearrangements of endogenous TCR are not possible (Lafaille et al., 1994). This study suggested the importance of regulatory lymphocytes in dampening EAE. Indeed, the transfer of polyclonal T cells completely suppressed spontaneous EAE (Olivares-Villagomez et al., 1998). PLP 139-151 specific TCR (obtained from both encephalitogenic and non-encephalitogenic clones) transgenic mice with a susceptible SJL/J genetic background developed severe spontaneous EAE but remained healthy with a resistant B10.S background (Waldner et al., 2000). This

resistance is attributed to the lower activation state and poor T cell stimulatory activity of APCs (Waldner et al., 2004). In addition, $CD4^+CD25^+$ regulatory cells (Tregs), which also contribute to the resistance and depletion of Tregs, restored their susceptibility to EAE induction by PLP 139-151 immunization (Reddy et al., 2005). Recently, an MOG 35-55-specific TCR transgenic mouse was developed with a C57BL/6 genetic background. Isolated optic neuritis (>30%) and low-grade EAE (4%) were observed in these mice (Bettelli et al., 2003). In addition to the CD4 TCR transgenic models, Goverman & colleagues developed the first TCR transgenic mice expressing MHC class I restricted TCR for MBP peptide (Perchellet et al., 2004)

Besides T cells, B cells might also play an important role in MS. B cells and antibodies have been shown to be essential for MS and EAE in several studies (Cross et al., 2001). Only one myelin antigen-specific BCR knock-in mouse model has been developed so far. It expresses a rearranged heavy chain from an MOG-specific antibody (8.18-C5). In contrast to TCR transgenic models, these mice never showed any sign of spontaneous CNS autoimmunity, but enhanced kinetics of diseased induction was observed when they were immunized with myelin antigens other than MOG (Litzenburger et al., 1998).

2.7.1.3 Novel model of T and B cell interaction

Undoubtedly, the above-described models (either induced or transgenic models) have contributed to our understanding of several facets of MS pathogenesis and allowed evaluation of therapeutic interventions. However, most of these animal models focus on either pathogenic T cells or B cells alone. Moreover, none of them reproduce the human disease in all its clinical and pathological aspects. Most importantly, none has shown that the interaction of pathogenic T and B cells precipitates autoimmunity.

To understand the interaction between antigen-specific T and B cells and their contribution to EAE, the present study used TCR and BCR transgenic mice available with the same genetic background. The TCR transgenic mice (TCR^{MOG}) used in the current study recognize the MOG 35-55 peptide in the context of $I-A^b$ and express

the rearranged TCR α and β chain from the pathogenic T cell clone obtained from immunized animals (Bettelli et al., 2003). A significant proportion (>30%) of the TCR^{MOG} mice used in the present study was shown to develop a spontaneous optic neuritis without evidence of clinical or histological EAE, and approximately 4% of the mice developed spontaneous EAE at an older age. The BCR knock-in mice (IgH^{MOG}) used in the present study were produced by gene targeting of the rearranged heavy chain VDJ sequence from the MOG-specific hybridoma 8.18-C5 to its natural locus (Litzenburger et al., 1998). This heavy chain recognizes the conformational epitope present in the extracellular portion of MOG. B cells in IgH^{MOG} mice develop normally and secrete high titers of pathogenic antibodies in serum. While they never show autoimmunity, enhanced kinetics of EAE after immunization was observed. The present study used both TCR^{MOG} and IgH^{MOG} mice to produce double-transgenic mice which developed a spontaneous EAE, and restricted localization of the inflammatory demyelinating lesions in the CNS.

3. Objectives

The role of CD4$^+$ T cells in the pathogenesis of MS has been studied extensively in animal models. Increasing evidence implicates B cells. So far, however, no animal model has shown a clear role of autoantigen-specific B cells and their interaction with autoreactive T cells to cause CNS autoimmunity.

This study was undertaken with the following objectives.

1. To generate an EAE mouse model that involves myelin antigen MOG-specific B and T cells.
2. To study the contribution of autoantigen-specific B cells in the pathogenesis of MS.
3. To study the interaction of autoantigen-specific B and T cells in precipitating autoimmunity.
4. To study the factors triggering CNS autoimmunity.

4. Materials and Methods

4.1. Materials

4.1.1 Antibodies
Antibodies for ELISA

	Specificity (anti-mouse)	Label	Clone	Antibody class	Company
Detection antibodies	IFNγ	Biotin	R4-6A2	Rat IgG1	Pharmingen
	IgG1	Biotin	A85-1	Rat IgG$_1$, κ	Pharmingen
	IgG1[a]	Biotin	10.9	Ms IgG$_{2a}$, κ (mouse IgG$_{2a}$[b])	Pharmingen
	IgG1[b]	Biotin	B68-2	Ms IgM, κ (mouse IgM[a])	Pharmingen
	IgG2a/2b	Biotin	R2-40	Rat IgG$_1$, κ	Pharmingen
	IgG2a/2b[a]	Biotin	8.3	Ms IgG$_{2a}$, κ (mouse IgG$_{2a}$[b])	Pharmingen
	IgG3	Biotin	R40-82	Rat IgG$_{2a}$, κ	Pharmingen
	IgM	Biotin	R6-60.2	Rat IgG$_{2a}$, κ	Pharmingen
	IgM[a]	Biotin	DS-1	Ms IgG$_1$, κ (mouse IgG$_1$[b])	Pharmingen
	IL2	Biotin	JES6-5H4	Rat IgG$_{2b}$	Pharmingen
	IL4	Biotin	BVD6-24G2	Rat IgG$_1$	Pharmingen
	IL5	Biotin	TRFK4	Rat IgG$_{2a}$	Pharmingen
Capture antibodies	IFNγ	-	AN-18	Rat IgG$_1$, κ	Pharmingen
	IgG$_1$	-	A85-3	Rat IgG$_{2a}$, κ	Pharmingen
	IgG2a	-	R11-89	Rat IgG$_1$, κ	Pharmingen
	IgG$_{2b}$	-	R9-91	Rat IgG$_1$	Pharmingen
	IgG3	-	R2-38	Rat IgG$_1$, κ	Pharmingen
	IgM	-	II/41	Rat IgG$_{2a}$, κ	Pharmingen
	IL2	-	JES6-1A12	Rat IgG$_{2a}$	Pharmingen
	IL4	-	BVD4-1D11	Rat IgG$_{2b}$	Pharmingen
	IL5	-	TRFK5	Rat IgG$_1$	Pharmingen

Isotype standards for Ig ELISA

Name	Clone	Company
Mouse IgG2a, κ isotype std (anti-TNP)	G155-178	Pharmingen
Mouse IgG1, λ isotype std	S1-68.1	Pharmingen
Mouse IgM, λ isotype std	PMG1-146.1	Pharmingen
Mouse IgG$_{2b}$, κ isotype std	MPC-11	Pharmingen
Mouse IgG$_3$, κ (anti-KLH)	A112-3	Pharmingen

The recombinant cytokine standards for cytokine ELISA were purchased from Pharmingen.

Antibodies (anti-mouse) for flow cytometry

Specificity	Label	Clone	Antibody class	Company
CD11b	PE	M1/70	Rat IgG$_{2b}$, κ	Pharmingen
CD154	PE	MR1	Ar Ham IgG3, κ	Pharmingen
CD19	FITC	1D3	Rat IgG$_{2a}$, κ	Pharmingen
CD19	PE	1D3	Rat IgG$_{2a}$, κ	Pharmingen
CD25	FITC	7D4	Rat IgM, κ	Pharmingen
CD25	PE	3C7	Rat IgG$_{2b}$, κ	Pharmingen
CD28	PE	37.51	Golden Syrian Hamster IgG	eBioscience
CD3e	APC	145-2C11	Ar Ham IgG1, κ	Pharmingen
CD3e	FITC	145-2C11	Ar Ham IgG1, κ	Pharmingen
CD4	PerCP	RM4-5	Rat IgG2a, κ	Pharmingen
CD44	FITC	IM7	Rat IgG$_{2b}$, κ	Pharmingen
CD44	PE	IM7	Rat IgG$_{2b}$, κ	Pharmingen
CD45R/B220	PerCP	RA3-6B2	Rat IgG$_{2a}$, κ	Pharmingen
CD62L	Biotin	MEL-14	Rat IgG$_{2a}$, κ	Pharmingen
CD69	FITC	H1.2F3	Ar Ham IgG1, λ3	Pharmingen
CD69	PE	H1.2F3	Ar Ham IgG1, λ3	Pharmingen
CD80	Biotin	16-10A1	Ar Ham IgG2, κ	Pharmingen
CD86	Biotin	GL1	Rat IgG2a, κ	Pharmingen
CD8a	APC	53-6.7	Rat IgG$_{2a}$, κ	Pharmingen
CDLA-4	PE	UC10-4B9	Armenian Hamster IgG	eBioscience
ICOS	PE	7E.17G9	Rat IgG2b,κ	eBioscience
ICOSL	PE	HK5.3	Rat IgG2a, κ	eBioscience
IFNγ	FITC	XMG1.2	Rat IgG$_1$	Pharmingen
IgM[a]	Biotin	DS-1	Ms IgG$_1$, κ (mouse IgG$_1$[b])	Pharmingen
IgM[a]	FITC	DS-1	Ms IgG$_1$, κ (mouse IgG$_1$[b])	Pharmingen
IgM[a]	PE	DS-1	Ms IgG$_1$, κ (mouse IgG$_1$[b])	Pharmingen
IgM[b]	FITC	AF6-78	Ms IgG$_1$, κ (mouse IgG$_1$[a])	Pharmingen
IgM[b]	PE	AF6-78	Ms IgG$_1$, κ (mouse IgG$_1$[a])	Pharmingen
IL2	FITC	S4B6	Rat IgG$_{2a}$	Pharmingen
IL4	FITC	BVD4-1D11	Rat IgG2b	Pharmingen
MHC Class II	Biotin	2G9	Rat IgG$_{2a}$, κ	Pharmingen
MOG	Biotin	8.18-C5	Mouse IgG1	In house
PD-1	PE	RMP1-30	Rat IgG2b, κ	eBioscience
PDL-1	PE	MIH5	Rat IgG2a, λ	eBioscience
PDL-2	FITC	122	Rat IgG2a, κ	eBioscience
TNFα	FITC	MP6-XT22	Rat IgG1	Pharmingen
Vα 3.2 TCR	FITC	RR3-16	Rat IgG2b, κ	Pharmingen
Vβ 11 TCR	PE	RR3-15	Rat IgG2b, κ	Pharmingen

4.1.2 Buffers and reagents

Tail digestion buffer

100 mM Tris HCl pH 8.5

5 mM EDTA

0.5% Tween 20

1 mg/ml Proteinase K (added before digestion)

FACS buffers

a. Staining buffer

PBS + 1% bovine serum albumin (BSA) + 0.1% sodium azide

b. Saponin buffer

0.1% saponin in PBS

c. PFA/saponin buffer

4% paraformaldehyde (PFA) + 0.1% saponin in PBS

Cell culture medium

RPMI 1640 or DMEM medium with sodium bicarbonate (Gibco)

1% MEM non essential amino acids (100 X; Gibco)

1% sodium pyruvate (100 mM; Gibco)

1% Pen-strep (Penicillin G 10,000 units/ml; streptomycin 10,000 μg/ml; Gibco)

1% glutamine solution (Gibco, 200 mM)

400 µl/ L β-mercaptoethanol (10 µl/10 ml media, pre-prepared)

10% heat-inactivated fetal calf serum (FCS)

Red blood cells (RBC) lysis buffer

0.83% ammonium chloride in PBS

Heparin solution

5000 units heparin (Sigma) in PBS

CFSE stock solution

5 mM in dimethyl sulfoxide (DMSO)

Isotonic percoll solution

9 parts (v/v) of percoll + 1 part (v/v) of 1.5 M sodium chloride

Neutralization buffer (for antibody purification)

   1 M Tris HCl pH 9.0

Elution buffer (for antibody purification)

   0.1 M glycine HCl pH 2.7

Binding buffer (for antibody purification)

   20 mM sodium phosphate pH 7.0

LB medium

   Peptone   10g

   Yeast extract   5g

   NaCl   5g

   Distilled water up to   1000 ml

Elution buffer (for MOG purification)

   6 M guanidium chloride + 0.5 M imidazole

Equilibration buffer (for MOG purification)

   6 M guanidium chloride pH 8.0

Wash buffer (for MOG purification)

   6 M guanidium chloride + 40 mM imidazole

Ni-NTA column regeneration buffer

   1 % EDTA + 0.05 % Tween-20

Solubilization buffer (for MOG purification)

   6 M guanidium chloride + 20 mM β-mercaptoethanol

Sonication buffer (for MOG purification)

   2 × PBS

Lysis buffer (for MOG purification)

   Sonication buffer + 0.5 % LDAO (N, N-dimethyldodecylamine-N-oxide, Fluka)
   + lysozyme

Wash buffer (ELISA)

   PBS + 0.05 % Tween 20

Assay diluent (ELISA)

   PBS + 10% FCS

4.1.3 Primers

Primers for gene expression analysis

Primer name	Gene	Oligo sequence (5' -> 3')	Label 5'	Label 3'
mGAPDH-sense #1	GAPDH	TCA CCA CCA TGG AGA AGG C	-	-
mGAPDH-AS #2	GAPDH	GCT AAG CAG TTG GTG GTG CA	-	-
mGAPDH-Probe #3	GAPDH	ATG CCC CCA TGT TTG TGA TGG GTG T	FAM	TAMRA
mFoxP3 sense #1	FoxP3	AGG AGA AGC TGG GAG CTA TGC	-	-
mFoxP3 AS #2	FoxP3	TGG CTA CGA TGC AGC AAG AG	-	-
mFoxP3 Probe #3	FoxP3	AAG GCT CCA TCT GTG GCC TCA ATG GA	FAM	TAMRA
mIL-5 sense #1	IL-5	CCG CTC ACC GAG CTC TGT T	-	-
mIL-5 AS #2	IL-5	AGA TTT CTC CAA TGC ATA GCT GG	-	-
mIL-5 Probe #3	IL-5	CAG GAA GCC TCA TCG TCT CAT TGC TTG T	FAM	TAMRA
mIL-10 sense	IL-10	CAGAGAAGCATGGCCCAGAA	-	-
mIL-10 AS	IL-10	TGCTCCACTGCCTTGCTCTT	-	-
mIL-10 Probe	IL-10	TGAGGCGCTGTCATCGATTTCTCCC	FAM	TAMRA
mEotaxin sense	Eotaxin	AGAGCTCCACAGCTTCTATT	-	-
mEotaxin AS	Eotaxin	CTTACTGGTCATGATAAAGCAGCAG	-	-
mEotaxin Probe	Eotaxin	ACGGTCACTTCCTTCACCTCCCAGG	FAM	TAMRA
mIFNγ sense	IFNγ	TCAAGTGGCATAGATGTGGAAGAA	-	-
mIFNγ AS	IFNγ	TGGCTCTGCAGGATTTTCATG	-	-
mIFNγ Probe	IFNγ	TCACCATCCTTTTGCCAGTTCCTCCAG	FAM	TAMRA
mTNFα sense	TNFα	CATCTTCTCAAAATTCGAGTGACAA	-	-
mTNFα AS	TNFα	TGGGAGTAGACAAGGTACAACCC	-	-
mTNFα probe	TNFα	CACGTCGTAGCAAACCACCAAGTGGA	FAM	TAMRA
mIL-4 sense	IL-4	ACAGGAGAAGGGACGCCAT	-	-
mIL-4 AS	IL-4	GAAGCCCTACAGACGAGCTCA	-	-
mIL-4 probe	IL-4	TCCTCACAGCAACGAAGAACACCACA	FAM	TAMRA
mIL-13 sense	IL-13	GGAGCTGAGCAACATCACACA	-	-
mIL-13 AS	IL-13	GGTCCTGTAGATGGCATTGCA	-	-
mIL-13 probe	IL-13	CGGGTTCTGTGTAGCCCTGGATTCC	FAM	TAMRA
mIP-10 sense	IP-10	GCCGTCATTTTCTGCCTCAT	-	-
mIP-10 AS	IP-10	GCTTCCCTATGGCCCTCATT	-	-
mIP-10 probe	IP-10	TCTCGCAAGGACGGTCCGCTG	FAM	TAMRA

IFN-γ, TNFα, IL-4, IL-13 and IP-10 Taqman probes were synthesized as described *(Giulietti et al., 2001)*.

Primers for genotyping transgenic mice

Primer name	Gene	Oligo sequence (5' -> 3')	Label	
			5'	3'
8.18C5-sense #1	anti-MOG IgH (8.18C5)	TGA GGA CTC TGC CGT CTA TTA CTG T	-	-
8.18C5-AS #2	anti-MOG IgH (8.18C5)	GGA GAC TGT GAG AGT GGT GCC T	-	-
8.18C5-Probe #3	anti-MOG IgH (8.18C5)	CCA GTA TGG CAT GTT TAC CAT CGT ATT ACC AGT T	FAM	TAMRA
mIgH-sense #1	Ig heavy chain	ATT GGT CCC TGA CTC AAG AGA TG	-	-
mIgH-AS #2	Ig heavy chain	TGG TGC TCC GCT TAG TCA AA	-	-
mIgH-Probe #3	Ig heavy chain	CCT TGC ACC AGT CAG AGA CCA CAG GG	FAM	TAMRA
Va3.2-2D2-M	Valpha 3.2 TCR	CCC GGG CAA GGC TCA GCC ATG CTC CTG	-	-
Ja18-2D2-M	Valpha 3.2 TCR	GCG GCC GCA ATT CCC AGA GAC ATC CCT CC	-	-
mRAG-2 sense #1	RAG2	GGG AGG ACA CTC ACT TGC CAG TA	-	-
mRAG-2 AS #2	RAG2	AGT CAG GAG TCT CCA TCT CAC TGA	-	-
Neo-2 #3	Neomycin resistance gene	AGG TGA GAT GAC AGG AGA TC	-	-
nlacZ	lacZ	GATGGGCGCATCGTAACCGTGC	-	-
mMOG-sense #1	MOG	AGG AAG GGA CAT GCA GCC GGA G	-	-
mMOG-AS #2	MOG	CTG CAT AGC TGC ATG ACA ACT G	-	-
oIMR1825	Ovalbumin	GCT GCT GCA CAG ACC TAC T	-	-
oIMR1826	Ovalbumin	CAG CTC ACC TAA CAC GAG GA	-	-

4. 2 Methods

4.2.1 Animals

All animals used in this study had a C57BL/6 genetic background and were maintained in the conventional and SPF animal facilities of Max-Planck Institute of Neurobiology, Martinsried, Germany. TCR^{MOG} (2D2; Bettelli et al., 2003) was generously provided by Drs. Estelle Bettelli and Vijay K. Kuchroo (Harvard Medical School, Boston, MS, USA). The transgenic IgH^{MOG} knock-in (Th) mouse was described previously (Litzenburger et al., 1998). MOG knock-out mice (Delarasse et al., 2003) was a kind gift from Dr. Danielle Pham-Dinh (INSERM, Unité 546, Paris, France). Ovalbumin-specific TCR transgenic (OT-II) mice were purchased from the Jackson Laboratories, and RAG2-deficient mice were obtained from Max-Planck Institute of Immunobiology, Freiburg, Germany. Wild-type (WT) C57BL/6 mice were obtained from the animal facility of the Max-Planck Institute of Biochemistry, Martinsried, Germany.

4.2.2 Genotyping

Transgenic animals were genotyped by either conventional polymerase chain reaction (PCR) or real-time PCR of genomic DNA extracted from a piece of tail. A small piece of tail was clipped after weaning and incubated overnight in tail digestion buffer containing proteinase K (Roche) at 55°C. Then 500 µl of phenol/chloroform/isoamyl alcohol (Roth) were added and mixed well. After spinning at a maximum speed for 5 min, an aqueous layer was transferred into a fresh test tube. DNA was precipitated with 1 ml of ethanol for 5 min at maximum speed and washed with 70% ethanol. Precipitated DNA was dissolved in 400 µl of 10 mM Tris buffer at pH 8.0 and stored at -20°C.

The typical PCR mixture consists of

       Tail genomic DNA   1 µl

       10X buffer   2.5 µl

10 µM Sense primer	0.5 µl
10 µM Anti-sense primer	0.5 µl
10 mM dNTPs	0.5 µl
Taq polymerase (5 units/µl)	0.1 µl
H_2O up to	25 µl

The typical real-time PCR reaction consists of

Tail genomic DNA	0.5 µl
10 µM Sense primer	0.5 µl
10 µM Anti-sense primer	0.5 µl
10 µM probe	0.5 µl
ROX 1:50	0.5 µl
Thermomix	10 µl
H_2O up to	20 µl

Taq polymerase was purchased either from Roche or Invitrogen, and real-time PCR mix was obtained from ABGene.

4.2.3 Disease scoring

All animals were examined at least once in 2 - 3 days for clinical signs of disease according to the classic EAE determination.

0 : healthy animal

1 : animal with a flaccid tail

2 : animal with impaired righting reflex and/or gait

3 : animal with one paralyzed hind leg

4 : animal with both hind legs paralyzed

5 : moribund or death after preceding clinical disease

4.2.4 Antigens

MOG peptide 35-55 (MEVGWYRSPFSRVVHLYRNGK) was synthesized at BioTrend, Cologne, Germany. Recombinant soluble MOG protein (MOG 1 – 125) was purified from bacterial inclusion bodies (Amor et al., 1994). Expression plasmid-pQE-12 containing rat MOG 1-125 was grown in LB medium containing ampicillin (100 mg/ml; Sigma) and kanamycin (25 mg/ml; Sigma). The bacterial cultures were induced with isopropyl thiogalactoside (IPTG),and the cells were pelletted. The pellet was resuspended in lysis buffer with lysozyme and sonicated. Lysed samples were washed, suspended in solubilization buffer, and loaded onto the Ni-NTA column prepared with chelating sepharose and 1% $NiCl_2$ (Amersham biosciences). The column was washed with wash buffer and eluted with elution buffer. Eluted MOG was dialyzed against 20 mM sodium acetate at pH 3.0.

4.2.5 Immunization of animals

Mice were injected (200 – 500 µl) subcutaneously (s.c.) at the tail base with an emulsion containing equal amounts of CFA (Difco) and 200 µg MOG 35-55 in PBS. CFA was supplemented with 5 mg/ml mycobacterium tuberculosis (strain H37Ra; Difco). Pertussis toxin (400 ng) was injected intraperitoneally (i.p.) on days 0 and 2 following immunization.

4.2.6 Serum collection

Mice were bled by retro-orbital puncture, and the samples were allowed to clot overnight at 4°C. Serum was collected after spinning at $4°C/400\ g$ for 10 min and stored at $-20°C$ until further analysis.

4.2.7 Isolation of CNS mononuclear cells

The entire spinal cord was removed with a syringe from the animal and pressed through nylon mesh into RPMI medium (without serum). After centrifugation for 10 min at 1200 rpm, it was suspended in 5 ml of RPMI and mixed with 2.16 ml of

isotonic percoll solution (Amersham Biosciences). The cell suspension was overlaid on 5 ml percoll and centrifuged at 20°C/1200 g for 20 min. The interface containing the mononuclear cells were collected and washed once with RPMI.

4.2.8 Preparation of PBMCs

Blood was collected from the mice by retro-orbital puncture in a tube containing 100 µl of heparin solution (5000 units/ml). RBC lysis buffer was added and incubated for 10 min on ice. Cells were spun down at 400 g/4°C for 10 min. The procedure was repeated once more and finally the cell pellet was suspended in PBS or processed as necessary.

4.2.9 Cell purification

Lymphocyte subpopulations were purified from the spleens of transgenic mice using B-cell or T-cell negative selection kits (Dynal Biotech, Norway). Single cell suspensions were prepared from the spleen of transgenic mice. RBC-lysed splenocytes were incubated with biotinylated antibody cocktail against cell surface antigens other than the cell population of interest. Dynabeads were mixed, and untouched CD4$^+$ or B cells were isolated after placing the cell suspension in a magnet. The viability and purity of the cells were evaluated by FACS analysis.

4.2.10 CFSE labeling of lymphocytes

The cells (2 x 10^7) were incubated at 37°C/dark for 10 min with 1% FCS/PBS containing 5 µM CFSE (Molecular Probes). After extensive washing with cold PBS, cells were suspended in medium or PBS.

4.2.11 *In vitro* proliferation assay

The proliferation assay was performed in 96 well U bottom plates in triplicates. Splenocytes or 1:1 mixed purified cells (2 × 10^5 /well) were cultured with the indicated concentrations of rMOG or MOG 35-55 in a final volume of 200 µl RPMI medium. After 48 h incubation, cultures were pulsed with ^{3}H-thymidine (specific

activity: 2 Ci/mmol; 1 µCi/well) (Amersham Biosciences). Samples were harvested after 16 h incubation, and the radioactivity was measured by the direct beta counter (Matrix^{TM} 9600, Packard).

4.2.12 Bone marrow chimera

Bone marrow cells from Devic mice were collected from both femur and tibia. RBCs were lysed from pooled bone marrow cells by RBC lysis buffer. Cells were counted and suspended in serum-free RPMI or PBS. Subsequently 7-10 week (wk)-old C57BL/6 females were sub-lethally irradiated at 1000 rad single dose just prior to injection. Then 10×10^6 RBC depleted bone marrow cells were injected intravenously (i.v) into each mouse and allowed to reconstitute. Serum antibody levels or levels of reconstitution were assessed after 4 wk by preparing PBMC or serum by retro-orbital bleeding.

4.2.13 Adoptive transfer

Transfer into TCR^{MOG} mice

Splenocytes obtained from IgH^{MOG} mice were depleted of RBCs and incubated with rMOG (1 µg/1 $\times$ 10^6) for 10 min at 37°C. Cells were washed extensively and suspended in PBS. Subsequently 20×10^6 cells were injected i.v. into recipient TCR^{MOG} mice. Some mice simultaneously received i.p. 50 µg of LPS (*E. coli* serotype O111:B4).

Transfer into RAG KO mice

Splenocytes obtained from Devic (healthy), IgH^{MOG} or TCR^{MOG} were incubated in RBS lysis buffer to remove RBCs. Then they were washed and suspended in PBS. Subsequently 50×10^6 cells were injected i.v into each RAG KO mice.

4.2.14 Histological analysis

Animals were perfused transcardially with 4% paraformaldehyde (PFA) in PBS, stored in PFA for 24 h, and then washed twice with PBS. Brain and spinal cord tissue was dissected and in part embedded in paraffin or snap-frozen for

immunocytochemistry. Adjacent serial sections were stained with hematoxylin/eosin, luxol fast blue (LFB), or Bielschowsky silver impregnation. All histological analysis was performed by Prof. Hans Lassmann, University of Vienna, Austria.

4.2.15 Immunohistochemistry

Tissues isolated from the animals were frozen in Tissue Tek OCT compound on dry ice and stored at -20°C. Tissue sections (8 - 12 µm) were incubated with primary rat antibodies recognizing mouse CD4, CD11b, CD8α, IgM, CD19, or B220 (all obtained from BD Pharmingen). A secondary biotinylated anti-rat antibody, a streptavidin-horseradish peroxidase complex (both from Vector Laboratories), and diaminobenzidine (Zymed) allowed the cell type-specific detection of mononuclear cells. Slides were counterstained with Meyer's hematoxylin and embedded in AquaMount (Fisher Scientific) prior to microscopic analysis.

4.2.16 Flow cytometry
Surface staining

Single cell suspensions were incubated with fluorochrome-labeled antibodies diluted in FACS staining buffer on ice/dark for 20 min. Stained cells were washed twice and suspended in PBS. Samples were acquired in FACSCalibur (BD Biosciences). Biotinylated antibodies were visualized by Streptavidin-APC (BD Pharmingen).

Intracellular staining

After surface staining, cells were suspended in PFA/saponin buffer for 10 min in the dark. After washing twice with saponin buffer, flurochorome-labeled anti-cytokine antibodies were added and incubated for another 30 min. Washed as above and suspended in PBS, samples were acquired in FACSCalibur.

Data were analyzed with CellQuest (BD Biosciences) or WinMDI (Joe Trotter) software.

4.2.17 Hybridoma generation

Splenocytes from the single transgenic mice were stimulated with 20 µg/ml LPS (*E. coli* serotype O111:B4) *in vitro*. After 3 days, cells were washed extensively to remove the serum. The hybridoma fusion partner cell line Sp2/0 growing in exponential phase was also harvested and washed. Splenocytes were mixed with Sp2/0 cells (5:1), and 0.5 ml of 50% polyethylene glycol was added slowly with gentle mixing. Cells were kept at 37°C for 1 min, diluted with serum-free media, and spun down and plated in 96-well plates at 1-2 × 10^6 cells/ml in Hybrimax® HAT (Sigma) containing DMEM/20% FCS. Seven days later medium was replaced with Hybrimax® HT (Sigma) containing DMEM/20% FCS, and growing clones were expanded in DMEM/10% FCS. Sub-cloning was done by single-cell sorting with FACSVantage.

4.2.18 Antibody purification

Antibody producing hybridomas were grown in cell stack (Corning) with DMEM/10% FCS. Culture supernatants were harvested and filtered to remove cell debris. Supernatants were applied to the Hitrap ® protein G column (Amersham Biosciences) and washed extensively with binding buffer to remove nonbinding proteins. Antibody was eluted from the column by the elution buffer and immediately neutralized in neutralization buffer. The antibody-containing fractions (measured by OD 280) were pooled and dialyzed against PBS overnight.

4.2.19 Enzyme linked immunosorbent assay (ELISA)
Cytokine ELISA

Splenocytes (2 × 10^5 cells/well) were either unstimulated or stimulated with rMOG in 96-well "U" bottom plates for 3 days, and supernatants were collected and frozen at -20°C. ELISA plates (Nunc) were coated with 100 µl of capture antibodies (1 µg/ml in 0.1 M $NaHCO_3$ pH 9.0) for overnight at 4°C. Plates were washed with wash buffer and blocked with assay diluent for 1 h. They were then washed and incubated with 100 µl of supernatants at room temperature for 2 h. Cytokine standards were serially

diluted from 2000 pg/ml to obtain standard curve in each individual assay. They were washed, and then 100 µl of the respective biotinylated secondary antibodies diluted in assay diluent was added and incubated for another 1 h. After extensive washing, streptavidin-HRP (1:2000) was added and incubated at room temperature for 30 min. After washing, 100 µl of ABTS (2, 2'-Azino-bis (3-ethyl-benzthiazoline-6-sulphonic acid; Sigma) activated with H_2O_2 was added and absorbance was measured at 405 nm in an ELISA reader (Victor2™ 1420 mutilabel counter; Perkin Elmer life sciences).

Serum antibody determination

 Plates were coated with rMOG (10 µg/ml in PBS) overnight at 4$^{°}$C. ELISA was performed as above with 1:100 diluted serum samples and incubation of for 1 h.

4.2.20 Enzyme linked immunospot (ELISPOT) assay

ELISPOT plates (Millipore) were coated with rMOG as in ELISA. Serially diluted splenocytes or BM cells were plated, and the rest of the procedure was similar to that of ELISA. Streptavidin-alkaline phosphatase was used to reveal the biotinylated antibodies. BCIP/NBT (Sigma) substrate was added to visualize the antibody secreting cells, and spots were counted by an ELISPOT reader (Carl Zeiss).

4.2.21 Quantitative real-time TaqMan PCR analysis

PBMCs or spinal cord tissue was mixed or homogenized in 0.5 – 1 ml of TRI® reagent (Sigma). To this 200 µl of chloroform was added and centrifuged at 12000 g/15 min. RNA was precipitated with 500 µl of isopropanol. It was washed once with 75% ethanol and dissolved in RNAse-free water. RNA (~ 5 µg) was treated with DNAse to remove DNA contamination and reverse transcribed with either random hexamer or oligo-dT primer using Superscript II reverse transcriptase. All reagents for cDNA synthesis were obtained from Invitrogen. Sense and antisense primers in combination with FAM/TAMRA TaqMan probes and gene-specific primers (synthesized at Metabion, Martinsried, Germany) were utilized for PCR analysis. The

PCR reaction was carried out as described previously in genotyping. Each reaction was run in triplicate on an ABI 5700 machine (Applied Biosystems) and was normalized to house-keeping gene GAPDH transcripts. Primary data were analyzed with GeneAmp SDS 5700 software (PE Biosystems).

4.2.22 Statistical analysis

Data were analyzed with Microsoft Excel and GraphPad prism version 4. A two-way ANOVA or t test was performed to analyze the statistical significance. A value of $p < 0.05$ was considered statistically significant.

5. RESULTS

5.1 Double transgenic IgH^{MOG} X TCR^{MOG} ("Devic") mice develop spontaneous EAE

MOG 35 – 55-specific TCR (2D2) transgenic mice (TCR^{MOG}) express the rearranged I-A^{b} restricted TCR. A large proportion (>30%) of these mice develop isolated spontaneous optic neuritis, but rarely EAE when observed for periods of up to 1 year (Bettelli et al., 2003).

MOG-specific BCR (Th) "knock-in mice" (IgH^{MOG}) contain the heavy chain of the demyelinating antibody 8.18-C5 and secrete large amounts of pathogenic antibodies. These mice never showed any spontaneous autoimmunity when observed over an extended period (Litzenburger et al., 1998).

Interbreeding of TCR^{MOG} and IgH^{MOG} mice, both with the C57BL/6 genetic background and housed under specific pathogen-free (SPF) conditions, generated double transgenic mice that had both MOG-specific CD4^{+} T and B cells. These double transgenic mice were termed "Devic mice" (Figure 5.1A). Surprisingly, more than 50% of the Devic mice developed spontaneous EAE, while all single transgenic littermates remained disease-free during the 9-week (wk) observation period. In contrast, neither breeding of IgH^{MOG} mice to non-self antigen ovalbumin (Ova 323 - 339)-specific TCR transgenic mice (OT-II; Barnden et al., 1998) nor MOG-deficient Devic mice (Devic X MOG$^{-/-}$; Delarasse et al., 2003) showed any spontaneous autoimmunity (Figure 5.1B). Clinical disease was observed at 6.1 ± 2 weeks of age, and the mean maximum disease score was 3.4 ± 1.2 (Table 5.1). Although male Devic mice showed a slightly earlier disease onset and a higher disease incidence than females, these differences were not statistically significant (Figure 5.1B).

The microbial environmental might be important for precipitating autoimmunity. To determine whether different housing conditions (i.e., different microbial environments) could influence spontaneous EAE, Devic mice were also bred under conventional housing conditions. About 46% of these animals developed spontaneous EAE as did Devic mice housed under SPF conditions. A comparison of

the disease kinetics did not reveal any statistically significant difference (Figure 5.1C). These data suggest that the presence of both MOG-specific T and B cells in a MOG-competent background is essential for spontaneous EAE. Environmental agents play (if at all) only a minor role in this spontaneous development.
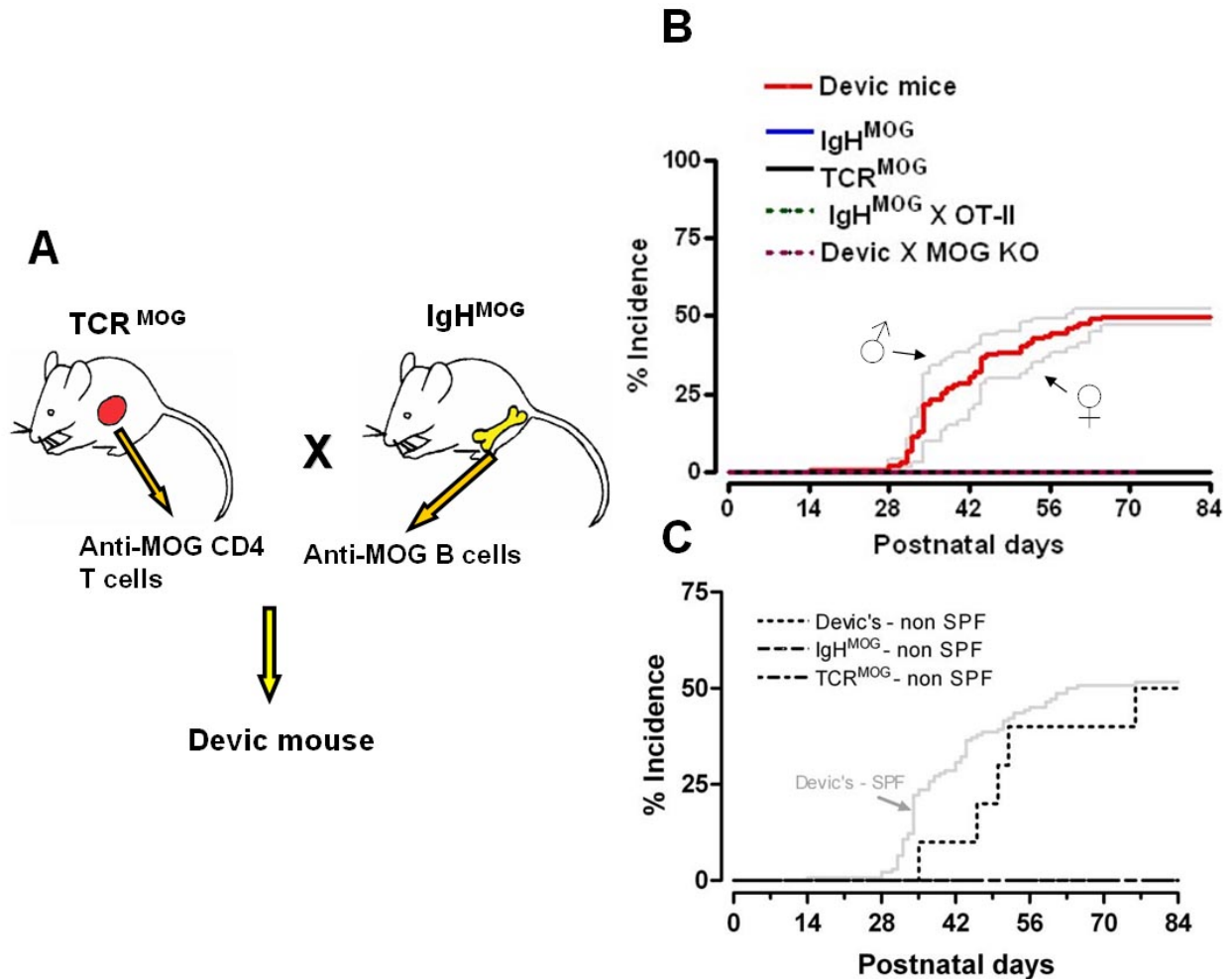
Figure 5.1

Spontaneous EAE-like disease in double transgenic IgH^MOG X TCR^MOG (Devic) mice. **(A)** F1 double transgenic (IgH^MOG X TCR^MOG) mice, from interbreeding of TCR transgenic mice containing MOG 35-55 specific CD4^+ T cells and IgH^MOG mice, which have MOG-specific B cells, were termed Devic mice. The genetic background of both parental mice was C57BL/6. **(B)** Spontaneous EAE-like disease was observed in Devic mice (red line) housed under SPF conditions, while single transgenic littermates IgH^MOG (blue line) and TCR^MOG (black line) did not show any clinical signs of EAE. Double transgenic IgH^MOG X OT-II (ovalbumin specific TCR) mice (green dotted line) and MOG-deficient Devic mice (IgH^MOG X TCR^MOG X MOG^-/-; violet dotted line) housed under the same conditions also never showed any clinical disease. Gray lines both above and below the red line show the disease kinetics of male and female Devic mice, respectively. The slightly earlier onset and higher incidence observed in male Devic mice (n = 73) when compared to female Devic mice (n = 60) was not statistically significant. **(C)** Devic mice housed under conventional conditions (n = 9) also showed EAE signs similar to the mice kept under SPF conditions (gray line; n = 133). Age-matched single transgenic littermates IgH^MOG (n = 7) and TCR^MOG (n = 3) were free of clinical disease during the same observation period.

Table 5.1
Spontaneous EAE incidence, onset, and severity in double transgenic IgH^{MOG} X TCR^{MOG} (Devic) mice.

Animal group	Incidence	Mean Clinical score	Mean age of onset (wk)
IgH^{MOG} X TCR^{MOG} (Devic mice)	51.13% (68/133)	3.4 ± 1.2 (n=8)	6.1 ± 2
TCR^{MOG}	0% (0/34)	NA	NA
IgH^{MOG}	0% (0/69)	NA	NA
IgH^{MOG} X OT-II	0% (0/11)	NA	NA
Devic X MOG$^{-/-}$	0% (0/6)	NA	NA

F1 mice from the interbreeding of IgH^{MOG} with TCR^{MOG}, IgH^{MOG} with OT-II, as well as the IgH^{MOG} and TCR^{MOG} with MOG$^{-/-}$ were assessed for clinical signs of EAE at least once in 2 - 3 days. Clinical score and age at spontaneous onset of EAE in Devic mice are shown as mean ± SD calculated from closely observed mice (n = 8). NA, Not applicable.

5.2 Causative CNS lesions in Devic mice mimic human opticospinal multiple sclerosis, Devic's neuromyelitis optica

The CNS of Devic mice with spontaneous EAE, housed under conventional conditions, was analyzed histologically. Pathological lesions in these mice were exclusively present in the optic nerves and spinal cord, whereas the brain was completely spared from any inflammation or tissue damage (Figure 5.2A). This peculiar localization of the lesions was highly similar to that in the human disease, Devic's neuromyelitis optica, an MS variant. In contrast, age-matched single transgenic TCR^{MOG} and IgH^{MOG} mice did not develop any CNS lesions. Only seldom did a few TCR^{MOG} animals show perivascular damage and mild infiltration. Healthy Devic mice also did not have any appreciable CNS lesions except sparse inflammatory infiltrates around perivascular areas (Figure 5.2B).
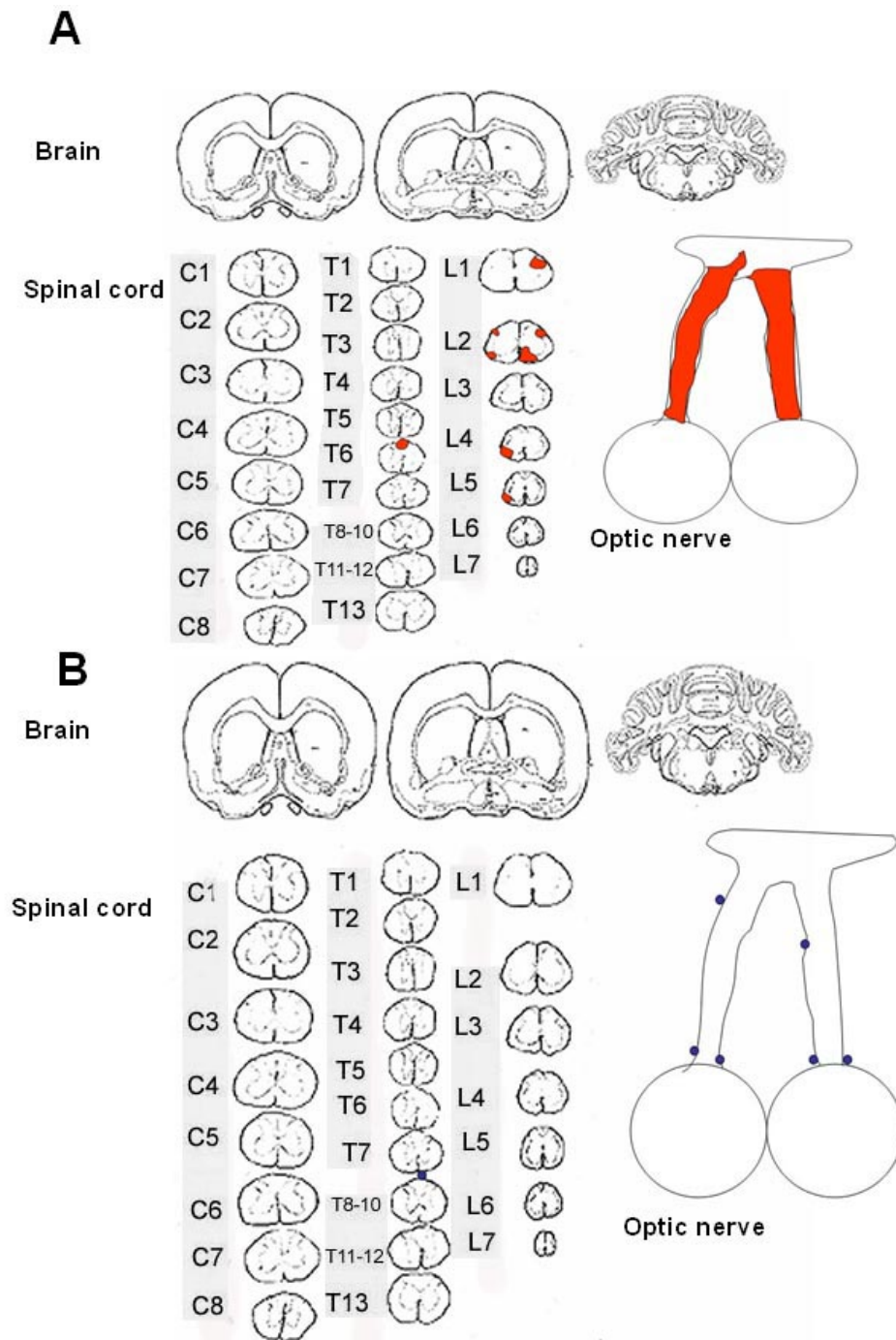
Figure 5.2

CNS lesions in sick Devic mice resemble those in the human MS variant, Devic's neuromyelitis optica. **(A)** A Devic mouse with clinical EAE was perfused transcardially with PFA, and after PFA fixation histological analysis was performed on different sections (cervical to lumbar) throughout the spinal cord. The histology of the entire CNS showed severe demyelination (red area) only in the optic nerve and the spinal cord, whereas the brain remained unaffected. **(B)** Analysis of the entire CNS of a healthy Devic mouse (7.5-wk-old) showed only slight focal inflammatory reaction (blue) in the optic nerve, whereas other parts of the CNS were completely free of any inflammation or demyelination. The histological analysis was performed by Prof. Hans Lassmann, University of Vienna, Austria.
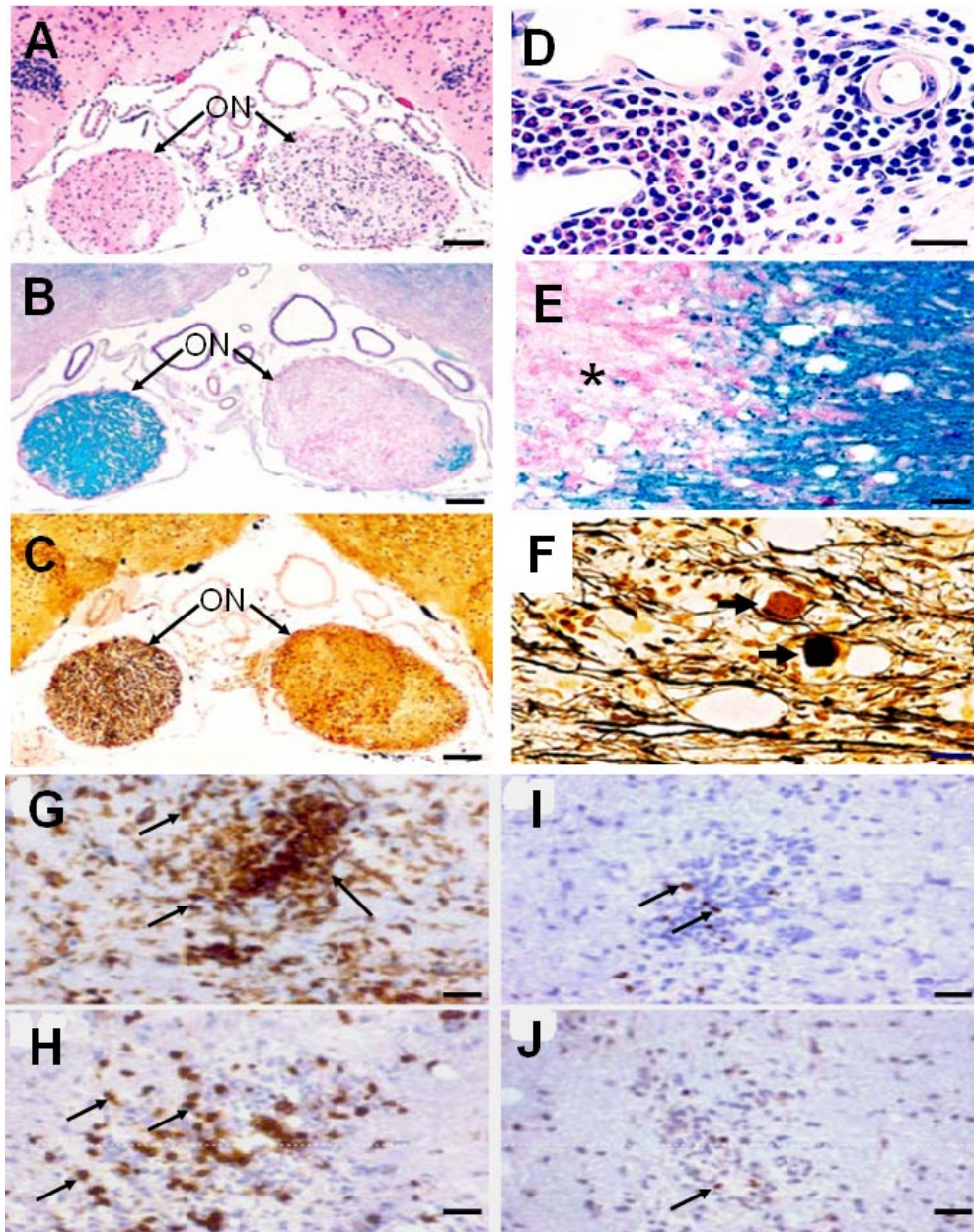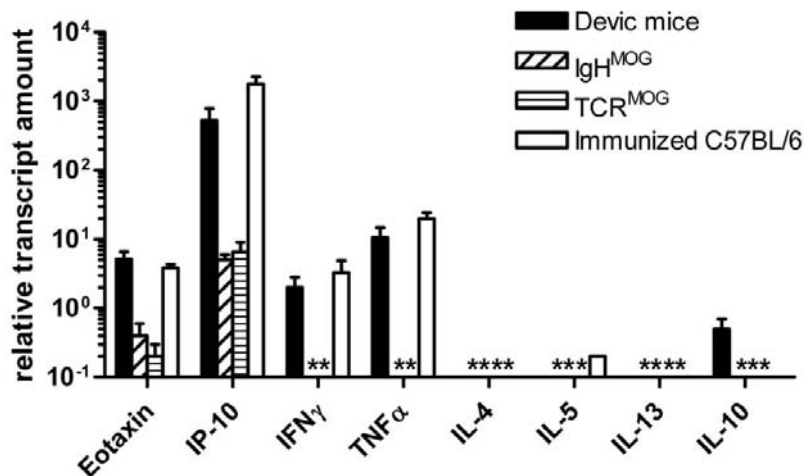
Figure 5.3

Histological analysis of optic nerves and spinal cords from a sick Devic mouse. Optic nerves (ON) **(A-F)** and spinal cords **(G-N)** were stained with hematoxylin & eosin (H&E), luxol fast blue (LFB), and Bielschowsky silver impregnation for cellular infiltration, demyelination and axonal damage, respectively. While hematoxylin/eosin stains mononuclear cells, luxol fast blue stains intact myelin as blue. Intact axons are stained dark brown with Bielschowsky silver impregnation and damaged axons stain yellowish brown. **(A-C)** The sections are from frontal brain sections and show both optic nerves; A: H & E; B: Luxol Fast Blue; C: Bielschowsky silver impregnation. Scale bar = 1mm. **(D)** Meninges surrounding the arterial spinalis anterior of the spinal cord with massive inflammatory infiltrates, composed of mononuclear cells and granulocytes, some of them being eosinophils; H&E staining; scale bar =100 µm. **(E)** Luxol fast blue staining of the anterior column of the spinal cord from the same animal. Shown is the actively demyelinating lesion (left side of the micrograph) with loss of myelin and Luxol fast blue myelin degradation products at the edge of the lesion. The asterisk shows the location of Fig 5.3 F; scale bar = 100µm. **(F)** Higher magnification of the lesion shown in Fig 1E, stained with Bielschowsky silver impregnation; profound reduction of axonal density and appearance of axonal spheroids, indicating acute axonal injury (arrow); scale bar= 100µm. **(G-J)** Conventional immunohistochemistry with antibodies against CD4, CD8, CD11b and B220/CD19 in the spinal cord. Shown is the predominant presence of CD11b^{+} macrophages **(G)** and CD4^{+} T cells **(H)** in the spinal cord, but B cells **(I)** and CD8+ cells **(J)** were not found in significant numbers. Arrows in G-J indicate the cells stained positive for the respective antibodies. Scale bar for G-J = 100µm. The histological analysis was performed by Prof. Hans Lassmann, University of Vienna, Austria.

Furthermore, the CNS lesions of sick Devic mice were circumscript and contained massive numbers of the inflammatory cells. Pronounced demyelination and axonal damage were observed to coincide with the infiltration of inflammatory cells. Immunohistochemistry showed that the inflammatory infiltrates were predominantly composed of macrophages and CD4^{+} T cells (Figure 5.3).

Occasionally a few B cells or CD8^{+} T cells were found. In some cases, significant numbers of eosinophils were also present in the actively demyelinating lesions (Figure 5.3). Devic mice kept under SPF conditions showed a similar localization of inflammatory lesions in the optic nerve and spinal cord with pronounced demyelination and massive infiltration of mononuclear cells in the meninges and perivascular areas. Eosinophilic infiltration was rarely observed.

5.3 Th1-cytokine milieu in CNS lesions

Cytokines and chemokines expressed by the CNS infiltrating cells create an inflammatory milieu and mediate the inflammatory process. The expression of cytokines and chemokines was assessed by quantitative real-time PCR of the spinal cords of Devic mice with spontaneous EAE, healthy IgH^{MOG}, healthy TCR^{MOG}, and wild-type C57BL/6 mice with actively induced EAE.

Figure 5.4
Th1 cytokine milieu of the spinal cord of sick Devic mice. Expression of cytokine and chemokine gene transcripts was measured by real-time quantitative PCR of the spinal cord of sick Devic (n = 5; clinical score ≥3), healthy IgH^{MOG} (n = 3), healthy TCR^{MOG} (n = 3), and MOG 35-55 immunized C57BL/6 (n = 3; clinical score ≥ 3) mice. Relative expression levels were normalized to endogenous control gene GAPDH transcripts x 10,000. Error bars indicate the SEM. * = not detectable gene expression.

Th1 cytokine transcripts (IFN-γ, TNF-α) and chemokines (IP-10, eotaxin) were expressed at similar levels in sick Devic mice and in WT mice with active EAE. In contrast, Th2 cytokine transcripts (IL-4, -5 -10, -13) remained low or undetectable. Healthy TCR^{MOG} or IgH^{MOG} single-transgenic littermates did not show expression of any of these cytokine transcripts, but they did express eotaxin and IP-10, albeit at low levels compared to sick Devic mice (Figure 5.4).

5.4 CNS-infiltrating transgenic CD4$^+$ T cells are highly activated

Consistent with the histological data, significant numbers of CNS infiltrating mononuclear cells could be isolated from the spinal cords of Devic mice with EAE by the percoll density gradient.
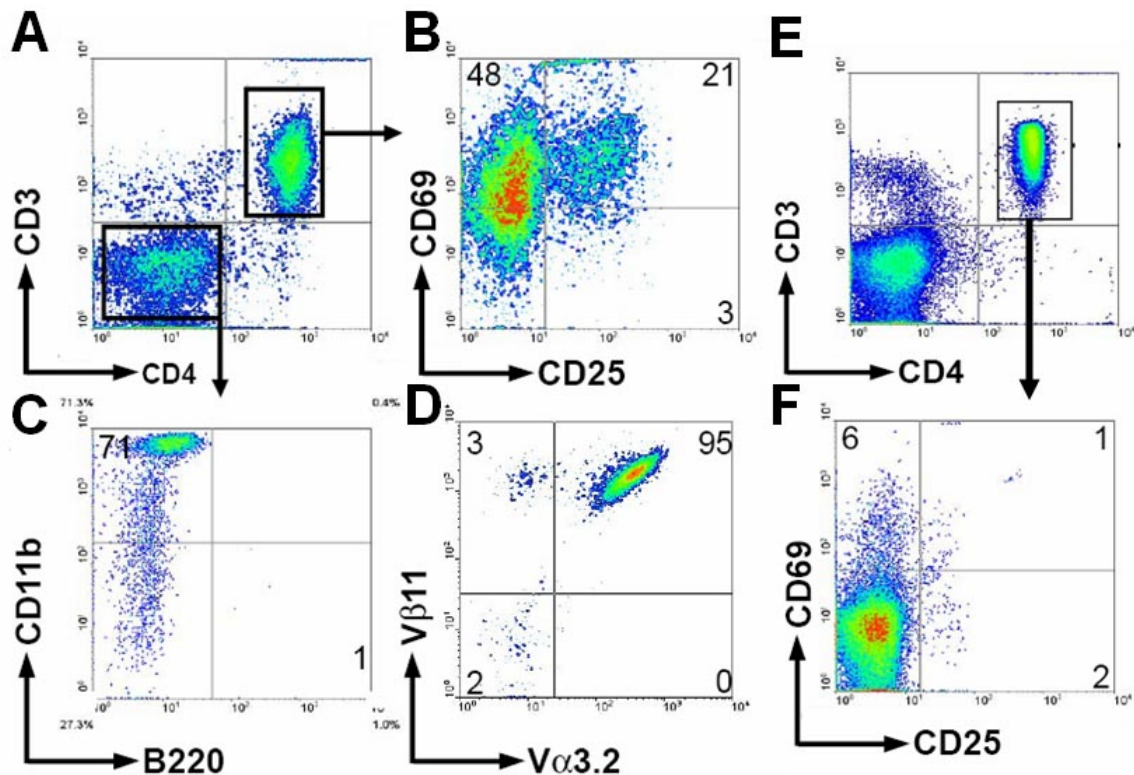
Figure 5.5

Transgenic CD4$^+$ T cells infiltrating the CNS were highly activated. **(A, B)** Spinal cord infiltrated cells from sick Devic mice isolated by percoll gradient were stained with antibodies against CD4, CD3, and the activation markers CD25 and CD69. Gated CD4$^+$CD3$^+$ T cells expressed CD69, and some of them also expressed CD25. **(C)** CD4$^-$CD3$^-$ cells stained for CD11b and B220 showed that they were predominantly CD11b$^+$ macrophages and a very few B220$^+$ cells were present. **(D)** CNS infiltrating CD4$^+$ cells were mainly transgenic T cells stained by Vα3.2/Vβ11 TCR antibodies. **(E, F)** Splenocytes from the same mice stained by the same antibodies, in contrast, did not show any significant expression of CD25 and CD69.

In contrast, only a few cells (if any) could be recovered from the spinal cords of healthy Devic, IgHMOG, or TCRMOG mice. FACS analysis was performed to identify the cellular composition and the activation status of the spinal cord infiltrating cells. Splenocytes from the same sick Devic mice, which yielded ample numbers of mononuclear cells from CNS, were used as control.

CNS infiltrating cells were mainly $CD4^+$ T cells and $CD11b^+$ macrophages, whereas $CD8^+$ T cells and B cells were practically undetectable. These $CD4^+$ T cells showed a highly activated phenotype when measured by the surface expression of CD25 (IL-2 receptor α chain) and CD69. In contrast, splenocytes from the same mice were not activated (Figure 5.5).

5.5 Enhanced anti-MOG proliferative response in Devic mice splenocytes

To determine the ability of transgenic splenocytes from Devic mice and single transgenic control mice to respond to the recombinant extracellular domain of MOG 1-125 (rMOG) and MOG 35-55, the immunodominant peptides for I-A^b were analyzed in a proliferation assay.

Dose response proliferation assays revealed that Devic mice splenocytes responded to rMOG by far more efficiently than TCR^{MOG} or IgH^{MOG} single transgenic splenocytes. While very low antigen doses (0.02 µg/ml) were sufficient to induce a significant proliferation in Devic splenocytes, high antigen doses (20 µg/ml) were required for a comparable proliferation of naive splenocytes obtained from TCR^{MOG} mice. The proliferation of IgH^{MOG} single transgenic splenocytes was the lowest of all, even at higher antigen dose (Figure 5.6A). In contrast, MOG 35-55 induced proliferation was similar in Devic and TCR^{MOG} mice. Only a high peptide dose (20 µg/ml) caused proliferation of Devic mice and TCR^{MOG} mice splenocytes, whereas IgH^{MOG} splenocytes completely failed to respond to MOG 35-55 (Figure 5.6B).

Splenocytes contain many cell types besides the autoreactive T and B cells. To identify the molecular mechanisms and the cell types that contribute to this enhanced reactivity to rMOG protein, mixing experiments were performed with either

whole splenocytes or purified cells (>90% purity as judged by FACS staining). First, equal numbers of IgH^MOG and TCR^MOG splenocytes were combined, and a proliferation assay was performed with rMOG. This reproduced the dose response reactivity, which was similar to that of the double transgenic Devic mice. The mixing of TCR^MOG or IgH^MOG splenocytes with WT splenocytes, however, did not show enhanced proliferation (Figure 5.6C).
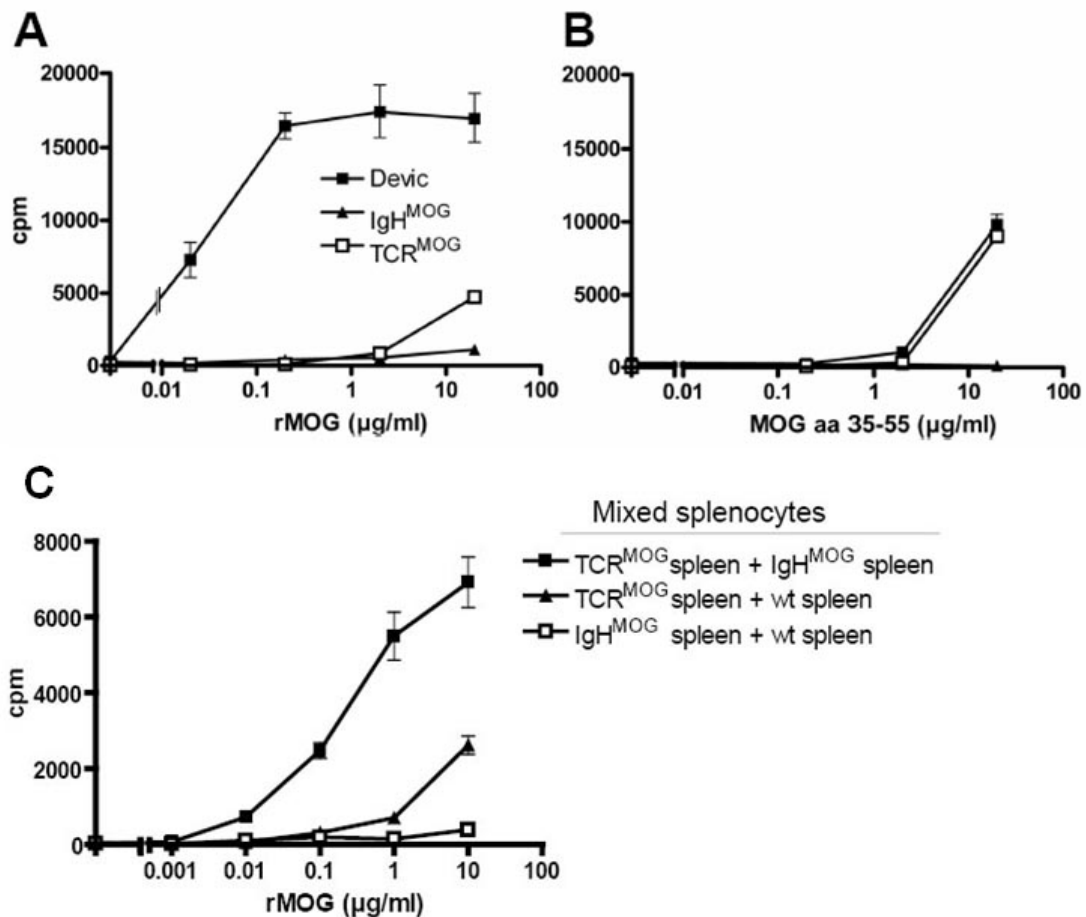
Figure 5.6

Enhanced MOG autoreactivity of Devic mice lymphocytes. **(A, B)** Dose response proliferation assay. Devic, IgH^MOG, and TCR^MOG splenocytes were incubated with increasing concentrations of rMOG **(A)** or MOG 35-55 **(B)**. **(C)** Dose response proliferation assay of mixed splenocytes. Equal numbers of IgH^MOG and TCR^MOG, TCR^MOG and WT, IgH^MOG and WT splenocytes were mixed, and a proliferation assay was performed with increasing concentrations of rMOG. Cells were cultured for 3 days and pulsed with ^{3}H-thymidine during the last 12 - 16 h. Cell-incorporated ^{3}H-thymidine, which indicates proliferation, was analyzed by measuring radioactivity in a beta counter and shown it as counts per minute (cpm). Each sample was run in triplicate; error bars indicate SEM. Shown data represent more than five independent experiments.

Second, to determine the relative contribution of MOG-reactive B and T cells, both cell types were purified from single transgenic mice and Devic mice by a negative isolation method. FACS analysis showed that the purity of the cell types was more than 90% (data not shown). Non-transgenic B and T cells were purified from TCR^{MOG} (TCR transgenic) and IgH^{MOG} (B cell transgenic), respectively. A similar synergistic proliferation in response to rMOG was observed by mixing both MOG-specific T and B cells but not by mixing non-transgenic T and B cells (Figure 5.7A).

Although enhanced proliferation was observed only when both MOG-specific B and T cells were present in the culture, it is not clear whether the role of B cells is limited to enhancing the proliferation of T cells or if both T and B cells stimulate each other to induce proliferation. To understand the mechanisms underlying this super-proliferation, TCR^{MOG} splenocytes were mixed with either irradiated or non-irradiated IgH^{MOG} splenocytes. While the mixing of non-irradiated IgH^{MOG} splenocytes reproduced the super-proliferation in response to rMOG, irradiation of IgH^{MOG} splenocytes drastically reduced the proliferation. In contrast, MOG 35-55 induced proliferation was not affected by irradiation (Figure 5.7B). This is consistent with the fact that the transgenic heavy chain of IgH^{MOG} B cells binds only the conformational epitope of MOG, but not the MOG 35-55 peptide. The observed synergistic proliferation is clearly due to the active co-operation between MOG-specific T cells and B cells, during which B cells efficiently bind and present antigen to the T cells.

To further demonstrate the active co-operation between MOG-specific B and T cells, Devic mouse splenocytes were labeled with the carboxy-fluorescein diacetate succinimidyl ester (CFSE), which emits green fluorescence when excited, and stimulated with rMOG. Cell proliferation was monitored by diluting cellular CFSE. FACS analysis of rMOG-stimulated CFSE-labeled splenocytes showed that both T and B cells proliferated equally (Figure 5.7C). The active co-operation between T and B cells was further substantiated by upregulation of the activation marker CD25 on T cells and the co-stimulatory molecule CD86 on the B cells (Figure 5.7D).
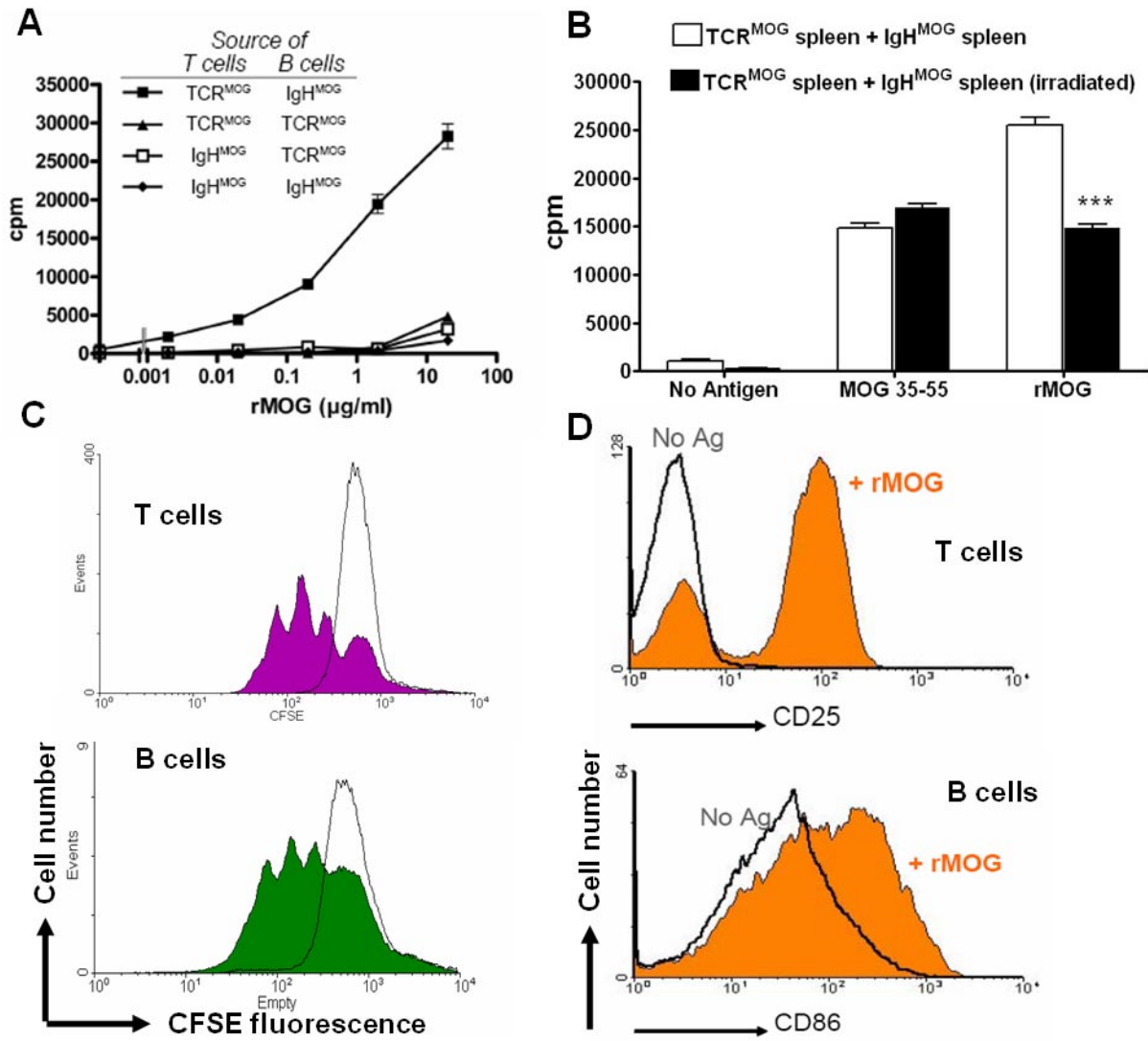
Figure 5.7

Active co-operation of MOG-specific T and B cells. **(A)** Purification and mixing of transgenic and non-transgenic CD4^{+} T and B cells. Equal numbers of highly purified CD4^{+} T cells and B cells from TCR[MOG] or from IgH[MOG] were mixed as indicated and exposed to increasing concentrations of rMOG. Proliferation was measured by the ^{3}H-thymidine incorporation assay. **(B)** TCR[MOG] splenocytes were mixed with equal numbers of either irradiated or non-irradiated IgH[MOG] splenocytes. The proliferation in response to MOG 35-55 (20 µg/ml) and rMOG (20 µg/ml) was measured by the ^{3}H-thymidine incorporation assay. **(C)** Devic mouse splenocytes were labeled with CFSE and exposed to optimal concentration of rMOG *in vitro* for 3 days. The proliferation of T and B cells (revealed by CD4 and B220 staining) was measured by diluting cellular CFSE (filled histogram) compared to no antigen control (open histogram). **(D)** FACS analysis of expression of the activation markers CD25 and CD86 by Devic mouse T and B cells, respectively, after activation with rMOG. Each sample in figures A and B was run in triplicate; error bars indicate SEM. *** - indicates statistical significance (p < 0.001).

5.6 Rapid activation and co-stimulatory expression of Devic lymphocytes *in vitro*

The enhanced reactivity of Devic lymphocytes to rMOG suggested efficient co-operation between MOG-specific T and B cells. The interaction between T and B cells is mediated by several cell surface molecules. For example, B cells present processed antigen to the CD4$^+$ T cells by MHC class II molecules. In addition, several cell surface, positive and negative co-stimulatory, molecules on the B cells interact with their respective ligands that are expressed on T cells to modulate the immune response. While positive co-stimulatory molecules such as CD80 (B7.1) and CD86 (B7.2) amplify the response, negative co-stimulatory molecules such as CTLA-4 and PD-1 dampen the reactivity to control an unwanted immune response.

Previous experiments measured the response of Devic lymphocytes to rMOG after 3 days of stimulation. To understand the kinetics of enhanced reactivity, Devic and single transgenic splenocytes were exposed to 20 µg/ml rMOG or remained without antigenic stimulus for 24 h. Expression of the activation markers CD25, CD44, and CD69, downregulation of CD62L, and expression of co-stimulatory molecule CD154 (CD40L) were measured by FACS.

CD4$^+$ T cells from Devic and TCR^{MOG} mice but not IgH^{MOG} mice rapidly upregulated CD25, CD69, and CD44 and downregulated CD62L after rMOG stimulation. The percentage of T cells of Devic mice expressing these molecules was considerably higher than T cells of TCR^{MOG} mice. In contrast, CD154 (CD40L) expression was not detectable in T cells of any mice (Figure 5.8 A & B). Stimulated Devic B cells (either B220$^+$ or CD19$^+$) upregulated CD69 and CD86, while CD80 expression was not modulated (Figure 5.8 C & D). These data demonstrate that significant numbers of Devic T cells are rapidly activated upon rMOG stimulation.

Next, the expression of co-stimulatory molecules on T and B cells was measured with or without rMOG stimulation (Figure 5.9). Large numbers of unstimulated B cells from IgH^{MOG}, TCR^{MOG}, and Devic mice expressed PDL-1 (programmed death ligand 1) and ICOSL (inducible co-stimulator ligand) constitutively. Although the percentage of B and T cells expressing PDL-1 was similar in all mice and was not altered by

rMOG stimulation, the cellular amount, measured by the mean fluorescence intensity, was significantly increased in rMOG-stimulated lymphocytes (Figure 5.10).
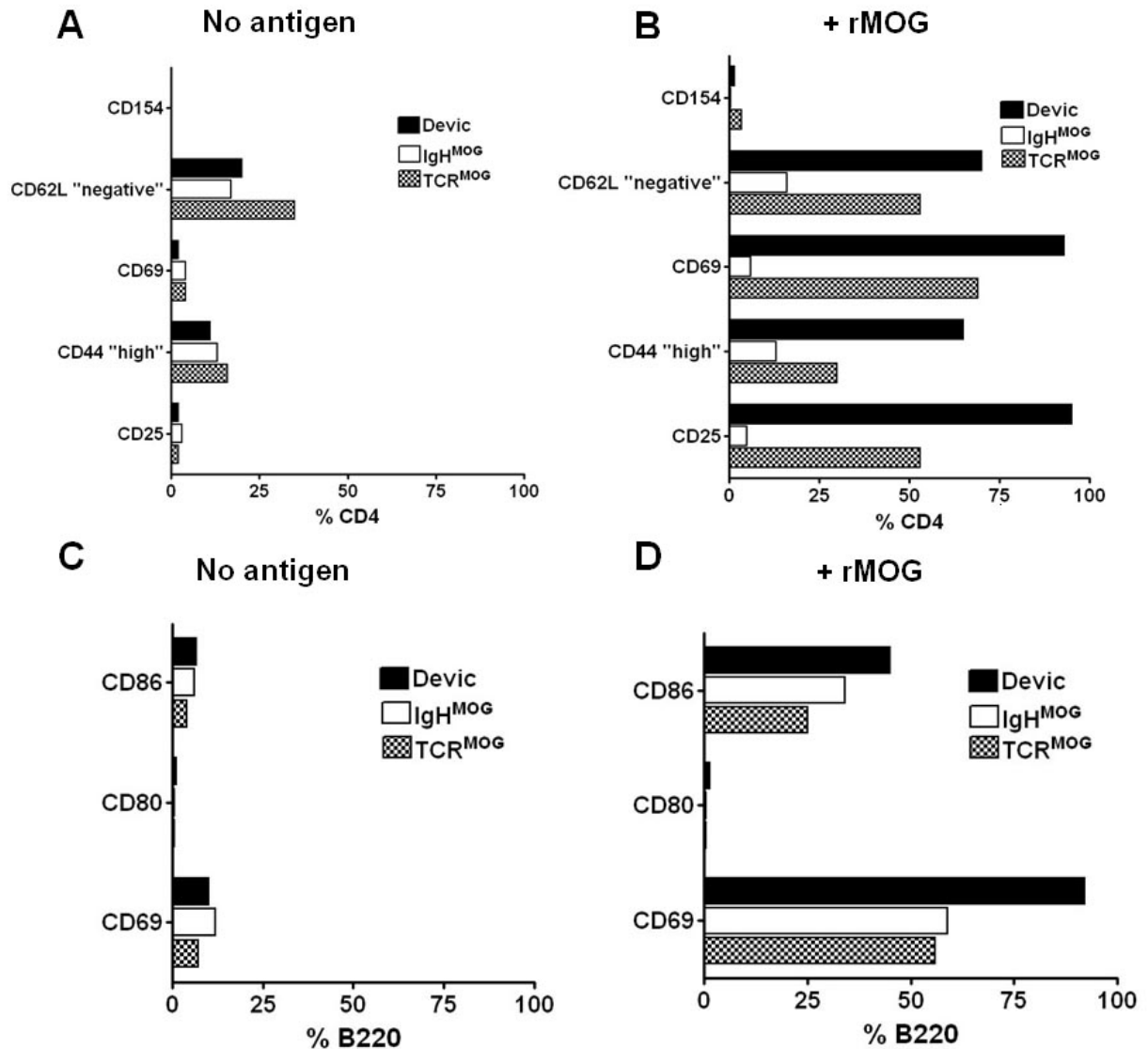
Figure 5.8

Rapid activation of Devic lymphocytes by rMOG *in vitro.* Devic, IgH[MOG] and TCR[MOG] , splenocytes were either left untreated **(A, C)** or exposed to 20 µg/ml of rMOG **(B, D)** for 24 h**.** Cells were stained with antibodies against CD154, CD62L, CD69, CD44, and CD25 and analyzed by FACSCalibur. Upregulation or downregulation (as indicated in the figure) of these molecules is shown as % of CD4^{+} T cells **(A, B)** and B220^{+} B cells **(C, D).**
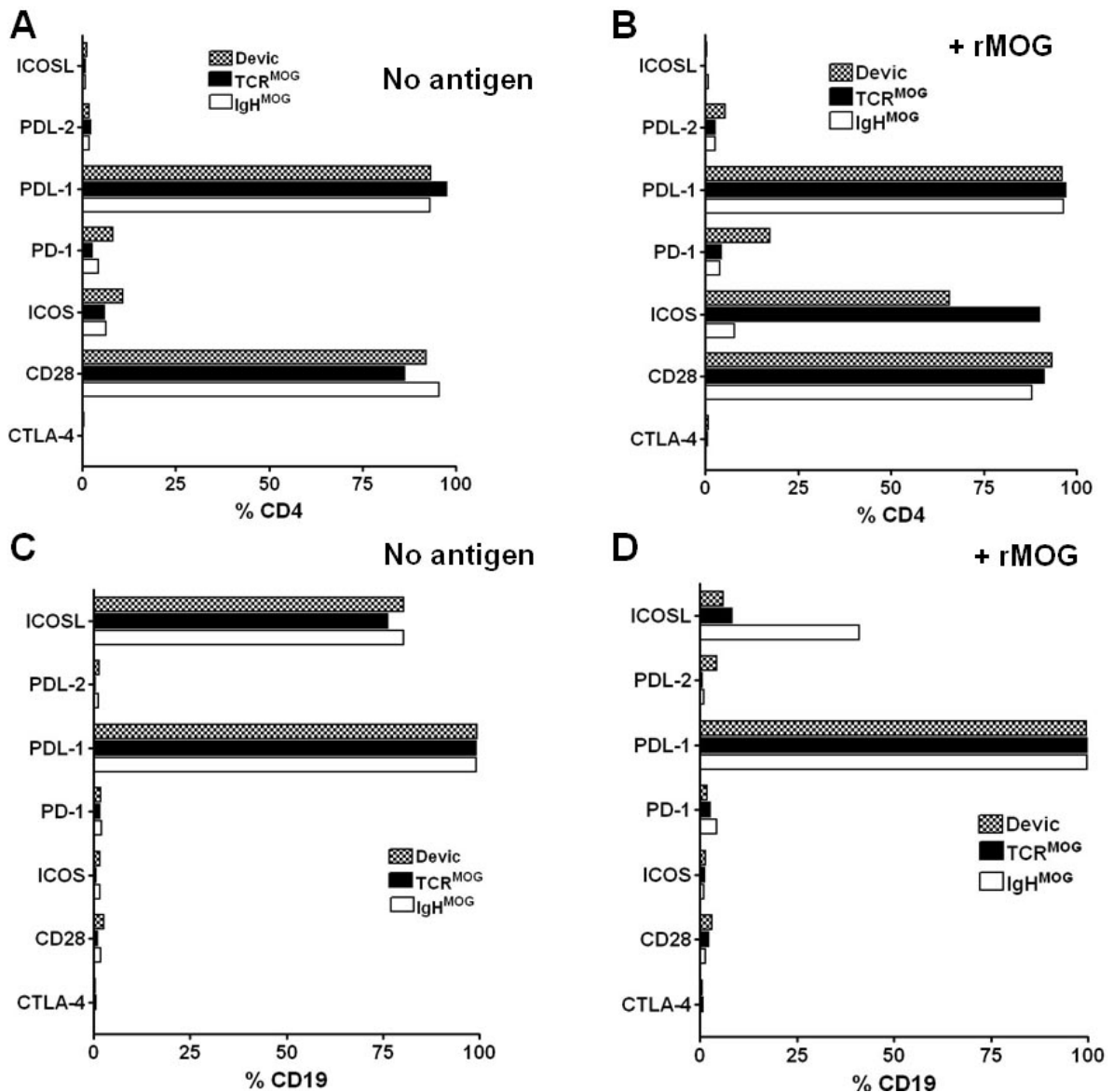
Figure 5.9

Expression of co-stimulatory molecules by transgenic lymphocytes after rMOG stimulation *in vitro*. Devic, IgH^{MOG} , and TCR^{MOG} splenocytes were either left untreated **(A, C)** or incubated with 20 μg/ml rMOG **(B, D)** for 24 h. Cells were stained with fluorochrome conjugated antibodies and analyzed by FACSCalibur. Percentages of gated CD4$^+$ T cells **(A, B)** and gated CD19$^+$ B cells **(C, D)** are shown.

The increased amount of PDL-1 on the surface of Devic T cells was similar to TCR^{MOG} T cells. In contrast, IgH^{MOG} T cells did not show a significant increase in PDL-1 surface expression. Upregulation of PDL-1 was observed on all rMOG stimulated B cells, although highest expression was detected among stimulated B cells from Devic spleen (Figure 5.10). B cells of Devic and TCR^{MOG} mice down-

regulated their constitutive ICOSL expression after treatment with rMOG, whereas about 40% of the IgH^{MOG} B cells retained ICOSL expression (Figure 5.9).
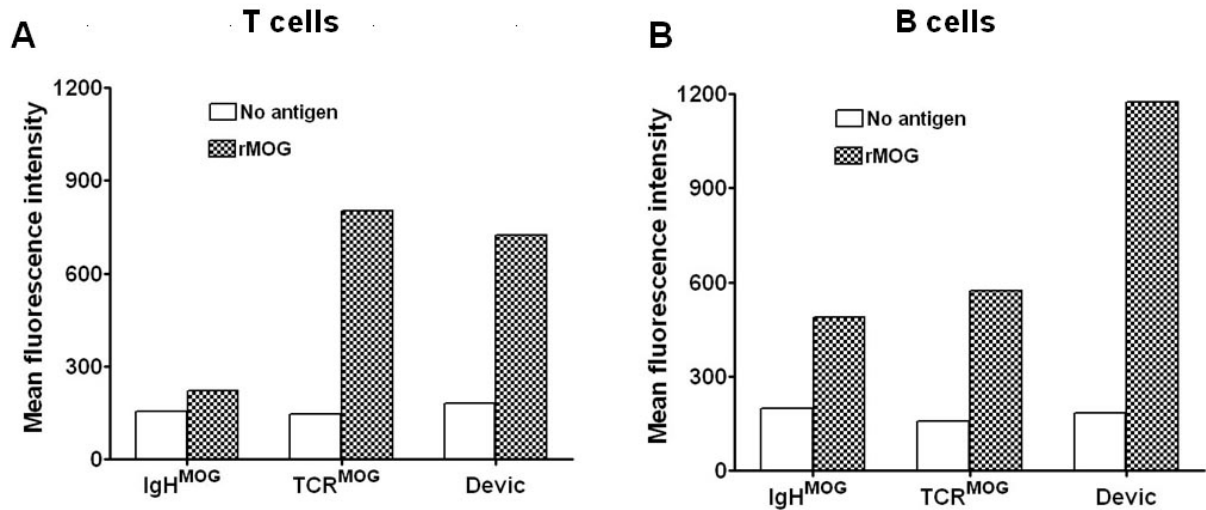
Figure 5.10

PDL-1 expression on transgenic T and B cells after *in vitro* rMOG stimulation. Devic, IgH^{MOG}, and TCR^{MOG} splenocytes were either left untreated or incubated with 20 µg/ml rMOG for 24 h. Cells were stained with fluorochrome conjugated antibodies and analyzed by FACSCalibur. PDL-1 expression measured by the mean fluorescence intensity of gated CD4^{+} T cells **(A)** and gated CD19^{+} B cells **(B)** are shown.

High frequencies of T cells from all mice expressed CD28 and PDL-1, independently of whether they were activated with rMOG or remained without a stimulus. It is of interest that a large proportion of T cells from TCR^{MOG} and Devic but not IgH^{MOG} spleens expressed the ICOS molecule when stimulated with rMOG. In contrast, PD-1 expression was detectable only in a negligible fraction of Devic T cells. Of note, ICOSL, PDL-2, and CTLA-4 on T cells and PDL-2, PD-1, ICOS, CD28, and CTLA-4 on B cells were not detected before or after rMOG activation (Figure 5.9).

## 5.7 Devic lymphocytes produce Th1 cytokines *in vitro*

The effector function of lymphocytes depends on the cytokines produced by them. To determine which cytokines are secreted by the lymphocytes, splenocytes from single transgenic mice and Devic mice were cultured in the presence of either MOG

35-55 or rMOG. Supernatants from stimulated cultures were collected 3 days after stimulation, and cytokines were measured by a sandwich ELISA.

Devic splenocytes secreted predominantly Th1 cytokines in a dose-dependent manner (Figure 5.11). Like the enhanced proliferation, the secretion of significant amounts of cytokines was noted in Devic splenocytes stimulated with even minute amounts of rMOG; in contrast, TCR^{MOG} and IgH^{MOG} splenocytes required much higher concentrations of rMOG. The Th1 cytokines IFNγ and IL-2 were prominent in the supernatants, whereas Th2 cytokine production was low. IL-4 was only marginally detectable, and low levels of IL-5 were evident only in Devic splenocytes stimulated with rMOG. In contrast, MOG 35-55 stimulation, much like proliferation, did not induce cytokine secretion at enhanced kinetics as observed with rMOG stimulation (Figure 5.11).

To determine which cell type(s) produce cytokines in response to rMOG *in vitro*, Devic splenocytes were labeled with CFSE, stimulated with rMOG, and intracellular cytokine staining was performed (Figure 5.12). T and B cells were distinguished by co-staining with anti-CD4 and anti-B220 antibodies, respectively. Stimulated but not unstimulated CD4$^+$ T cells from Devic mice produced TNFα and IFNγ, whereas B cells from the same cultures did not produce these cytokines. TNFα producing Devic T cells appeared as early as 24 h (day 1) after stimulation. Their numbers were gradually reduced by days 2 and 3 (Figure 5.12 A). The frequency of TNFα producing Devic T cells showed a clear dose-dependent response to rMOG (Figure 5.12 D).

In contrast, TCR^{MOG} single-transgenic T cells did not produce TNFα (Figure 5.12 D). Devic T cells also expressed IFN-γ when stimulated with rMOG. However, the kinetics of IFN-γ production was significantly slower when compared to TNFα production. Moreover, the frequency of IFN-γ^+ T cells was relatively low (Figure 5.12 C). IgH^{MOG} T cells did not produce any of the tested cytokines (Figure 5.12).
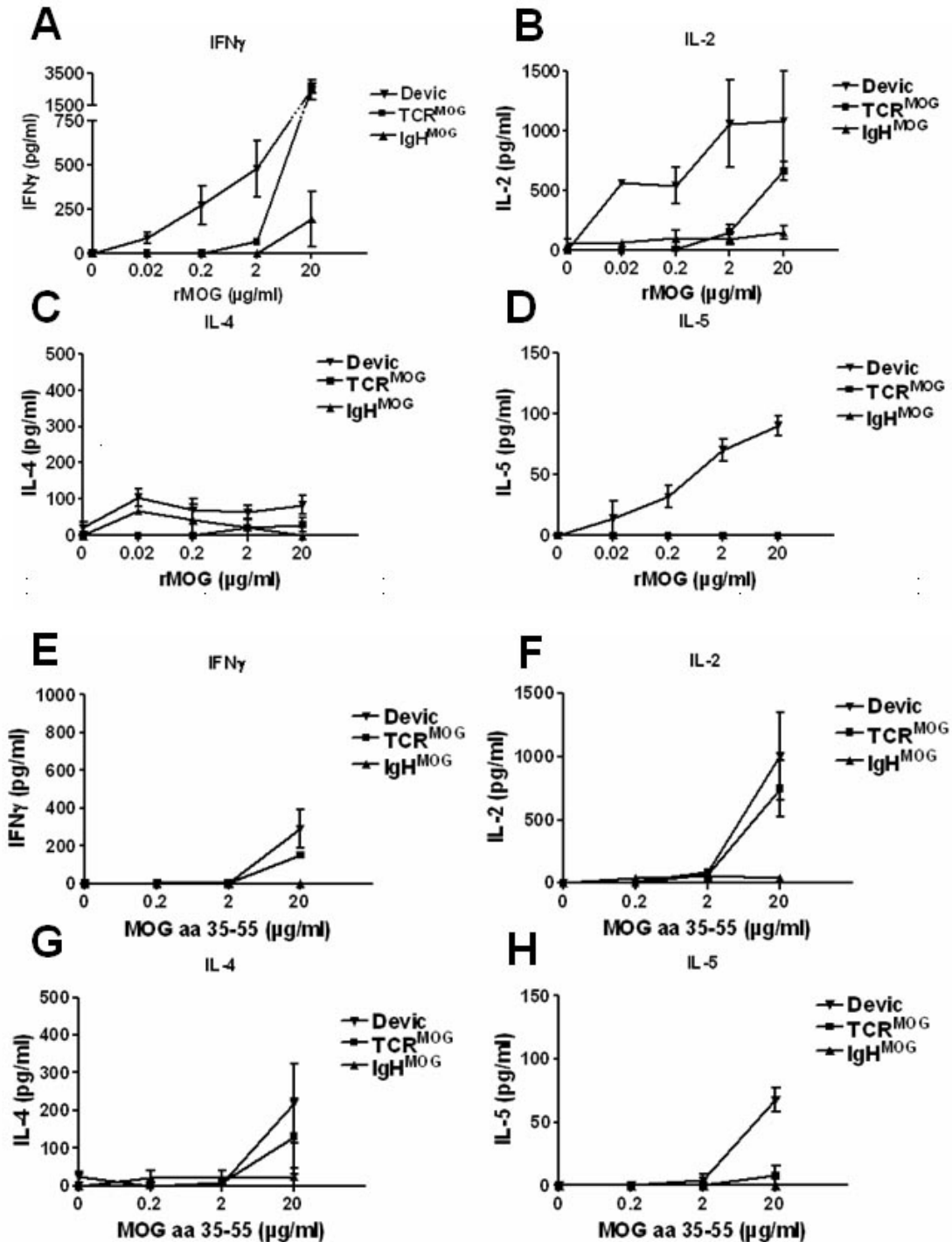
Figure 5.11

Enhanced cytokine secretion by Devic mice lymphocytes. Devic mice, IgH^{MOG}, and TCR^{MOG} splenocytes were incubated with increasing concentrations of rMOG **(A-D)** or MOG 35-55 **(E-H)** for 3 days. Cytokines released from stimulated cultures were measured by sandwich ELISA. Absolute amounts of IFNγ **(A, E)**, IL-2 **(B, F)**, IL-4 **(C, G)** and IL-5 **(D, H)** were calculated from standard curve constructed using recombinant cytokine standard. Representative results of a total of seven Devic, three TCR^{MOG}, and three IgH^{MOG} animals analyzed during three independent experiments. Error bars indicate the SEM.
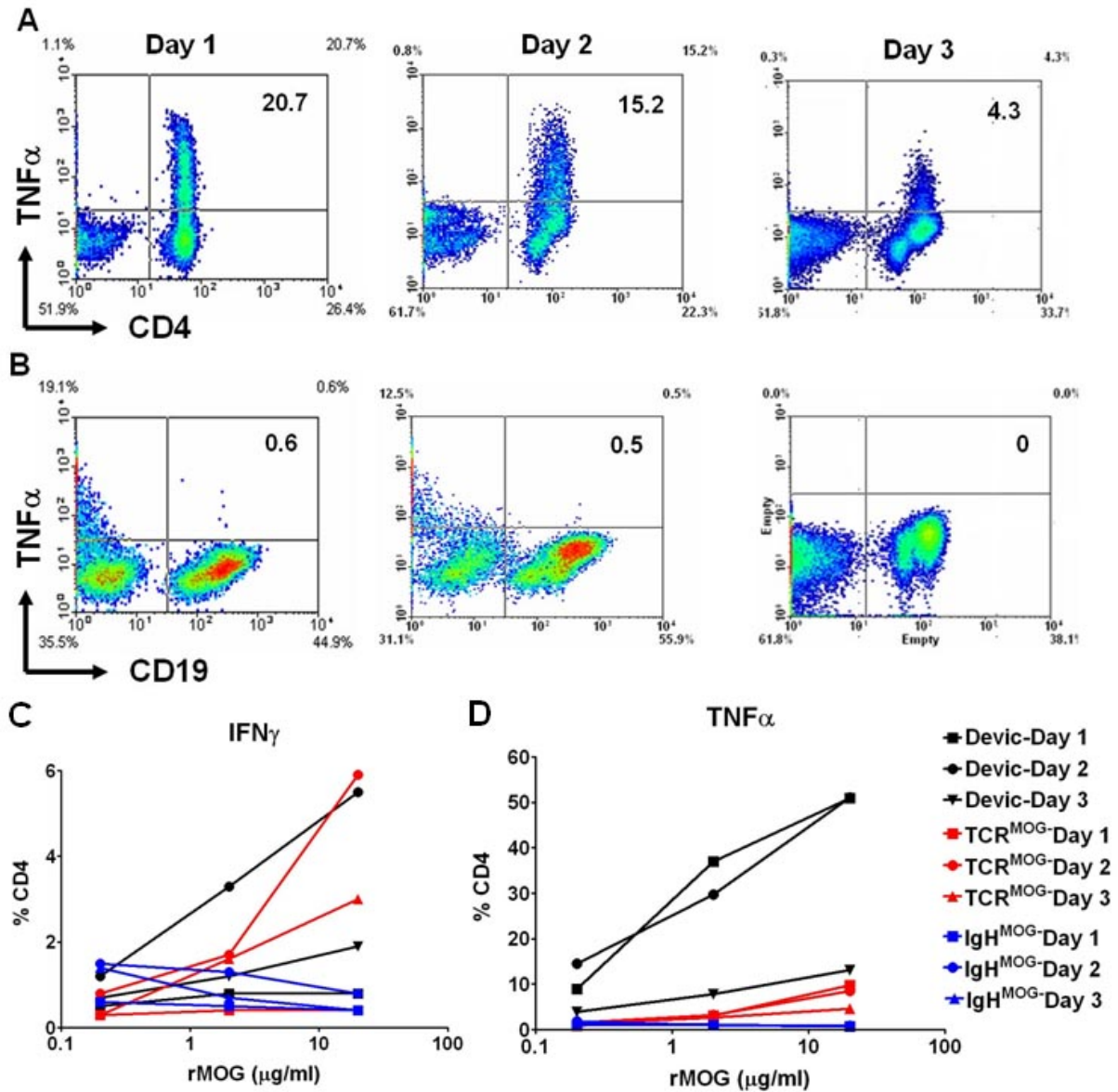
Figure 5.12
Relative contribution of Th1 cytokine secretion by T and B cells. **(A, B)** show the intracellular TNFα
FACS staining of rMOG stimulated (20 µg/ml) Devic mouse splenocytes. Brefeldin A was added to
stimulated cells for 6 h before FACS staining on day 1 (left panel), day 2 (middle panel) and day 3
(right panel) and stained with antibodies against CD4, CD19, and TNF as described in the Methods.
(C, D) Devic, TCR^{MOG} and IgH^{MOG} splenocytes were stimulated *in vitro* with rMOG as indicated, and
the frequency of TNFα and IFNγ secreting CD4$^+$ T cells was quantified on day 1, 2, and 3 after
stimulation. Values are expressed as percentage of gated CD4$^+$ T cells.

5.8 *In vivo* antigen presentation in Devic mice

To address the question as to whether the efficient antigen presentation by MOG-specific B cells observed *in vitro* is also applicable *in vivo*, naive rMOG-incubated IgH^{MOG} splenocytes were adoptively transferred to TCR^{MOG} mice.
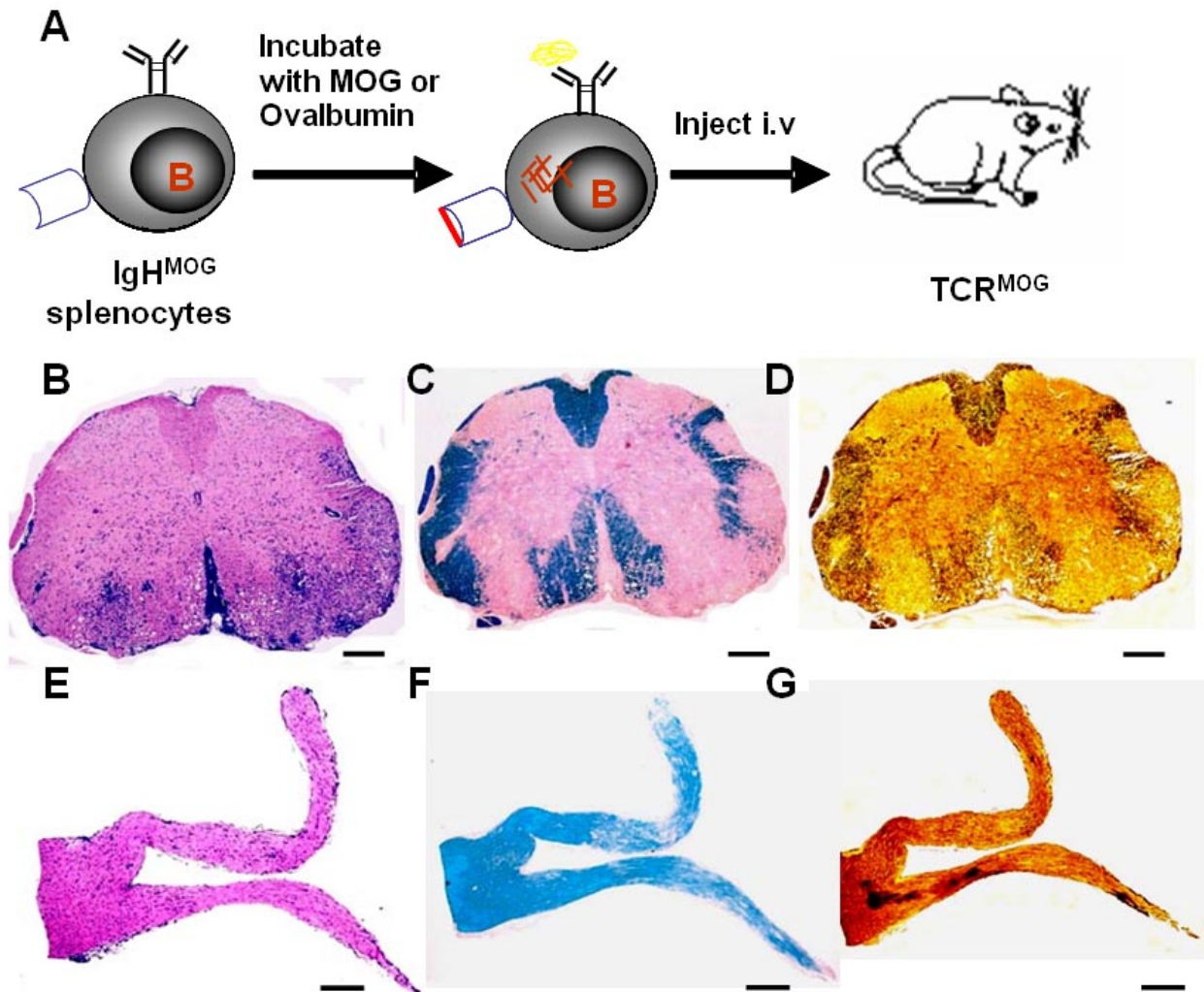
Figure 5.13

MOG-incubated transgenic B cells transfer EAE. **(A)** Depicts the strategy to evaluate the antigen presentation efficiency of MOG-specific B cells *in vivo*. IgH^{MOG} spleen cells were incubated with MOG or ovalbumin for 10 min and transferred into TCR^{MOG} mice. **(B-D)** Spinal cord with large inflammatory demyelinating lesions mainly in the anterior and lateral columns. **(B)** H&E showing inflammation; **(C)** Luxol fast blue showing demyelination; **(D)** Bielschowsky silver impregnation showing axonal loss; Scale bar of B-D = 1mm **(E-G)** Serial sections through optic nerve and chiasm with inflammatory demyelinating lesions. **(E)** H&E; **(F)** Luxol fast blue; **(G)** Bielschowsky silver impregnation. Scale bar of E-F = 1mm. The histological analysis was performed by Prof. Hans Lassmann, University of Vienna, Austria.

Brief incubation (10 min) with rMOG protein might facilitate antigen uptake, if any, by the transgenic B cells via their surface Ig. Subsequently, the cells were washed extensively to remove unbound protein and transferred via the tail vein into TCR^{MOG} mice. As a control, ovalbumin-incubated IgH^{MOG} splenocytes were transferred into TCR^{MOG} mice at the same time. Some animals additionally received LPS (50 µg/mouse; i.p.), which is known to activate B cells (Figure 5.13). The transfer of MOG-incubated splenocytes, but not ovalbumin-incubated splenocytes, induced EAE in about 20% of the mice. Further, activation of B cells by LPS did not significantly alter the incidence of EAE (Table 5.2). Histological examination of the sick mice showed the presence of mononuclear cells in the spinal cord and optic nerve. This was similar to the Devic mice with spontaneous EAE. In addition, they exhibited a loss of myelin and moderate axonal damage (Figure 5.13).

Table 5.2
Incidence of EAE following adoptive transfer of MOG or ovalbumin incubated IgH^{MOG} splenocytes.

Treatment	n	Incidence (%)
MOG incubated IgH^{MOG} splenocytes	15	3/15 (20%)
MOG incubated IgH^{MOG} splenocytes + LPS	11	3/11 (27.3%)
Ova incubated IgH^{MOG} splenocytes	6	0/6 (0%)

IgH^{MOG} splenocytes were incubated with rMOG or ovalbumin (1 µg/1 $\times$ 10^6 cells) for 10 min at 37°C and washed extensively. 20 $\times$ 10^6 cells were transferred i.v. into TCR^{MOG} mice and observed for clinical signs of EAE for 30 days.

5.9 Anti-MOG autoantibodies and their influence in Devic mice

Autoreactive B cells differentiate with the help of T cells to produce self-reactive antibodies, which recognize self-antigens and induce tissue damage. To analyze the changes in humoral immunity and the ability of Devic mice to secrete self-reactive antibodies, total serum immunoglobulins (Ig), and MOG-specific Ig were measured by ELISA. Serum from Devic mice, control single transgenic littermates, IgH^{MOG} X OT-II double transgenic mice, and Devic X MOG KO mice were used.

Devic mice did not differ from their single transgenic parental IgH^{MOG} and TCR^{MOG} mice in the absolute amounts of total serum IgM, IgG1 or IgG2b levels. However, there was a slight reduction in the IgG3 levels and an increase in the IgG2a amounts (Figure 5.14). This indicates that Devic mice have no major abnormalities in their humoral immunity.
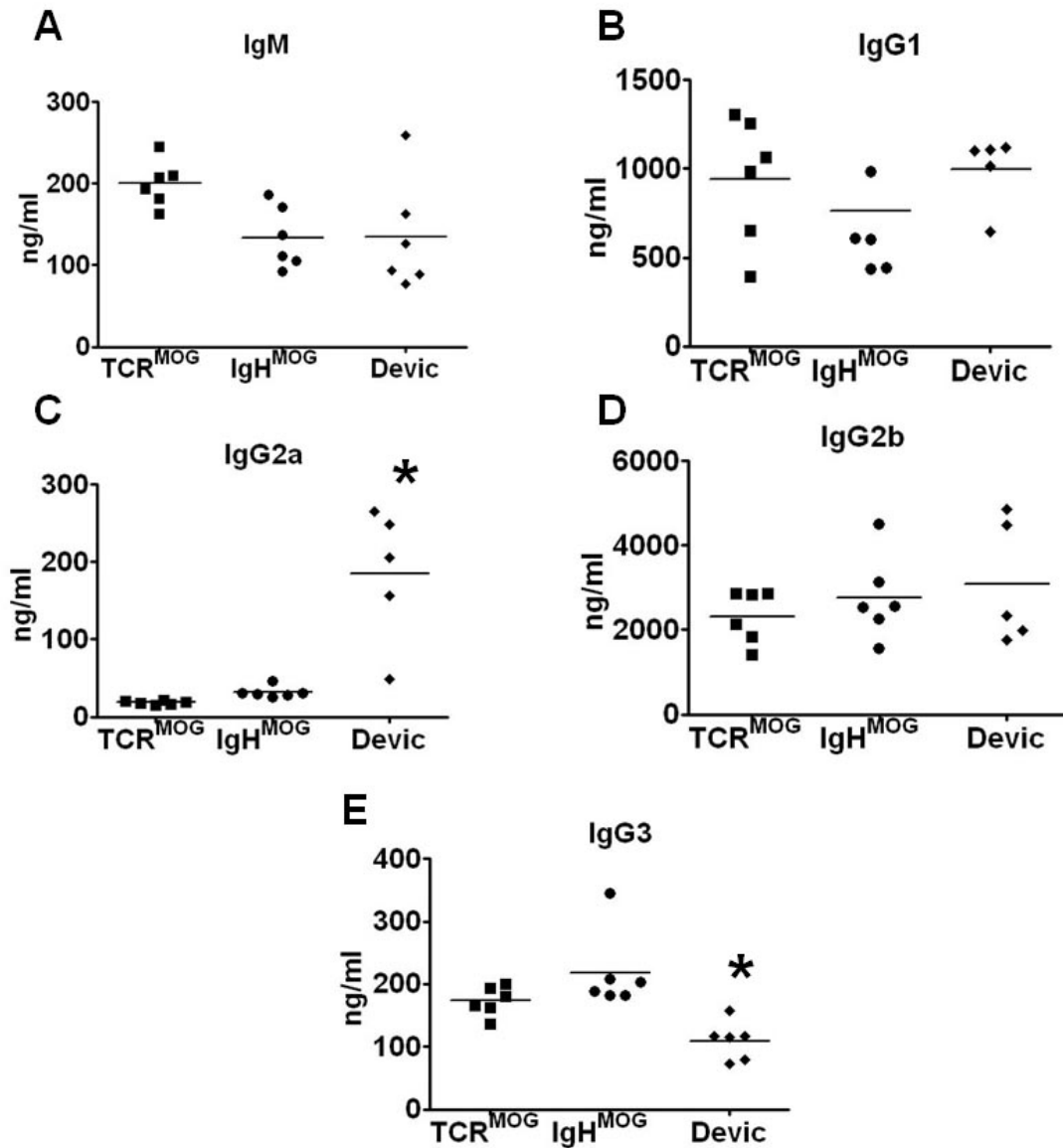
Figure 5.14

Total serum Ig levels. 1:100 diluted serum, collected by retro-orbital puncture, from Devic and single transgenic littermates was measured for the presence of IgM **(A)**, IgG1 **(B)**, IgG2a **(C)**, IgG2b **(D)**, and IgG3 **(E)** by an isotype specific sandwich ELISA. Purified antibodies were used as standard to quantify the absolute amounts. Mean values are indicated for each animal group (n = 5 – 6). * indicates statistical significance (p < 0.01).

Subsequently, MOG-specific antibodies were measured from the serum of these transgenic mice. Strikingly, Devic mice differed from single-transgenic IgH[MOG] mice in the amounts of MOG-specific IgG1 serum autoantibodies. While MOG-specific IgM antibodies were readily detectable in the serum of IgH[MOG] animals, MOG-specific IgG1 antibodies remained at low serum titers in these mice. In contrast, Devic mice produced high serum levels of anti-MOG antibodies of both IgM and IgG1 isotypes. MOG-specific antibodies could not be detected in naive TCR[MOG] mice. However, anti-MOG IgG1 antibodies were observed irrespective of the clinical status of the Devic mice. Interestingly, Devic mice deficient in MOG (i.e. triple-transgenic IgH[MOG] x TCR[MOG] x MOG$^{-/-}$ mice) also had elevated serum levels of MOG-specific IgG1 antibodies. This indicates that a spontaneous isotype switching of MOG-specific antibodies from IgM to IgG1 isotopes occurred independently of MOG antigen.
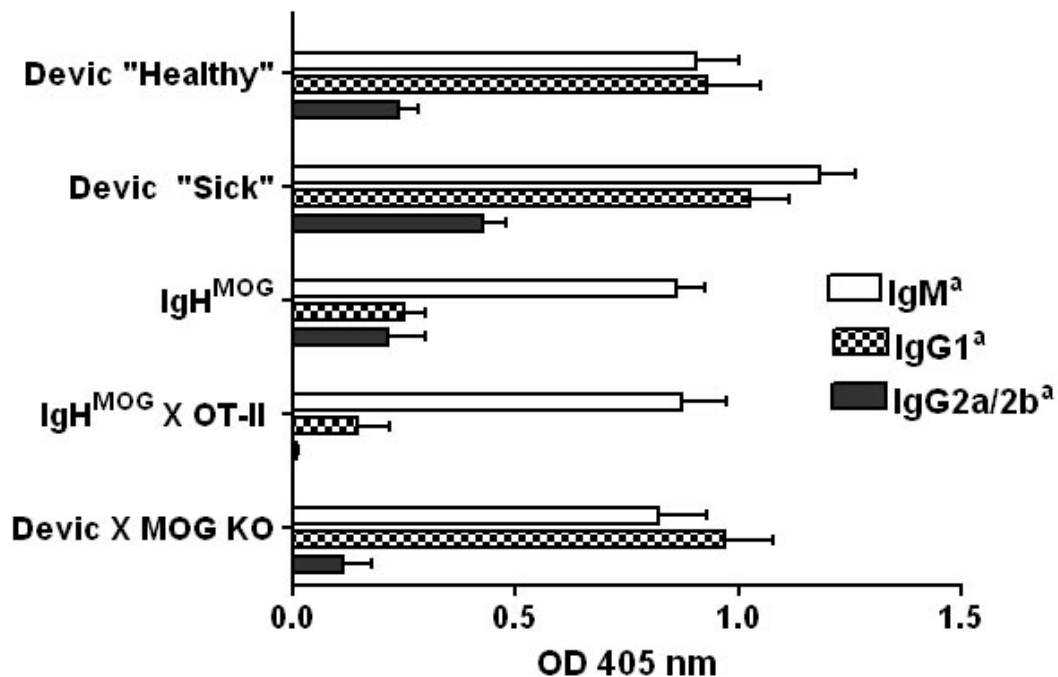
Figure 5.15

MOG-specific serum autoantibodies in transgenic mice. Sera obtained from healthy (n = 18) and sick (n = 24) Devic, healthy IgH[MOG] (n = 16), healthy OT-II (TCR[OVA]) x IgH[MOG] (n = 7), and healthy Devic x MOG KO (n = 3) mice were diluted to 1:100 and incubated with plates coated with rMOG. Bound MOG-specific Ig was detected by allotype/isotype specific antibodies recognizing IgM[a], IgG1[a], or IgG2a/b[a]. Values are expressed as the mean absorbance (at OD 405 nm) measured during more than five independent experiments. Error bars indicate the SEM.

This spontaneous isotype switching was observed only in Devic mice, whereas double transgenic IgH^{MOG} x OT-II, which contain non-self antigen ovalbumin-specific TCR together with IgH^{MOG}, did not have high amounts of MOG-specific IgG1. However, these mice had similar titers of MOG-specific IgM autoantibodies (Figure 5.15).

Antibody secreting cells (ASCs) can be identified by an ELISPOT assay. To understand the anatomical location where the MOG-specific B cells undergo spontaneous isotype switching, bone marrow (BM) cells and splenocytes, in which isotype switching presumably happens, were plated onto rMOG-coated plates for either a brief period (5 h) or overnight (12-16 h). Subsequently, bound antibody secreting cells were detected by isotype-specific antibody. The IgM ASCs were present in the BM as well as in splenocytes, but IgG1 ASCs were neither detectable among splenocytes nor among bone marrow cells obtained from either healthy or sick Devic mice (Figure 5.16). This suggests that isotype switching most likely occurred outside the BM and spleen at an as yet unidentified location.
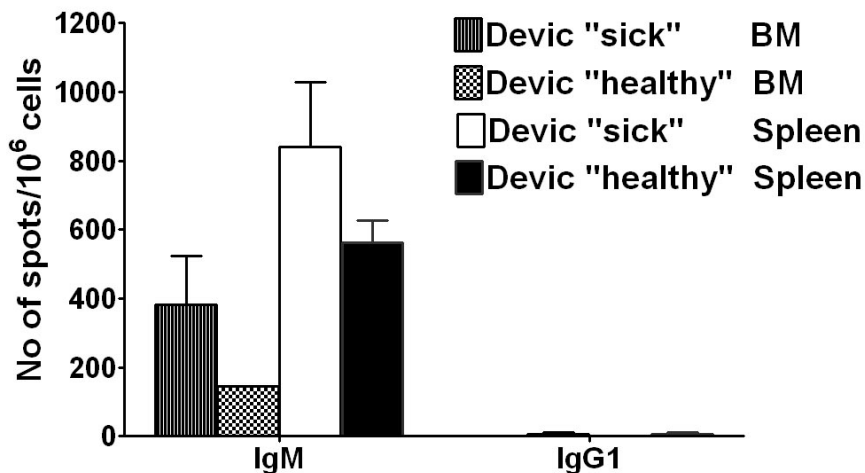
Figure 5.16

Anti-MOG autoantibody-secreting cells in transgenic mice. Serially diluted bone marrow cells and splenocytes were seeded onto the rMOG-coated plates and after 5 h bound anti-MOG antibody-secreting cells were visualized by the isotype/allotype specific secondary antibody with BCIP/NBT as substrate. The number of spots, indicating the antibody-secreting cells, was counted (dilution gives clearly countable spots) by the Carl Zeiss ELISPOT reader. Data are expressed as the number of spots per million cells + SEM. The data is representative of two independent experiments.

IgH^{MOG} B cells express the heavy chain of the anti-MOG antibody 8.18-C5 which is paired with the endogenous light chains. FACS analysis showed that about 30% of B cells in these mice bind MOG. To analyze the MOG-binding activity and possibly to isolate MOG binding IgG1 B cells, a significant number of hybridomas (see table 5.3) were produced from splenocytes of healthy IgH^{MOG} and healthy or sick Devic mice by standard techniques. Hybridoma supernatants were screened for the presence of MOG-binding Ig and their isotype.

Table 5.3

B cell hybridomas from splenocytes of transgenic mice

Animal No	Animal group	Score	Master hybridomas			Sub clones		
			n	IgM^a/ MOG binding	IgG1^a/ MOG binding	n	IgM^a/ MOG binding	IgG1^a/ MOG binding
#3277	Devic mouse	2.5	14	5/5	0/0	34	17/17	0/0
#3023	Devic mouse	0	13	2/2	0/0	64	3/3	0/0
#3756	Devic mouse	3.5	118	118/118	0/0	ND	ND	ND
#3769	Devic mouse	2.5	22	11/11	0/0	ND	ND	ND
#3279	IgH^{MOG}	0	13	9/9	0/0	ND	ND	ND
#3395	IgH^{MOG}	0	6	1/1	0/0	3	0/0	ND
#3214	IgH^{MOG}	0	3	1/1	0/0	30	24/24	ND
#3278	IgH^{MOG}	0	168	168/168	0/0	ND	ND	ND

Devic and IgH^{MOG} mice splenocytes were stimulated with LPS for 2 days. After washing, the activated B cells were fused with non Ig secreting Sp2/0 cells using polyethylene glycol and were plated on 96-well plates. Growing clones were expanded, and supernatants were screened for the presence of MOG-binding antibodies of IgM or IgG1 isotype by ELISA. Some master hybridomas were cloned by single cell sorting, were expanded, and supernatants were assayed for the MOG-binding antibodies by ELISA. ND, not determined

Fusion of LPS-activated IgH^{MOG} or Devic splenocytes with the non-Ig producing hybridoma cell line Sp2/0 yielded several antibody-producing hybridomas. Surprisingly, the screening of hybridomas that contained more than one antibody-

secreting cell (master hybridoma) revealed that all of them were of the IgM isotype and able to bind MOG. In view of the fact that only 30% of the transgenic B cells bind MOG in FACS assays, the ability of all the generated hybridomas to bind MOG is contradictory. In addition, no single IgG1- secreting hybridoma was found. Some master hybridomas were sub-cloned by single cell sorting. Analysis of the sub-clones showed that all of them also bound MOG and they were of the IgM isotype (Table 5.3). These data point out that IgG1 isotype switching must happen outside the spleen and/or at low frequency.

Isotype switching is a highly co-ordinated event that requires the interaction of T cells and B cells and is facilitated by certain cytokines. Furthermore, the interaction of constitutively expressed CD40 on B cells and CD40L (CD154) expressed on activated T cells leads to a pronounced expansion and differentiation of B cells into Ig- secreting plasma cells. It has been reported that the blockade of the interaction of CD40 – CD40L prevents isotype switching (Howard et al., 1999).

Initially, the effect of MR1 (anti-mouse CD40L) antibody on the rMOG-induced proliferation of Devic splenocytes was measured by the thymidine incorporation assay. It was observed that the blockade of CD40L significantly reduced the *in vitro* proliferation of Devic splenocytes (Figure 5.17 A). However, *in vivo* administration of the anti-CD40L antibody to young Devic and IgH^{MOG} mice (3 – 4-wk-old) did not prevent a spontaneous isotype switching from MOG-specific IgM to IgG1. The levels of MOG-specific antibodies were comparable in MR1 antibody- and PBS-treated Devic mice. MOG-specific IgM antibody levels were unaffected in IgH^{MOG} or in Devic mice after CD40L blockade (Figure 5.17 B).
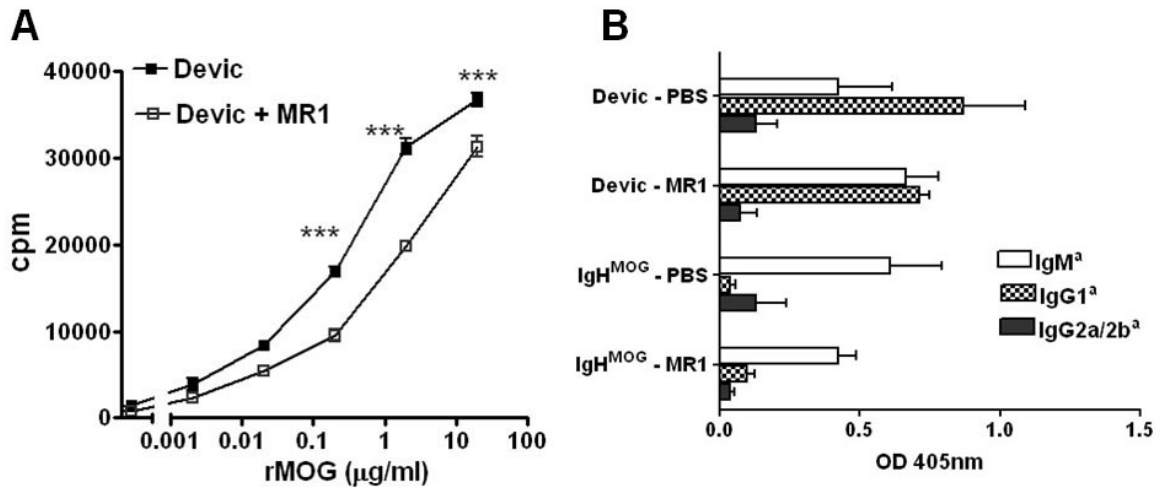
Figure 5.17

Effect of CD40L blockade on *in vitro* proliferation and *in vivo* isotype switching. **(A)** Dose response proliferation of Devic splenocytes to rMOG with or without the presence of 10 µg/ml MR1 (anti-mouse CD40L). Data shown as mean cpm measured by ^{3}H-thymidine incorporation ± SEM measured from triplicates. *** indicates statistically significant (p < 0.01). **(B)** Serum MOG-specific antibody levels of PBS or MR1 antibody-treated IgH^{MOG} and Devic mice (three mice per group). 1:100 diluted serum samples were incubated with MOG-coated plates, and bound Ig was detected by isotype/allotype specific antibody. Values are expressed as mean absorbance at 405 nm + SEM.

Table 5.4

Incidence of spontaneous EAE after *in vivo* CD40L blockade

Animal group	Treatment	n	Incidence (%)
IgH^{MOG}	PBS	4	0/4 (0%)
IgH^{MOG}	MR1	4	0/4 (0%)
Devic mice	PBS	2	2/2 (100%)
Devic mice	MR1	2	1/2 (50%)

500 µg MR1 (anti-CD40L) antibody were injected into young (3 - 4 wk-old) Devic and IgH^{MOG} mice on days 0, 3, 6, and the incidence of spontaneous EAE was monitored for 60 days.

CD40L blockade also did not prevent spontaneous EAE in Devic mice. MR1 antibody treatment did not induce EAE in single transgenic IgH^{MOG} mice (Table 5.4). Spleen cells from these antibody-treated mice were isolated after 2 months and evaluated for the proliferation in response to rMOG. Surprisingly, the MR1-antibody treated mice splenocytes proliferated more strongly than PBS-treated mice (Figure

5.18). This paradoxical *in vivo* effect when compared to the inhibition of *in vitro* proliferation by the MR1 antibody may be due to the multiple effects of CD40L blockade *in vivo*.
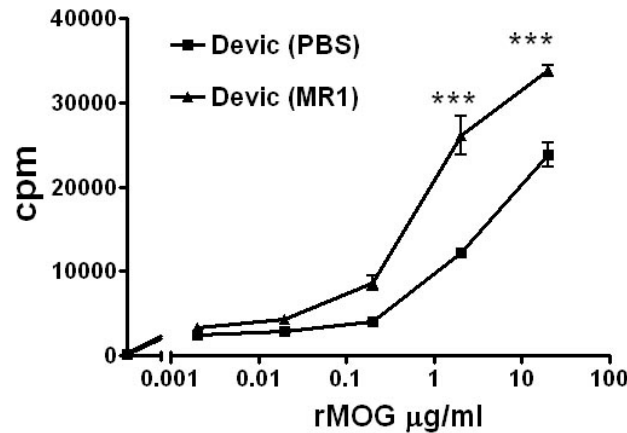
Figure 5.18

Effect of *in vivo* CD40L blockade on proliferation. 500 µg MR1 (anti-CD40L) antibody were injected into young (3 - 4 wk-old) Devic and IgH^{MOG} mice on days 0, 3, 6, and splenocytes were isolated after the mice developed spontaneous EAE (~2 months). Splenocytes were exposed to increasing concentrations of rMOG, and proliferation was measured by the ^{3}H-thymidine incorporation assay. Shown as mean cpm ± SEM measured from triplicate samples.

5.10 Activation status of lymphocytes in Devic mice

To understand which peripheral changes lead to the development of spontaneous EAE, a FACS analysis was performed on the splenocytes obtained from Devic mice and single transgenic control mice.

Healthy Devic mice and single transgenic mice did not differ in the absolute numbers of their splenocytes. There was a slight reduction in the total numbers of splenocytes from sick Devic mice. Splenocytes were stained with fluorochrome-conjugated antibodies against various cell surface markers to further clarify their cellular composition. The percentage of the B220^{+} or CD19^{+} cells, CD4,$^{+}$ and CD3^{+} T cells was similar in all groups, whereas only a few CD8^{+} T cells were present in Devic and TCR^{MOG} mice when compared to IgH^{MOG} mice (Table 5.5).

Table 5.5

Total cell numbers and composition of splenocytes from Devic and single transgenic mice.

Animal group	Splenocytes (x 10^6 cells)*	CD19$^\pm$/B220$^\pm$ (%)§	CD3$^\pm$ (%)§	CD4$^\pm$ (%)§	CD8$^\pm$ (%)§
Devic mice *Healthy*	86.6 ± 45.4	32.2 ± 12.6	45.2 ± 3.1	44.0 ± 3.0	0.9 ± 0.2
Devic mice *Sick*	52.8 ± 24.8	26.9 ± 12.6	39.0 ± 10.2	31.6 ± 11.3	2. 7 ± 1.4
TCR^{MOG}	97.5 ± 25.6	36.0 ± 18.0	36.4 ± 11.0	29.1 ± 10.8	3.7 ± 2.4
IgH^{MOG}	60.4 ± 15.2	34.4 ± 10.5	40.0 ± 5.1	23.5 ± 1.3	15.9 ± 3.7

* The amounts of total splenocytes ± SD. Number of animals analyzed: Devic healthy, n=14; Devic sick, n = 15; TCR^{MOG}, n = 14; IgH^{MOG}, n = 13. § indicates the percentage of the indicated cell type among live-gated splenocytes ± standard deviation. Number of animals analyzed: Devic healthy, n=3; Devic sick, n = 12; TCR^{MOG}, n = 7; IgH^{MOG}, n = 7.

Naive lymphocytes, which normally do not cross the blood-brain barrier, might enter the CNS after activation in peripheral lymphoid organs. It is well documented that activated lymphocytes express several distinct surface markers. To identify the activation status of the T and B cells, splenocytes were stained with several surface markers. It was found that B cells obtained either from healthy IgH^{MOG} or Devic mice expressed comparable amounts of CD80, CD86, and MHC class II (Figure 5.19). Likewise, B cells from sick Devic mice showed very similar levels of surface expression of these markers, indicating that their peripheral B cells were not strongly activated.
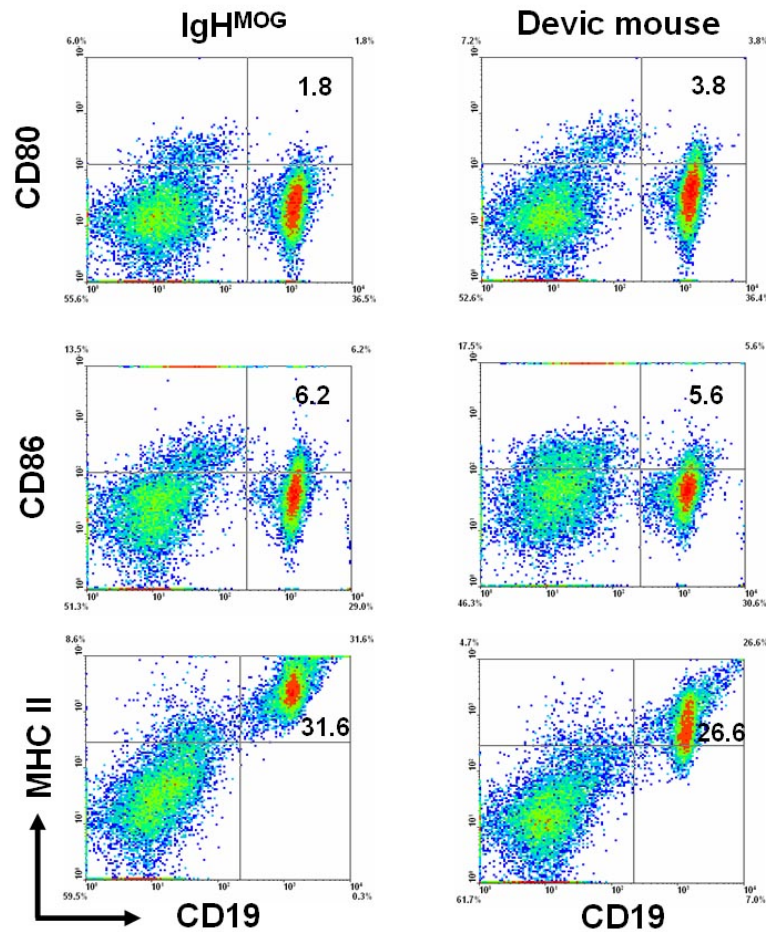
Figure 5.19

The expression of activation markers in B cells of transgenic mice. RBC-depleted splenocytes from IgH^{MOG} and Devic mice were stained with fluorochrome-conjugated antibodies against CD80, CD86, and MHC class II and CD19. Samples were acquired in FACSCalibur and analyzed by WinMDI software. Numbers in quadrants refer to the percentage of the gated-cell population.

IgH^{MOG} transgenic B cells efficiently bind MOG via their cell surface IgM. To test whether the enhanced proliferation and cytokine secretion are due to an increase in the capacity to bind MOG antigen by transgenic B cells, splenocytes from IgH^{MOG} and Devic mice were incubated with labeled rMOG protein and analyzed by FACS. About 20 - 30% of the single-transgenic IgH^{MOG} B cells were able to bind MOG through their surface IgM. Devic mice also showed similar MOG binding, quantitatively and qualitatively, irrespective of the clinical status of the animals. Moreover, the number of B cells expressing the transgenic heavy chain (IgM^a allotype) was similar in Devic and IgH^{MOG} mice, and there was no change in the expression of the endogenous heavy chain (IgM^b allotype; Figure 5.20).
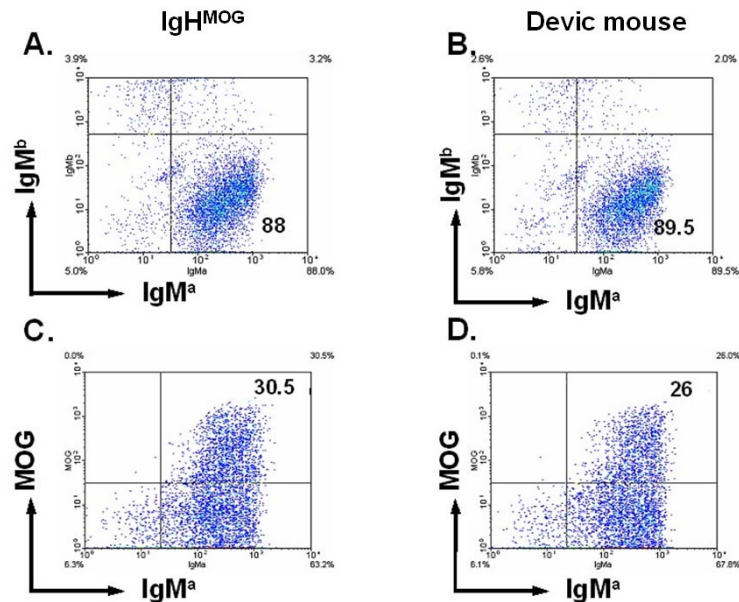
Figure 5.20

MOG binding by transgenic B cells from Devic mice and single transgenic IgH^MOG mice. Splenocytes from Devic mice and IgH^MOG mice were stained with antibodies against IgM^a (transgenic allotype), IgM^b (wild-type allotype), B220, and biotinylated rMOG. Streptavidin-APC was used to develop biotin conjugate. Results are shown as B220 gated cells. **(A)** and **(B)** refer to the expression of the transgenic heavy chain in B cells of IgH^MOG and Devic mouse, respectively. **(C)** and **(D)** show the ability of transgenic B cells IgH^MOG or Devic mice, respectively, to bind MOG. Numbers in quadrants indicate the percentage of the gated-cell population.

Activated, but not naive, T cells express several specific surface molecules. Analysis of TCR^MOG and Devic mice for the expression of the activation markers CD25 (IL-2 receptor α chain), CD69, CD44, and CD62L (L-selectin) revealed no significant difference, irrespective of the clinical status of the mice (Figure 5.21).

The above data demonstrate that there is minimal activation of lymphocytes in peripheral lymphoid organs of Devic mice. To verify and delineate the location of T cell activation, adoptive transfer experiments were performed. Naive Devic mouse splenocytes were labeled with CFSE *in vitro* and injected i.v. into sick as well as healthy Devic mice. CNS infiltrating cells and splenocytes were harvested after 3 days and analyzed for dilution of cellular CFSE (indication of T cell proliferation) and for expression of CD69. Percoll gradient separation yielded significant numbers of cells from the spinal cord of sick Devic mice, but only a few cells (if any) could be recovered from healthy mice.
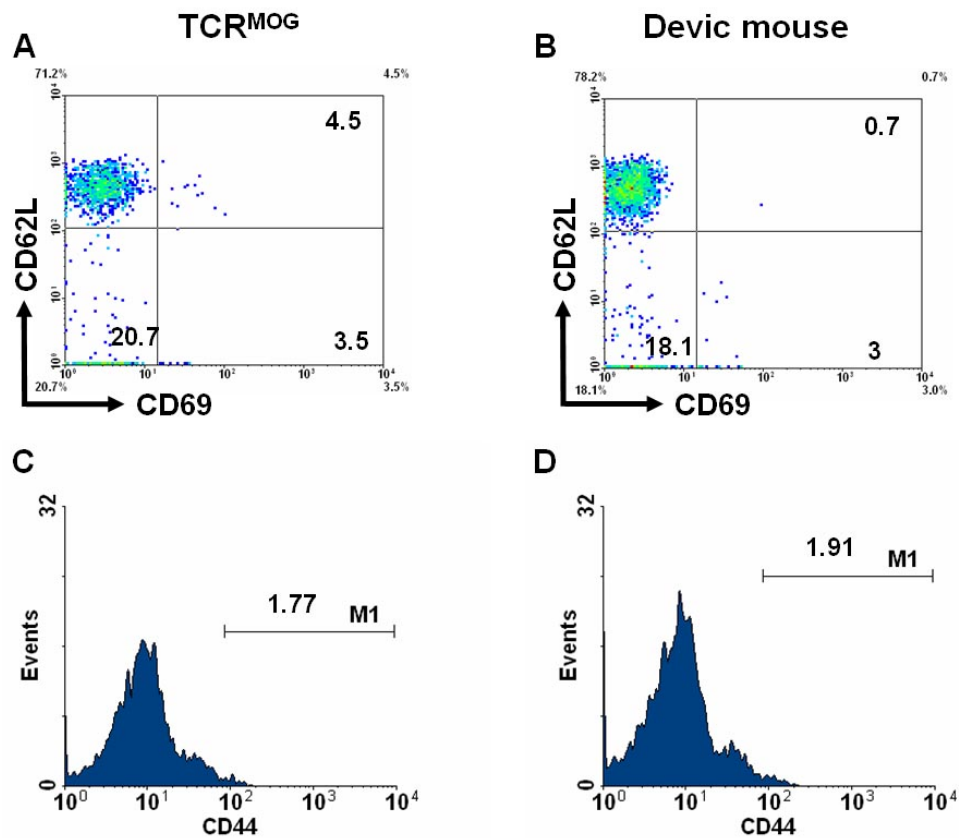
Figure 5.21

Activation status of T cells in transgenic mice. Splenocytes from TCR^{MOG} and Devic mice with EAE (Score 4) were stained with antibodies against CD69, CD44, CD62L, and CD4. Results shown are gated on CD4$^+$ T cells. Numbers in quadrants refer to percentage of the gated cell populations.

Cells isolated from the spinal cord of sick Devic mice contained significant numbers of CD4$^+$ T cells, but only a very few CD19$^+$ B cells (Figure 5.22 A). While in the spleen, CFSE-loaded cells showed a meager proliferation, CNS infiltrated T cells proliferated vigorously, as indicated by the decrease in the fluorescence intensity of CFSE. CNS-infiltrated cells expressed the activation marker CD69 at comparable levels to that of host-derived cells (CFSE negative quadrant; Figure 5.22). It can be concluded that the CNS is a major site of T cell activation.
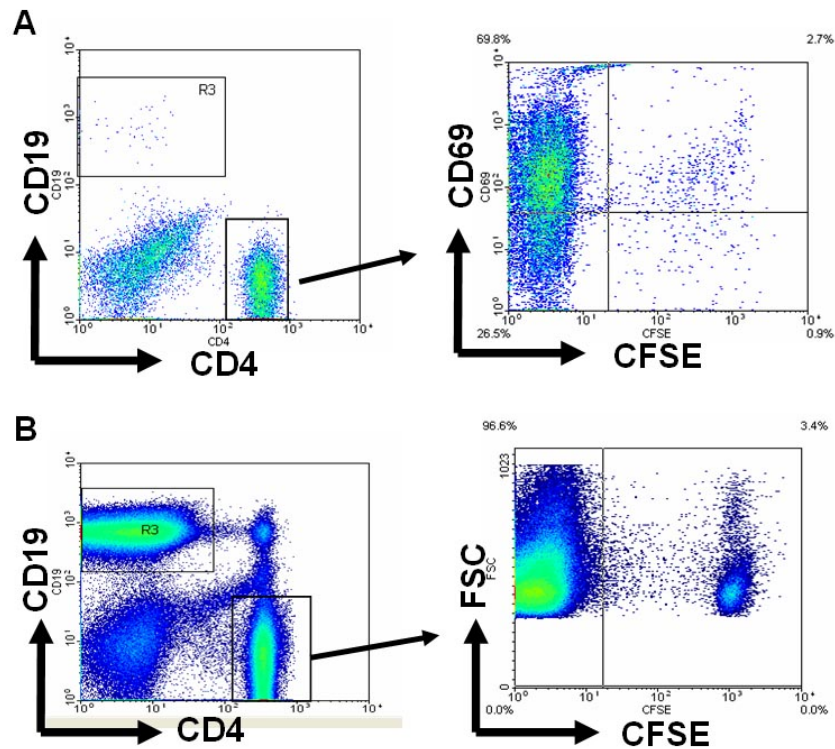
Figure 5.22

Proliferation of T cells in the CNS. **(A)** Percoll gradient separated CNS infiltrating mononuclear cells (3 days after injection) from sick Devic mice, which received CFSE-labeled naive Devic splenocytes stained for CD4, CD69, and CD19. Right panel shows gated CD4$^+$ T cells for the expression of CD69 and CFSE fluorescence. **(B)** Splenocytes from the same sick mice stained as above. CFSE fluorescence in gated CD4$^+$ T cells is shown in right panel.

5.11 Reconstitution of wild-type (WT) mice with Devic mice bone marrow (BM) reproduces spontaneous EAE

To further clarify whether bone marrow-derived B and T cells or yet another defect in the architecture of Devic mice induces spontaneous EAE, bone marrow reconstitution experiments were performed.

Lethally irradiated WT C57BL/6 mice were reconstituted with bone marrow cells derived from Devic mice. Analysis of the PBMCs 1 month after injection confirmed the reconstitution of the immune system with the transgenic T and B cells. Reconstituted mice also showed high titers of serum MOG-specific IgG1 autoantibodies as commonly found in Devic mice. In contrast, titers of MOG-specific IgM autoantibodies were significantly low (Figure 5.23 A). Despite the reconstitution of WT mice with transgenic B and T cells and the isotype switching to IgG1

autoantibodies, the disease incidence in these mice was surprisingly low (12.5%). Those few chimeric mice that had developed spontaneous EAE-like disease exhibited CNS lesions only in the optic nerves and spinal cord with severe demyelination and axonal damage (Figure 5.23 B & C). This clearly shows that transgenic MOG-specific B cells and T cells can induce spontaneous EAE-like disease, which is dependent on other endogenous factors.
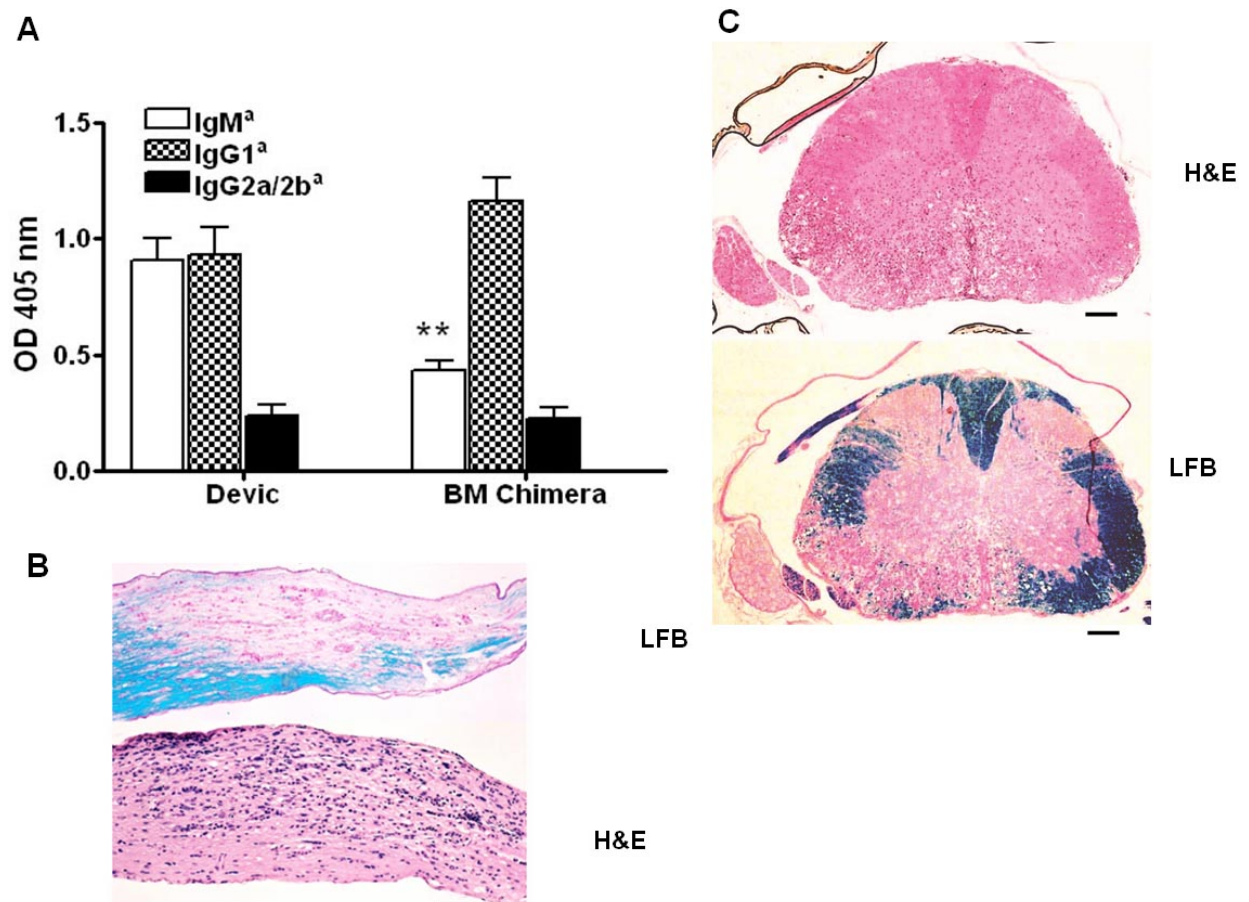
Figure 5.23

BM reconstitution reproduces spontaneous EAE. **(A)** Serum MOG-specific antibody levels 1 month after Devic BM injection into WT mice (n = 7). ** indicates statistically significant (p < 0.01). **(B, C)** Histological analysis of the spinal cord and optic nerve from BM reconstituted mice with spontaneous EAE. **(B)** Serial sections through optic nerve (longitudinal sections) showing demyelinated plaques in Luxol fast blue staining (upper picture) and inflammatory infiltrates in H&E staining (lower picture). Scale bar = 1mm. **(C)** Spinal cord with inflammatory demyelinating lesions mainly in the left anterior column; upper picture: H&E, lower picture: Luxol fast blue. Scale bar = 1mm. The histological analysis was performed by Prof. Hans Lassmann, University of Vienna, Austria.

5.12 Devic lymphocytes transfer spontaneous EAE in immunodeficient mice.

The use of adoptive transfer models allows determination of the relative contribution of specific cells types that are necessary to induce EAE. To establish an adoptive transfer model of Devic mice, naive splenocytes from healthy Devic mice were injected into recombinase-activating gene 2-deficient mice (RAG2 KO), which lacked T and B cells. RAG2 KO mice, however, are normally able to present antigen and show normal amounts of NK cells. The transfer of splenocytes from naive healthy young (< 8-wk-old) Devic mice into RAG2 KO mice induced severe spontaneous EAE in 75% of the recipient animals 13.7 ± 2.2 days after transfer. In contrast, TCR^{MOG} splenocytes transferred into RAG2 KO mice induced a low incidence of EAE, and IgH^{MOG} splenocytes did not transfer EAE (Table 5.6).

Table 5.6

Incidence of EAE following adoptive transfer of Devic and single transgenic mice splenocytes into RAG KO mice.

Transferred cells	Incidence	Mean severity	Mean day of onset
Devic splenocytes	6/8 (75%)	2.8 ± 1.3	13.7 ± 2.2
TCR^{MOG} splenocytes	1/4 (25%)	4	20
IgH^{MOG} splenocytes	0/2 (0%)	NA	NA

Devic or single transgenic mice splenocytes (50 × 10^6) were transferred into RAG-deficient mice and the incidence of spontaneous EAE was noted. Data pooled from two independent experiments. NA-Not applicable.

Histological analysis of the spinal cord from sick mice that received Devic splenocytes showed lesions, infiltration, and demyelination similar to that in Devic mice (data not shown). Analysis of serum immunoglobulin identified MOG-specific IgM antibodies in RAG2 KO mice which had previously received Devic or IgH^{MOG} splenocytes. Surprisingly, the spontaneous isotype switching to IgG1 observed in Devic mice was completely absent in these mice. In addition, mice that received IgH^{MOG} splenocytes showed high titers of MOG-specific IgG2a/2b levels in their

serum. In contrast, TCR^{MOG} cell transfer did not produce any MOG-specific antibodies (Figure 5.24).
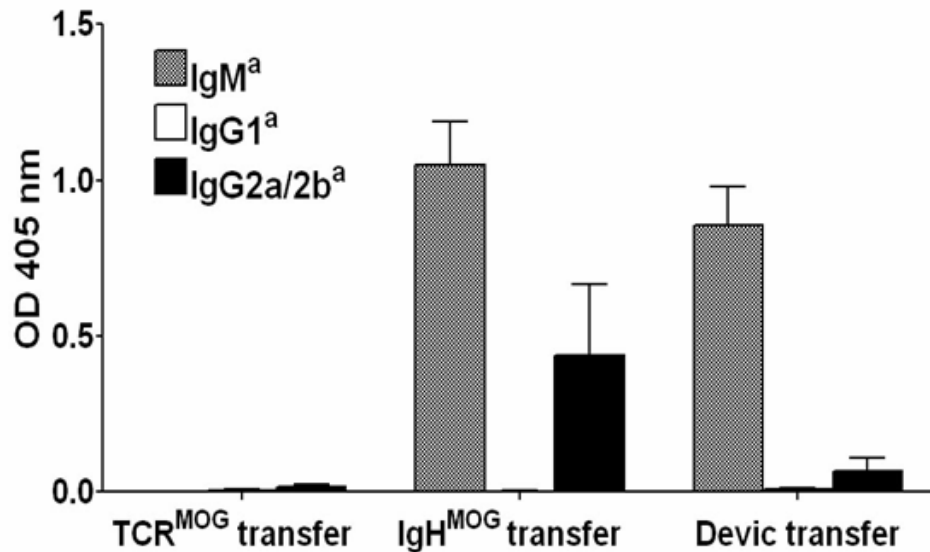
Figure 5.24

Serum immunoglobulin levels after adoptive transfer. Devic or single transgenic mice splenocytes (50 × 10^6) were transferred into RAG-deficient mice. Serum was collected at least 12 days after transfer, and MOG-specific antibodies were measured by sandwich ELISA. Number of animals: TCR^{MOG} transfer, n = 4; IgH^{MOG} transfer, n = 2; Devic transfer, n = 7.

To determine if any peripheral proliferation or activation occurs in this adoptive transfer EAE, Devic and OT-II X IgH^{MOG} splenocytes were labeled with CFSE before transfer into RAG recipients. Mice were bled every 3rd day to identify proliferation indicated by CFSE-negative cells; CFSE$^+$ cells indicate non-proliferated cells. Both control (OT-II X IgH^{MOG}) and Devic T cells proliferated equally in RAG$^{-/-}$ mice but without any appreciable activation as measured by the surface expression of CD25 (data not shown). The B cells initially underwent rapid proliferation, but the numbers stayed constant throughout the observation period (Figure 5.25).
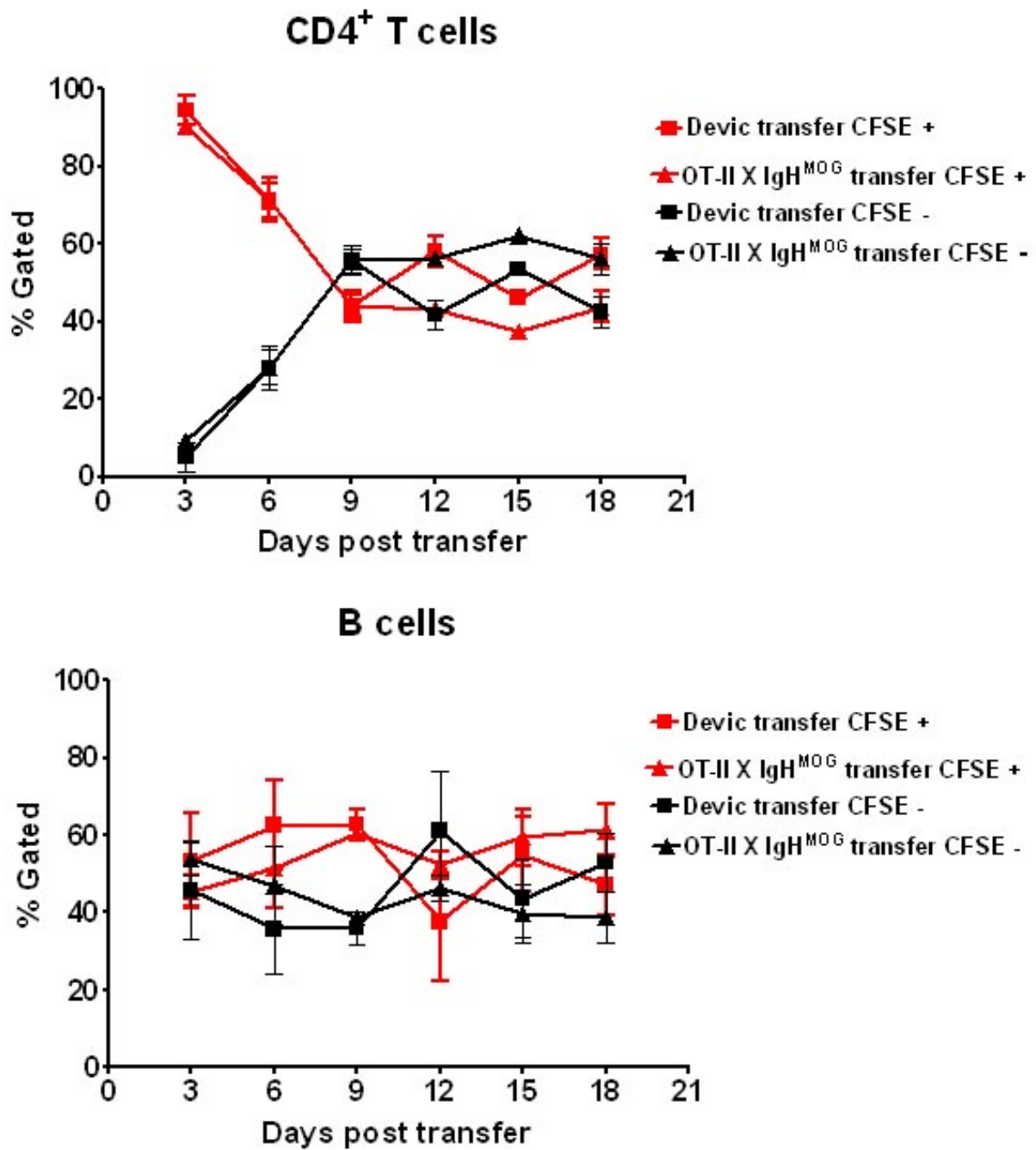
Figure 5.25

Proliferation of T and B cells following adoptive transfer. Devic and OT-II X IgH[MOG] splenocytes were labeled with CFSE and injected into RAG2 KO mice via the tail vein. Mice were bled every 3rd day and stained with antibodies against CD4 and B220. Green CFSE fluorescence-positive and negative CD4^{+} T cells and B220^{+} B cells were quantified. Each data point represents the mean percentage of gated cells from three animals. Error bars indicate SEM.

5.13 Regulatory T cells and their influence on spontaneous EAE

Although pathogenic T cells and B cells are present in normal individuals, they might be kept under control by several tolerance mechanisms. Regulatory cells, which exclusively express the transcription factor FoxP3, may be able to dampen self-reactive cells and hence prevent autoimmunity.
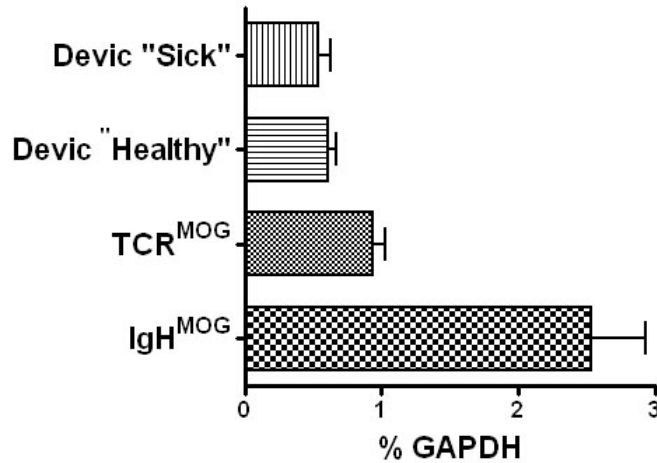
Figure 5.26

Expression of Foxp3 in the spleen of transgenic mice. Foxp3 transcripts from splenocytes of 4 – 8 wk-old transgenic mice were measured by quantitative real-time PCR. Each sample was measured in triplicate. Values are expressed as mean percentage of endogenous gene GAPDH transcripts + SEM. Data were pooled from more than three independent experiments. Numbers of animals analyzed: Devic healthy, n = 9; Devic sick, n = 9; TCR^{MOG}, n = 7; IgH^{MOG} n = 8.

Expression of Foxp3 was measured by the quantitative real-time PCR from splenocytes of Devic mice with or without EAE and single transgenic mice. Healthy or sick Devic mice and TCR^{MOG} single transgenic mice expressed similar amounts of Foxp3. In contrast, IgH^{MOG} mice expressed significantly higher amounts of Foxp3 (Figure 5.26).

However, this does not account for the variable expression of Foxp3 within the same individual and changes in expression before and after clinical EAE. To address this point, Foxp3 gene expression was determined by real-time quantitative PCR of PBMCs isolated from the same Devic mouse every week. Foxp3 gene expression in PBMCs was quite variable in these mice. During young age (around 4 - 5 weeks) both sick and healthy Devic mice showed low levels of Foxp3 gene expression. On the one hand, Foxp3 expression was higher and increased over time

in Devic mice that did not develop spontaneous EAE. On the other, the majority of sick Devic mice expressed low levels of Foxp3 transcripts, which, interestingly, remained low over time (Figure 5.27).
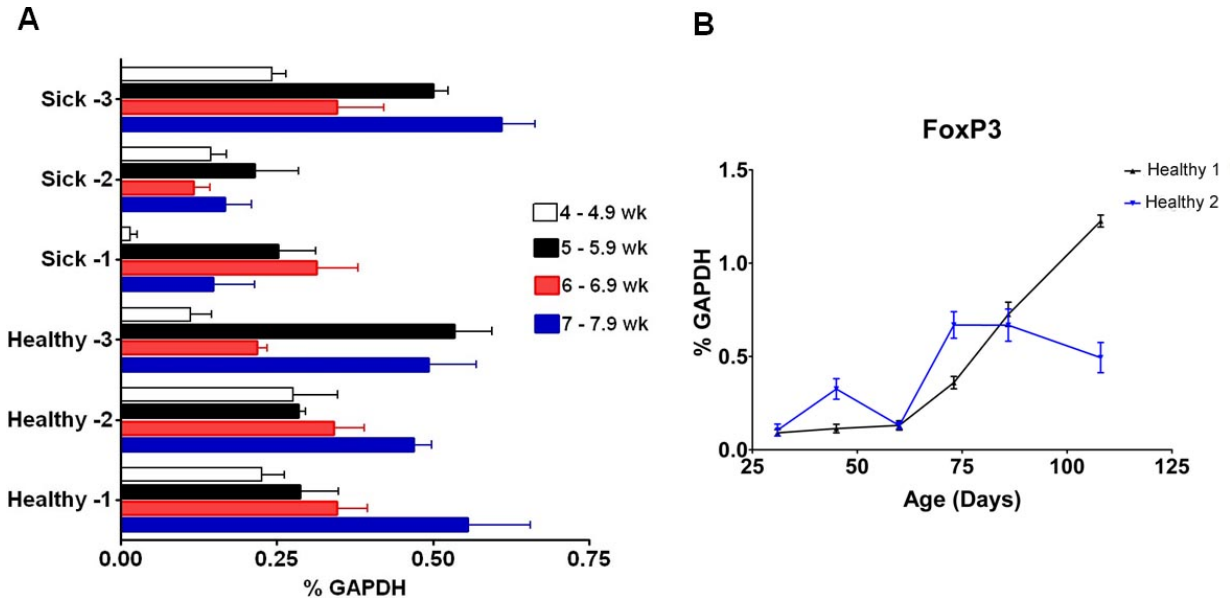
Figure 5.27

Variable Foxp3 expression in sick and healthy Devic mice. **(A)** and **(B)** show the expression of Foxp3 in PBMCs. Three sick and three healthy Devic mice were bled 4 times once a wk starting from 4 – 5 wk of age, and Foxp3 expression was assessed by quantitative real-time PCR **(A)**. Two healthy Devic mice were bled once every 2 wk, and Foxp3 expression was measured by real-time PCR **(B)**. Relative expression values are expressed as percentage of endogenous GAPDH gene transcript ± SEM measured from triplicate samples.

To confirm Foxp3 expression at the protein level, intracellular staining was performed. Foxp3 expression in splenocytes from relatively young (4 – 8 wk old) Devic mice was undetectable, perhaps due to the limits of detection of the assay. Nevertheless, 8-month-old healthy Devic mice clearly showed expression of Foxp3 (2.6%), confirming the possibly protective role of Foxp3 expressing cells. Foxp3 expression is variable even among the healthy Devic mice of the same age (Figure 5.28).

Foxp3-expressing regulatory cells are known to express GITR (glucocorticoid-induced tumor necrosis factor receptor family-related gene) and CD25 (IL-2 receptor α chain). Blocking antibodies (anti-GITR; DTA-1, anti-CD25; PC61) against these molecules have been shown to deplete regulatory cells and promote autoimmunity.
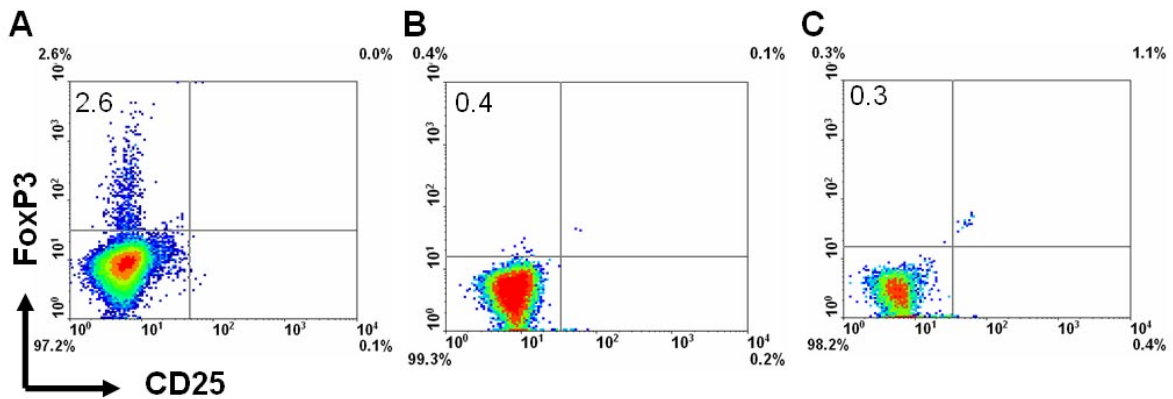
Figure 5.28

Intracellular Foxp3 expression in Devic splenocytes. Splenocytes from ~8-month-old (**A** and **B**) and 8-wk-old **(C)** Devic mice were stained with antibodies against the cell surface molecules CD25, CD4, and CD3. Intracellular Foxp3 staining was done after permeabilization and fixing of the cells. Shown are CD4$^+$CD3$^+$ gated cells expressing CD25 and Foxp3.

The effect of the antibodies DTA-1 and PC61 on the proliferation of Devic splenocytes was measured. Anti-CD25 antibody (PC61) greatly diminished the proliferation induced by rMOG, and anti-GITR antibody (DTA-1) enhanced the proliferation, thus confirming the effectiveness of these antibodies on transgenic cells (Figure 5.29).
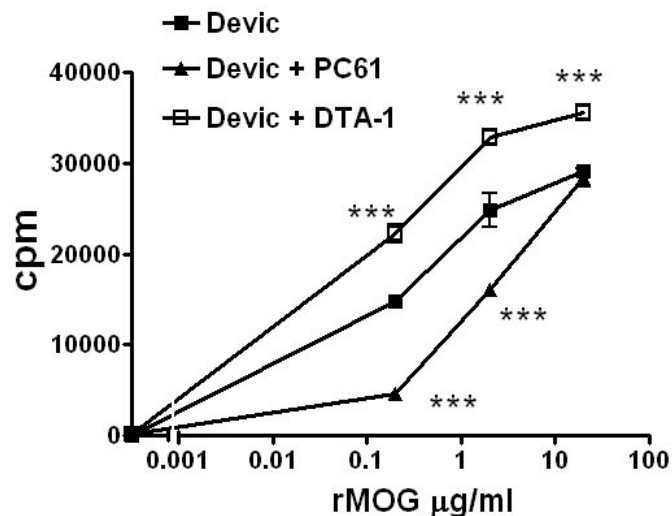
Figure 5.29

The effect of anti-CD25 and anti-GITR antibodies on proliferation. Devic splenocytes were left untreated or added to 10 µg/ml PC61 (anti-CD25) or DTA-1 (anti-GITR) and exposed to increasing concentrations of rMOG. Proliferation measured in triplicates by ^{3}H-thymidine incorporation is expressed as mean cpm ± SEM.

These antibodies were administered to Devic mice, and their influence on disease incidence was observed. When administered to either young (3 – 4 wk-old) or adult (4 – 8 wk-old) mice, they did not have a major impact on the incidence and kinetics of clinical disease. The PC61 antibody treatment did not significantly affect clinical EAE compared to control Ig or PBS-treated mice. However, DTA-1 treatment enhanced the disease incidence (Table 5.7).

Table 5.7

Incidence of spontaneous EAE after depletion of regulatory T cells

Antibody	Target	n	EAE incidence
DTA-1	GITR	12	9/12 (75%)
PC61	CD25	6	2/6 (33.3%)
Rat IgG or PBS	-	12	5/12 (41.7%)

Healthy Devic mice (3 - 7 wk-old) were injected with 500 µg of the indicated antibody once a week 3 - 4 times, and the incidence of spontaneous EAE was monitored.

6. Discussion

MS is a complex CNS disorder that has multiple pathogenic manifestations but no known trigger. Although existing EAE models are important for studying the pathogenic mechanisms of MS, they do not reproduce human MS pathology in all its structural and clinical aspects.

The double-transgenic mouse model presented here has several advantages. Foremost among them is that it recapitulates several pathological aspects of the human disease, Devic's neuromyelitis optica, a variant form of MS. For this reason it is aptly termed, the "Devic mouse". The pathological hallmark of Devic's disease is the restricted localization of demyelinating lesions in the optic nerve and spinal cord (Cree et al., 2002). Devic mice show similar demyelinating lesions in the spinal cord and optic nerve, but not in the brain or cerebellum. Serological and clinical evidence suggest that B cells and autoantibodies are involved in Devic's disease, and Ig deposition and eosinophilic infiltration are prominent features of its pathology (Lucchinetti et al., 2002). In the Devic mouse both MOG-specific B and T cells interact at multiple levels to precipitate EAE. Although eosinophilic infiltration was observed in some Devic mice, Ig deposition is rare. Another difference is sex bias. Many human autoimmune diseases including MS are more prevalent in females than males. Sex differences in susceptibility to autoimmune disease have also been reported in several mouse models. For example, female NOD mice are more susceptible than males to develop spontaneous diabetes (Kikutani and Makino, 1992; Whitacre et al., 1999). Susceptibility to induced EAE is also characteristic of females in some inbred strains, most notably in SJL/J mice (Levine and Sowinski, 1973; Papenfuss et al., 2004). Devic mice, however, do not show any sex bias in spontaneous EAE incidence or in kinetics.

A second crucial feature of the Devic mouse is that it spontaneously develops EAE. Conventional EAE models suffer from many shortcomings, for example, the need to activate T cells before transfer or to use a strong adjuvant to artificially induce an immune response. In contrast, about 50% of the Devic mice develop spontaneous EAE at about 12 wk of age. Neither of the single transgenic parental

mice develops EAE within that time. Spontaneous, organ-specific autoimmune mouse models are rare. The non-obese diabetic (NOD) mouse (Makino et al., 1980), which spontaneously develops diabetes, is a widely studied spontaneous model of autoimmunity. Several transgenic and knock-out mice have been reported to develop spontaneous, organ-specific, and systemic autoimmune diseases (Burkhardt and Kalden, 1997). Spontaneous EAE was also reported in TCR transgenic mice for MBP in the context of I-A^u (Goverman et al., 1993; Lafaille, 2004), and PLP 139-151-specific TCR transgenic mice in the context of I-A^s. MBP-specific TCR transgenic mice developed EAE at variable frequencies, depending on the housing conditions or the absence of endogenous regulatory lymphocytes.

Third, the Devic mouse is unique because of the presence of B and T cells that have same myelin autoantigen specificity. No other animal model has been reported to have such properties. The relevance of antigen specificity in spontaneous EAE was confirmed by two control breeding experiments. First, the breeding of IgH^{MOG} transgenic mice with non-specific antigen ovalbumin (IgH^{MOG} X OT-II) never showed any spontaneous EAE. Second, MOG-deficient Devic mice also did not develop CNS autoimmunity.

The Devic mouse is being used to investigate several issues that remain open and may serve as a better model to study those issues.

1. Triggers of spontaneous autoimmunity

One major issue involves the triggers of spontaneous autoimmunity. They are currently at the forefront of autoimmune research. So far both positive and negative mechanisms have been proposed. Positive mechanisms include microbial antigens, which have the potential to initiate autoreactivity by molecular mimicry, by polyclonal activation of autoreactive lymphocytes, or by the release of previously sequestered antigens. Their relative involvement is still controversial. Goverman and colleagues have shown that 14 - 44% of MBP-specific transgenic mice develop spontaneous EAE when housed under conventional conditions, whereas none of these mice developed EAE under SPF conditions. However, in a follow-up study, they observed spontaneous EAE in about 15% of the mice under SPF conditions, and they linked microbial triggers to this development of spontaneous EAE (Brabb et al., 1997;

Goverman et al., 1993). The NOD mouse, in contrast, exhibits spontaneous diabetes more frequently when housed under SPF than under "dirty" conditions (Pozzilli et al., 1993; Singh and Rabinovitch, 1993). The present study has shown that there is a similar incidence of EAE in Devic mice grown under conventional or SPF conditions.

2. The site of priming of autoreactive lymphocytes

It is commonly believed that the priming of autoreactive lymphocytes must occur in the peripheral lymphoid organs, since under normal conditions the BBB does not permit the passage of immune cells. Activated T cells express a set of adhesion molecules, which are important for their transmigration across the BBB. While the activation of lymphocytes in actively induced EAE occurs in the lymph nodes, the exact site of activation of T cells in human CNS autoimmune disease and in spontaneous animal models must still be identified. In a monkey model of EAE, it has been suggested that CNS antigen can be transported to the cervical lymph nodes, where it contributes to the priming of the autoreactive T cells (de Vos et al., 2002). Besides the presence of APCs, an inflammatory milieu is necessary for this priming. A search for lymphocyte activation molecules in secondary lymphoid organs of healthy and sick Devic mice did not identify any distinguishable activation status of T or B cells. However, CNS infiltrated cells from the sick Devic mice upregulated several activation markers. This raises the question of the presence of (if any) putative triggering factors in the peripheral lymphoid organs of Devic mice.

The transfer of CFSE-labeled lymphocytes confirmed that T cells are not activated in the peripheral lymphoid organs even during an ongoing inflammatory immune process. Both the proliferation and activation of transgenic T cells were only detectable in the CNS of sick Devic mice. It is not clear which APCs induce the activation of T cells. Recently, however, it was demonstrated that CNS-resident dendritic cells or microglia can activate autoreactive cells (Greter et al., 2005; Heppner et al., 2005). Furthermore, McMahon *et al.* showed that even during ongoing CNS inflammation the activation of PLP transgenic T cells occurred only in the CNS and not in the cervical lymph nodes or in other peripheral lymphoid organs (McMahon et al., 2005).

It is a well-documented fact that EAE can be induced in normal mice by autoantigen, mycobacteria, and adjuvant. Innate immune signals elicited on APCs through toll-like receptors exacerbate EAE in PLP-reactive transgenic mouse as well as in WT SJL/J mice (Waldner et al., 2004; Ichikawa et al., 2002). Microglia acting as CNS sentinels for danger signals have been shown to increase TLR expression in response to inflammatory mediators as well as microbial products (Olson and Miller, 2004). Augmented TLR expression during EAE was observed within the CNS, even in the absence of any apparent microbial involvement (Prinz et al., 2006). However, in our preliminary experiments, the injection of Devic mice with TLR ligands failed to influence the disease incidence.

3. The role of regulatory lymphocytes

Autoaggressive T and B cells might be controlled by regulatory lymphocytes and hence autoimmunity could be facilitated by the depletion of regulatory cells. The presence of many types of regulatory cells has been shown in different models. Naturally occurring $CD4^+CD25^+$ regulatory T cells (Treg) are thought to control autoimmunity through multiple mechanisms (Sakaguchi, 2004). The adoptive transfer of $CD4^+CD25^+$ regulatory T cells conferred significant protection from clinical EAE (Kohm et al., 2002), and the depletion of putative regulatory cells from EAE-resistant B10.S mice (Reddy et al., 2005) or SJL/J mice exacerbated EAE (Kohm et al., 2004). However, both healthy and sick Devic mice harbored a very low frequency of $CD4^+CD25^+$ T cells (< 2%). Furthermore, the administration of depleting antibodies (anti-CD25 and anti-GITR) had only a marginal influence on the development of EAE.

Foxp3, which encodes a transcription factor, is expressed in naturally arising regulatory T cells and is the only available specific marker for them (Hori et al., 2003). The naturally occurring Foxp3 mutant scurfy mice or the targeted disruption of the Foxp3 gene led to a severe autoimmune syndrome (Fontenot et al., 2003). Splenocytes of young Devic mice expressed Foxp3 in amounts similar to that of TCR^{MOG} splenocytes, but at much lower levels than single transgenic IgH^{MOG} mice. This might partly explain why optic neuritis is observed in TCR^{MOG} mice and EAE in Devic mice. Reduced Foxp3 expression might be due to a restricted endogenous

TCR-encoded repertoire. The higher frequencies of EAE observed after removal of endogenous T cells (putative regulatory), cells of MBP-specific TCR transgenic mice, and the transfer of polyclonal T cells completely prevented EAE (Lafaille et al., 1994). Interestingly, preliminary experiments showed that Devic mice with EAE had even more reduced expression of Foxp3 in PBMCs than healthy mice over time. Conversely, 8-month-old resistant mice expressed much higher levels of Foxp3 in the spleen. The elevated expression of Foxp3 found in some sick mice, however, suggests that additional factors are involved.

4. The complex role of B cells and antibodies

Although MS is considered to be mainly a T cell-mediated disease, evidence is emerging that, at least in one subset of MS cases, B cells and antibodies are involved (Lassmann et al., 2001). This applies also to patients with Devic's disease who have pronounced Ig reactivity co-localizing with complement activation at sites of blood vessel damage (Lucchinetti et al., 2002). Indeed, B cells, plasma cells, and oligoclonal Ig bands are quite common components of MS lesions (Baranzini et al., 1999; Esiri, 1980; Walsh and Tourtellotte, 1986).

EAE models have so far been used to study T cell responses in CNS autoimmunity. Studies on neonatally B-cell depleted mice (Myers et al., 1992) and B cell-deficient transgenic μMT mice (Wolf et al., 1996) have shown that B cells in general might play a significant role in the pathogenesis of EAE. However, the contribution of autoantigen-specific B cells has been largely ignored due to the lack of suitable animal models. Here the Devic mice offer unique advantages as a double-transgenic model with T and B cells specific for the same myelin autoantigen, MOG. The interaction of autoreactive B and T cells can occur at multiple levels. Antigen-specific B cells can act as efficient APCs. By virtue of the presence of antigen-binding receptor on the surface, B lymphocytes are able to efficiently capture specific antigen and present it to antigen-specific T cells (Rock et al., 1984; Zimecki et al., 1988; Lanzavecchia, 1985). This is definitely the case in Devic mice. When Devic mouse B cells were mixed with MOG-specific T cells, they greatly enhanced the proliferation of T cells, even when recombinant MOG protein was highly diluted, but not with the immunodominant MOG 35-55 peptide. This is

consistent with the fact that the transgenic H chain binds only a conformational epitope of MOG but not the MOG 35-55 peptide (Litzenburger et al., 1998). The increased response, however, cannot be attributed to the increased MOG-binding activity of transgenic B cells, since both single transgenic mice and Devic mice B cells showed similar MOG-binding activity. This result certainly has *in vivo* relevance; the availability (if any) of the autoantigen during the initial phase of disease would be a critical factor. The significant role of antigen presentation by MOG-specific B cells in the pathogenesis is further supported by the finding that the transfer of MOG-incubated IgH^{MOG} B cells to TCR^{MOG} single-transgenic mice was sufficient to induce spontaneous EAE. These results are consistent with the proteoglycan-induced arthritis model, in which antigen presentation of antigen-specific B cells is important for the induction of arthritis (O'Neill et al., 2005).

MOG-specific B cells in Devic mouse not only present antigen to T cells but also respond to MOG by proliferation and activation. The interaction between T and B cells is an active co-operation, since irradiation of the transgenic B cells abolishes the enhanced proliferation of mixed cultures. An effective humoral response also requires that the B cells receive contact-mediated signals from activated T cells (Bishop and Hostager, 2001). B7 family ligand and receptor pairs expressed on B and T cells are known to serve as potential mediators of such interactions (Greenwald et al., 2005; Sharpe and Freeman, 2002).

ICOS expressed on activated T cells provides a co-stimulatory signal to B cells and induces isotype switching (McAdam et al., 2001; Hutloff et al., 1999). ICOS has also been shown to be important in the immunopathogenesis of EAE (Rottman et al., 2001). Devic mouse T cells rapidly upregulated ICOS after MOG activation. This might be one of the important factors responsible for the spontaneous isotype switching as well as spontaneous EAE observed in Devic mice. In addition, while B cells of single transgenic mice downregulated ICOSL rapidly and completely, Devic mouse B cells downregulated it only partially. This would lead to a sustained activation of T and B cells. It was also shown previously that the ICOSL expression on B cells is completely extinguished after antigen engagement without the help of T

cells, and signaling through CD40 mediated by T cells restored ICOSL expression (Liang et al., 2002).

Furthermore, the negative co-stimulatory molecule PD-1 and its ligand PDL-1,-2 interactions inhibit the proliferation and effector cytokine production of T cells (Sharpe and Freeman, 2002). PD-1 was upregulated only on a fraction of Devic T cells, but on much larger amounts of Devic B cells than in single transgenic mice after MOG activation. The rapid upregulation of PD-1 on Devic T cells not only confirms the antigen-specific interaction between B and T cells but also the presence of negative regulatory mechanisms that limit the activation of self-reactive T cells. In addition to the expression of co-stimulatory molecules, Devic lymphocytes are also rapidly activated by MOG. This supports the hypothesis that minimal antigen doses would be sufficient to rapidly activate autoreactive T cells *in vivo.*

Another cardinal feature of antigen-specific B cells is the production of autoantibodies, which either directly induce tissue damage or form an immune complex and mediate complement activation (Martin and Chan, 2004). Furthermore, T-B cell interactions play a critical role in controlling Ig affinity maturation and isotype switching. The cytokines produced by T cells can be divided into Th1 or Th2, which mediate distinct effector functions (Gor et al., 2003). They might help B cells to undergo class switching. Anti-MOG Igs were present in the Devic mouse. B cells from the Devic mouse, but not IgH^{MOG} X OT-II or IgH^{MOG} knock-in mice, underwent spontaneous isotype switching from IgM to IgG1. This is commonly observed in Th2 immune conditions. Surprisingly, Devic mice splenocytes produced Th1 cytokines (IFNγ, IL-2) in response to MOG stimulation *in vitro,* and low levels of the Th2 cytokines IL-5, but not IL-4. IL-5 is a well-known cytokine that helps B cells to switch to IgG1 and IgE (Purkerson and Isakson, 1992), but its low level in Devic mice suggest that additional factors must contribute to the isotype switching. In principle, both T cells and B cells can produce cytokines. Intracellular cytokine staining after MOG stimulation showed that only T cells (but not B cells) produced Th1 cytokines. Consistent with these *in vitro* observations, only Th1 cytokines were present in the spinal cord of sick Devic mice; Th2 cytokines were not.

Ig isotype switching is considered to be a regulated event during which B cells bind antigen and present it to T cells, which in turn help the B cells. This conventional dogma is challenged by the fact that MOG-deficient (MOG$^{-/-}$) Devic mice also showed isotype switching that was indistinguishable from MOG-sufficient (MOG$^{+/+}$) Devic mice. This raises the question of a putative cross-reactive antigen that links MOG-specific T and B cells *in vivo* or perhaps the MOG-deficient mouse is an incomplete knock-out mouse. It has been postulated that a self-antigen other than MOG must cross-link to induce receptor editing (Litzenburger et al., 2000). Interactions between CD40 and CD154 (CD40L) provide a number of signals that regulate activation of T and B cells as well as isotype switching (Quezada et al., 2004). Therapeutic blockade with CD40L-specific antibody has been shown to ameliorate EAE (Howard et al., 1999). In Devic mice, the blockade of CD40-CD40L interaction neither prevented spontaneous isotype switching nor affected EAE development.

The definitive involvement of MOG-specific B and T cells in spontaneous EAE has been clearly indicated by the induction of EAE after BM reconstitution. Furthermore, the ability of naive splenocytes obtained from young healthy Devic mice to transfer a similar clinical and histopathological EAE into RAG$^{-/-}$ mice suggests that MOG-specific T and B cells do interact to precipitate spontaneous EAE. It is nevertheless still not known, where and how the entire disease process is initiated.

In summary, the Devic mouse model described here has several salient features. The peculiar localization of lesions in the optic nerve and the spinal cord differs from the classic EAE models and strikingly resembles Devic's neuromyelitis optica in humans. The factors that determine this selective attack are not known. Presumably, target autoantigen, genetic factors, and the inherent leakiness of the BBB at the optic nerve and spinal cord may play a role in directing the autoimmune lymphocytes. MOG-induced EAE in BN rats favors antibody response and also produces a chronic demyelination, most frequently in the spinal cord and optic nerve. In contrast, immunization of dark agouti (DA) rats with MOG results in inflammation throughout the CNS (Storch et al., 1998). Furthermore, MHC and MHC-linked genes strongly influence the disease severity and clinical course

(Stefferl et al., 1999). The TCR^{MOG} (2D2) mice used in the current study frequently showed isolated optic neuritis, but rarely EAE (Bettelli et al., 2003). In a recent study, aquaporin-4 binding antibodies were described in about 30% of the sera of patients with Devic's disease. But the widespread expression of AQP4 (Badaut et al., 2002) does not coincide with the restricted lesion distribution in NMO patients (Lennon et al., 2005).

Although many questions await definite answers, the Devic mouse is the first CNS autoimmune model that shows the interaction of antigen-specific B and T cells. The MOG-specific B cells can efficiently bind MOG and present it to the MOG-specific T cells. The anti-MOG autoantibodies can also have direct access to the MOG present on the membrane and induce damage. As a model of spontaneous immunity, the Devic mouse may prove instrumental in finally elucidating the triggering factors of autoimmune disease and for validating novel therapies of autoimmune CNS disease.

7. References

Agre, P. and Kozono, D. (2003) Aquaporin water channels: molecular mechanisms for human diseases. *FEBS Lett*, **555**, 72-78.

Altmann, D.M., Douek, D.C., Frater, A.J., Hetherington, C.M., Inoko, H. and Elliott, J.I. (1995) The T cell response of HLA-DR transgenic mice to human myelin basic protein and other antigens in the presence and absence of human CD4. *J Exp Med*, **181**, 867-875.

Amor, S., Groome, N., Linington, C., Morris, M.M., Dornmair, K., Gardinier, M.V., Matthieu, J.M. and Baker, D. (1994) Identification of epitopes of myelin oligodendrocyte glycoprotein for the induction of experimental allergic encephalomyelitis in SJL and Biozzi AB/H mice. *J Immunol*, **153**, 4349-4356.

Andersson, M., Yu, M., Soderstrom, M., Weerth, S., Baig, S., Solders, G. and Link, H. (2002) Multiple MAG peptides are recognized by circulating T and B lymphocytes in polyneuropathy and multiple sclerosis. *Eur J Neurol*, **9**, 243-251.

Babbe, H., Roers, A., Waisman, A., Lassmann, H., Goebels, N., Hohlfeld, R., Friese, M., Schroder, R., Deckert, M., Schmidt, S., Ravid, R. and Rajewsky, K. (2000) Clonal expansions of CD8(+) T cells dominate the T cell infiltrate in active multiple sclerosis lesions as shown by micromanipulation and single cell polymerase chain reaction. *J Exp Med*, **192**, 393-404.

Bach, J.F. (2002) The effect of infections on susceptibility to autoimmune and allergic diseases. *N Engl J Med*, **347**, 911-920.

Badaut, J., Lasbennes, F., Magistretti, P.J. and Regli, L. (2002) Aquaporins in brain: distribution, physiology, and pathophysiology. *J Cereb Blood Flow Metab*, **22**, 367-378.

Baranzini, S.E., Jeong, M.C., Butunoi, C., Murray, R.S., Bernard, C.C. and Oksenberg, J.R. (1999) B cell repertoire diversity and clonal expansion in multiple sclerosis brain lesions. *J Immunol*, **163**, 5133-5144.

Barnden, M.J., Allison, J., Heath, W.R. and Carbone, F.R. (1998) Defective TCR expression in transgenic mice constructed using cDNA-based alpha- and beta-chain genes under the control of heterologous regulatory elements. *Immunol Cell Biol*, **76**, 34-40.

Baumann, N. and Pham-Dinh, D. (2001) Biology of oligodendrocyte and myelin in the mammalian central nervous system. *Physiol Rev*, **81**, 871-927.

Ben-Nun, A., Wekerle, H. and Cohen, I.R. (1981) Vaccination against autoimmune encephalomyelitis with T-lymphocyte line cells reactive against myelin basic protein. *Nature*, **292**, 60-61.

Bettelli, E., Pagany, M., Weiner, H.L., Linington, C., Sobel, R.A. and Kuchroo, V.K. (2003) Myelin oligodendrocyte glycoprotein-specific T cell receptor transgenic

mice develop spontaneous autoimmune optic neuritis. *J Exp Med*, **197**, 1073-1081.

Bishop, G.A. and Hostager, B.S. (2001) B lymphocyte activation by contact-mediated interactions with T lymphocytes. *Curr Opin Immunol*, **13**, 278-285.

Bourquin, C., Schubart, A., Tobollik, S., Mather, I., Ogg, S., Liblau, R. and Linington, C. (2003) Selective unresponsiveness to conformational B cell epitopes of the myelin oligodendrocyte glycoprotein in H-2b mice. *J Immunol*, **171**, 455-461.

Brabb, T., Goldrath, A.W., von Dassow, P., Paez, A., Liggitt, H.D. and Goverman, J. (1997) Triggers of autoimmune disease in a murine TCR-transgenic model for multiple sclerosis. *J Immunol*, **159**, 497-507.

Breithaupt, C., Schubart, A., Zander, H., Skerra, A., Huber, R., Linington, C. and Jacob, U. (2003) Structural insights into the antigenicity of myelin oligodendrocyte glycoprotein. *Proc Natl Acad Sci U S A*, **100**, 9446-9451.

Bronstein, J.M., Micevych, P.E. and Chen, K. (1997) Oligodendrocyte-specific protein (OSP) is a major component of CNS myelin. *J Neurosci Res*, **50**, 713-720.

Bruno, R., Sabater, L., Sospedra, M., Ferrer-Francesch, X., Escudero, D., Martinez-Caceres, E. and Pujol-Borrell, R. (2002) Multiple sclerosis candidate autoantigens except myelin oligodendrocyte glycoprotein are transcribed in human thymus. *Eur J Immunol*, **32**, 2737-2747.

Burkhardt, H. and Kalden, J.R. (1997) Animal models of autoimmune diseases. *Rheumatol Int*, **17**, 91-99.

Cepok, S., Zhou, D., Srivastava, R., Nessler, S., Stei, S., Bussow, K., Sommer, N. and Hemmer, B. (2005) Identification of Epstein-Barr virus proteins as putative targets of the immune response in multiple sclerosis. *J Clin Invest*, **115**, 1352-1360.

Christen, U. and von Herrath, M.G. (2005) Infections and autoimmunity--good or bad? *J Immunol*, **174**, 7481-7486.

Clements, C.S., Reid, H.H., Beddoe, T., Tynan, F.E., Perugini, M.A., Johns, T.G., Bernard, C.C. and Rossjohn, J. (2003) The crystal structure of myelin oligodendrocyte glycoprotein, a key autoantigen in multiple sclerosis. *Proc Natl Acad Sci U S A*, **100**, 11059-11064.

Coo, H. and Aronson, K.J. (2004) A systematic review of several potential non-genetic risk factors for multiple sclerosis. *Neuroepidemiology*, **23**, 1-12.

Cree, B.A., Goodin, D.S. and Hauser, S.L. (2002) Neuromyelitis optica. *Semin Neurol*, **22**, 105-122.

Cross, A.H., Trotter, J.L. and Lyons, J. (2001) B cells and antibodies in CNS demyelinating disease. *J Neuroimmunol*, **112**, 1-14.

Davidson, A. and Diamond, B. (2001) Autoimmune diseases. *N Engl J Med*, **345**, 340-350.

de Vos, A.F., van Meurs, M., Brok, H.P., Boven, L.A., Hintzen, R.Q., van der Valk, P., Ravid, R., Rensing, S., Boon, L., t Hart, B.A. and Laman, J.D. (2002) Transfer of central nervous system autoantigens and presentation in secondary lymphoid organs. *J Immunol*, **169**, 5415-5423.

Delarasse, C., Daubas, P., Mars, L.T., Vizler, C., Litzenburger, T., Iglesias, A., Bauer, J., Della Gaspera, B., Schubart, A., Decker, L., Dimitri, D., Roussel, G., Dierich, A., Amor, S., Dautigny, A., Liblau, R. and Pham-Dinh, D. (2003) Myelin/oligodendrocyte glycoprotein-deficient (MOG-deficient) mice reveal lack of immune tolerance to MOG in wild-type mice. *J Clin Invest*, **112**, 544-553.

Dyment, D.A., Ebers, G.C. and Sadovnick, A.D. (2004) Genetics of multiple sclerosis. *Lancet Neurol*, **3**, 104-110.

Ellmerich, S., Takacs, K., Mycko, M., Waldner, H., Wahid, F., Boyton, R.J., Smith, P.A., Amor, S., Baker, D., Hafler, D.A., Kuchroo, V.K. and Altmann, D.M. (2004) Disease-related epitope spread in a humanized T cell receptor transgenic model of multiple sclerosis. *Eur J Immunol*, **34**, 1839-1848.

Esiri, M.M. (1980) Multiple sclerosis: a quantitative and qualitative study of immunoglobulin-containing cells in the central nervous system. *Neuropathol Appl Neurobiol*, **6**, 9-21.

Flugel, A., Berkowicz, T., Ritter, T., Labeur, M., Jenne, D.E., Li, Z., Ellwart, J.W., Willem, M., Lassmann, H. and Wekerle, H. (2001) Migratory activity and functional changes of green fluorescent effector cells before and during experimental autoimmune encephalomyelitis. *Immunity*, **14**, 547-560.

Fontenot, J.D., Gavin, M.A. and Rudensky, A.Y. (2003) Foxp3 programs the development and function of CD4+CD25+ regulatory T cells. *Nat Immunol*, **4**, 330-336.

Friese, M.A. and Fugger, L. (2005) Autoreactive CD8+ T cells in multiple sclerosis: a new target for therapy? *Brain*, **128**, 1747-1763.

Fujinami, R.S. and Oldstone, M.B. (1985) Amino acid homology between the encephalitogenic site of myelin basic protein and virus: mechanism for autoimmunity. *Science*, **230**, 1043-1045.

Genain, C.P., Cannella, B., Hauser, S.L. and Raine, C.S. (1999) Identification of autoantibodies associated with myelin damage in multiple sclerosis. *Nat Med*, **5**, 170-175.

Genain, C.P., Nguyen, M.H., Letvin, N.L., Pearl, R., Davis, R.L., Adelman, M., Lees, M.B., Linington, C. and Hauser, S.L. (1995) Antibody facilitation of multiple sclerosis-like lesions in a nonhuman primate. *J Clin Invest*, **96**, 2966-2974.

Gilden, D.H. (2005) Infectious causes of multiple sclerosis. *Lancet Neurol*, **4**, 195-202.

Giulietti, A., Overbergh, L., Valckx, D., Decallonne, B., Bouillon, R. and Mathieu, C. (2001) An overview of real-time quantitative PCR: applications to quantify cytokine gene expression. *Methods*, **25**, 386-401.

Gold, R., Hartung, H.P. and Toyka, K.V. (2000) Animal models for autoimmune demyelinating disorders of the nervous system. *Mol Med Today*, **6**, 88-91.

Gor, D.O., Rose, N.R. and Greenspan, N.S. (2003) TH1-TH2: a procrustean paradigm. *Nat Immunol*, **4**, 503-505.

Goverman, J., Woods, A., Larson, L., Weiner, L.P., Hood, L. and Zaller, D.M. (1993) Transgenic mice that express a myelin basic protein-specific T cell receptor develop spontaneous autoimmunity. *Cell*, **72**, 551-560.

Greenwald, R.J., Freeman, G.J. and Sharpe, A.H. (2005) The B7 family revisited. *Annu Rev Immunol*, **23**, 515-548.

Greter, M., Heppner, F.L., Lemos, M.P., Odermatt, B.M., Goebels, N., Laufer, T., Noelle, R.J. and Becher, B. (2005) Dendritic cells permit immune invasion of the CNS in an animal model of multiple sclerosis. *Nat Med*, **11**, 328-334.

Hafler, D.A. (2004) Multiple sclerosis. *J Clin Invest*, **113**, 788-794.

Hauser, S.L., Bhan, A.K., Gilles, F., Kemp, M., Kerr, C. and Weiner, H.L. (1986) Immunohistochemical analysis of the cellular infiltrate in multiple sclerosis lesions. *Ann Neurol*, **19**, 578-587.

Hemmer, B., Archelos, J.J. and Hartung, H.P. (2002) New concepts in the immunopathogenesis of multiple sclerosis. *Nat Rev Neurosci*, **3**, 291-301.

Heppner, F.L., Greter, M., Marino, D., Falsig, J., Raivich, G., Hovelmeyer, N., Waisman, A., Rulicke, T., Prinz, M., Priller, J., Becher, B. and Aguzzi, A. (2005) Experimental autoimmune encephalomyelitis repressed by microglial paralysis. *Nat Med*, **11**, 146-152.

Holz, A., Bielekova, B., Martin, R. and Oldstone, M.B. (2000) Myelin-associated oligodendrocytic basic protein: identification of an encephalitogenic epitope and association with multiple sclerosis. *J Immunol*, **164**, 1103-1109.

Hori, S., Nomura, T. and Sakaguchi, S. (2003) Control of regulatory T cell development by the transcription factor Foxp3. *Science*, **299**, 1057-1061.

Howard, L.M., Miga, A.J., Vanderlugt, C.L., Dal Canto, M.C., Laman, J.D., Noelle, R.J. and Miller, S.D. (1999) Mechanisms of immunotherapeutic intervention by anti-CD40L (CD154) antibody in an animal model of multiple sclerosis. *J Clin Invest*, **103**, 281-290.

Huseby, E.S., Liggitt, D., Brabb, T., Schnabel, B., Ohlen, C. and Goverman, J. (2001a) A pathogenic role for myelin-specific CD8(+) T cells in a model for multiple sclerosis. *J Exp Med*, **194**, 669-676.

Huseby, E.S., Sather, B., Huseby, P.G. and Goverman, J. (2001b) Age-dependent T cell tolerance and autoimmunity to myelin basic protein. *Immunity*, **14**, 471-481.

Hutloff, A., Dittrich, A.M., Beier, K.C., Eljaschewitsch, B., Kraft, R., Anagnostopoulos, I. and Kroczek, R.A. (1999) ICOS is an inducible T-cell co-stimulator structurally and functionally related to CD28. *Nature*, **397**, 263-266.

Ichikawa, H.T., Williams, L.P. and Segal, B.M. (2002) Activation of APCs through CD40 or Toll-like receptor 9 overcomes tolerance and precipitates autoimmune disease. *J Immunol*, **169**, 2781-2787.

Ito, K., Bian, H.J., Molina, M., Han, J., Magram, J., Saar, E., Belunis, C., Bolin, D.R., Arceo, R., Campbell, R., Falcioni, F., Vidovic, D., Hammer, J. and Nagy, Z.A. (1996) HLA-DR4-IE chimeric class II transgenic, murine class II-deficient mice are susceptible to experimental allergic encephalomyelitis. *J Exp Med*, **183**, 2635-2644.

Jacobsen, M., Cepok, S., Quak, E., Happel, M., Gaber, R., Ziegler, A., Schock, S., Oertel, W.H., Sommer, N. and Hemmer, B. (2002) Oligoclonal expansion of memory CD8+ T cells in cerebrospinal fluid from multiple sclerosis patients. *Brain*, **125**, 538-550.

Jacobson, D.L., Gange, S.J., Rose, N.R. and Graham, N.M. (1997) Epidemiology and estimated population burden of selected autoimmune diseases in the United States. *Clin Immunol Immunopathol*, **84**, 223-243.

Johns, T.G. and Bernard, C.C. (1999) The structure and function of myelin oligodendrocyte glycoprotein. *J Neurochem*, **72**, 1-9.

Kawamura, K., Yamamura, T., Yokoyama, K., Chui, D.H., Fukui, Y., Sasazuki, T., Inoko, H., David, C.S. and Tabira, T. (2000) Hla-DR2-restricted responses to proteolipid protein 95-116 peptide cause autoimmune encephalitis in transgenic mice. *J Clin Invest*, **105**, 977-984.

Kieseier, B.C. and Hartung, H.P. (2003) Current disease-modifying therapies in multiple sclerosis. *Semin Neurol*, **23**, 133-146.

Kikutani, H. and Makino, S. (1992) The murine autoimmune diabetes model: NOD and related strains. *Adv Immunol*, **51**, 285-322.

Kira, J. (2003) Multiple sclerosis in the Japanese population. *Lancet Neurol*, **2**, 117-127.

Klein, L., Klugmann, M., Nave, K.A., Tuohy, V.K. and Kyewski, B. (2000) Shaping of the autoreactive T-cell repertoire by a splice variant of self protein expressed in thymic epithelial cells. *Nat Med*, **6**, 56-61.

Kohm, A.P., Carpentier, P.A., Anger, H.A. and Miller, S.D. (2002) CD4+CD25+ regulatory T cells suppress antigen-specific autoreactive immune responses and central nervous system inflammation during active experimental autoimmune encephalomyelitis. *J Immunol*, **169**, 4712-4716.

Kohm, A.P., Williams, J.S. and Miller, S.D. (2004) Ligation of the glucocorticoid-induced TNF receptor enhances autoreactive CD4+ T cell activation and experimental autoimmune encephalomyelitis. *J Immunol*, **172**, 4686-4690.

Kuchroo, V.K., Anderson, A.C., Waldner, H., Munder, M., Bettelli, E. and Nicholson, L.B. (2002) T cell response in experimental autoimmune encephalomyelitis (EAE): role of self and cross-reactive antigens in shaping, tuning, and regulating the autopathogenic T cell repertoire. *Annu Rev Immunol*, **20**, 101-123.

Lafaille, J.J. (2004) T-cell receptor transgenic mice in the study of autoimmune diseases. *J Autoimmun*, **22**, 95-106.

Lafaille, J.J., Nagashima, K., Katsuki, M. and Tonegawa, S. (1994) High incidence of spontaneous autoimmune encephalomyelitis in immunodeficient anti-myelin basic protein T cell receptor transgenic mice. *Cell*, **78**, 399-408.

Lang, H.L., Jacobsen, H., Ikemizu, S., Andersson, C., Harlos, K., Madsen, L., Hjorth, P., Sondergaard, L., Svejgaard, A., Wucherpfennig, K., Stuart, D.I., Bell, J.I., Jones, E.Y. and Fugger, L. (2002) A functional and structural basis for TCR cross-reactivity in multiple sclerosis. *Nat Immunol*, **3**, 940-943.

Lanzavecchia, A. (1985) Antigen-specific interaction between T and B cells. *Nature*, **314**, 537-539.

Lassmann, H., Bruck, W. and Lucchinetti, C. (2001) Heterogeneity of multiple sclerosis pathogenesis: implications for diagnosis and therapy. *Trends Mol Med*, **7**, 115-121.

Lebar, R., Lubetzki, C., Vincent, C., Lombrail, P. and Boutry, J.M. (1986) The M2 autoantigen of central nervous system myelin, a glycoprotein present in oligodendrocyte membrane. *Clin Exp Immunol*, **66**, 423-434.

Lennon, V.A., Kryzer, T.J., Pittock, S.J., Verkman, A.S. and Hinson, S.R. (2005) IgG marker of optic-spinal multiple sclerosis binds to the aquaporin-4 water channel. *J Exp Med*, **202**, 473-477.

Lennon, V.A., Wingerchuk, D.M., Kryzer, T.J., Pittock, S.J., Lucchinetti, C.F., Fujihara, K., Nakashima, I. and Weinshenker, B.G. (2004) A serum autoantibody marker of neuromyelitis optica: distinction from multiple sclerosis. *Lancet*, **364**, 2106-2112.

Levine, S. and Sowinski, R. (1973) Experimental allergic encephalomyelitis in inbred and outbred mice. *J Immunol*, **110**, 139-143.

Liang, L., Porter, E.M. and Sha, W.C. (2002) Constitutive expression of the B7h ligand for inducible costimulator on naive B cells is extinguished after activation by distinct B cell receptor and interleukin 4 receptor-mediated pathways and can be rescued by CD40 signaling. *J Exp Med*, **196**, 97-108.

Linares, D., Mana, P., Goodyear, M., Chow, A.M., Clavarino, C., Huntington, N.D., Barnett, L., Koentgen, F., Tomioka, R., Bernard, C.C., Freire-Garabal, M. and Reid, H.H. (2003) The magnitude and encephalogenic potential of autoimmune response to MOG is enhanced in MOG deficient mice. *J Autoimmun*, **21**, 339-351.

Linington, C. and Lassmann, H. (1987) Antibody responses in chronic relapsing experimental allergic encephalomyelitis: correlation of serum demyelinating activity with antibody titre to the myelin/oligodendrocyte glycoprotein (MOG). *J Neuroimmunol*, **17**, 61-69.

Linthicum, D.S. and Frelinger, J.A. (1982) Acute autoimmune encephalomyelitis in mice. II. Susceptibility is controlled by the combination of H-2 and histamine sensitization genes. *J Exp Med*, **156**, 31-40.

Litzenburger, T., Bluthmann, H., Morales, P., Pham-Dinh, D., Dautigny, A., Wekerle, H. and Iglesias, A. (2000) Development of myelin oligodendrocyte glycoprotein autoreactive transgenic B lymphocytes: receptor editing in vivo after encounter of a self-antigen distinct from myelin oligodendrocyte glycoprotein. *J Immunol*, **165**, 5360-5366.

Litzenburger, T., Fassler, R., Bauer, J., Lassmann, H., Linington, C., Wekerle, H. and Iglesias, A. (1998) B lymphocytes producing demyelinating autoantibodies: development and function in gene-targeted transgenic mice. *J Exp Med*, **188**, 169-180.

Lucchinetti, C., Bruck, W., Parisi, J., Scheithauer, B., Rodriguez, M. and Lassmann, H. (2000) Heterogeneity of multiple sclerosis lesions: implications for the pathogenesis of demyelination. *Ann Neurol*, **47**, 707-717.

Lucchinetti, C.F., Mandler, R.N., McGavern, D., Bruck, W., Gleich, G., Ransohoff, R.M., Trebst, C., Weinshenker, B., Wingerchuk, D., Parisi, J.E. and Lassmann, H. (2002) A role for humoral mechanisms in the pathogenesis of Devic's neuromyelitis optica. *Brain*, **125**, 1450-1461.

Lyons, J.A., San, M., Happ, M.P. and Cross, A.H. (1999) B cells are critical to induction of experimental allergic encephalomyelitis by protein but not by a short encephalitogenic peptide. *Eur J Immunol*, **29**, 3432-3439.

Madsen, L.S., Andersson, E.C., Jansson, L., krogsgaard, M., Andersen, C.B., Engberg, J., Strominger, J.L., Svejgaard, A., Hjorth, J.P., Holmdahl, R., Wucherpfennig, K.W. and Fugger, L. (1999) A humanized model for multiple sclerosis using HLA-DR2 and a human T-cell receptor. *Nat Genet*, **23**, 343-347.

Makino, S., Kunimoto, K., Muraoka, Y., Mizushima, Y., Katagiri, K. and Tochino, Y. (1980) Breeding of a non-obese, diabetic strain of mice. *Jikken Dobutsu*, **29**, 1-13.

Mandler, R.N., Davis, L.E., Jeffery, D.R. and Kornfeld, M. (1993) Devic's neuromyelitis optica: a clinicopathological study of 8 patients. *Ann Neurol*, **34**, 162-168.

Marta, C.B., Montano, M.B., Taylor, C.M., Taylor, A.L., Bansal, R. and Pfeiffer, S.E. (2005a) Signaling cascades activated upon antibody cross-linking of myelin oligodendrocyte glycoprotein: potential implications for multiple sclerosis. *J Biol Chem*, **280**, 8985-8993.

Marta, C.B., Oliver, A.R., Sweet, R.A., Pfeiffer, S.E. and Ruddle, N.H. (2005b) Pathogenic myelin oligodendrocyte glycoprotein antibodies recognize glycosylated epitopes and perturb oligodendrocyte physiology. *Proc Natl Acad Sci U S A*, **102**, 13992-13997.

Marta, C.B., Taylor, C.M., Coetzee, T., Kim, T., Winkler, S., Bansal, R. and Pfeiffer, S.E. (2003) Antibody cross-linking of myelin oligodendrocyte glycoprotein leads

to its rapid repartitioning into detergent-insoluble fractions, and altered protein phosphorylation and cell morphology. *J Neurosci*, **23**, 5461-5471.

Martin, F. and Chan, A.C. (2004) Pathogenic roles of B cells in human autoimmunity; insights from the clinic. *Immunity*, **20**, 517-527.

McAdam, A.J., Greenwald, R.J., Levin, M.A., Chernova, T., Malenkovich, N., Ling, V., Freeman, G.J., Sharpe, A.H., Hutloff, A., Dittrich, A.M., Beier, K.C., Eljaschewitsch, B., Kraft, R., Anagnostopoulos, I. and Kroczek, R.A. (2001) ICOS is critical for CD40-mediated antibody class switching *Nature*, **409**, 102-105.

McMahon, E.J., Bailey, S.L., Castenada, C.V., Waldner, H. and Miller, S.D. (2005) Epitope spreading initiates in the CNS in two mouse models of multiple sclerosis. *Nat Med*, **11**, 335-339.

Minagar, A., Alexander, J.S., Fowler, M.R., Long, A.C. and Kelley, R.E. (2002) Devic disease: clinical course, pathophysiology, and management. *Pathophysiology*, **9**, 33.

Morris-Downes, M.M., McCormack, K., Baker, D., Sivaprasad, D., Natkunarajah, J. and Amor, S. (2002) Encephalitogenic and immunogenic potential of myelin-associated glycoprotein (MAG), oligodendrocyte-specific glycoprotein (OSP) and 2',3'-cyclic nucleotide 3'-phosphodiesterase (CNPase) in ABH and SJL mice. *J Neuroimmunol*, **122**, 20-33.

Myers, K.J., Sprent, J., Dougherty, J.P. and Ron, Y. (1992) Synergy between encephalitogenic T cells and myelin basic protein-specific antibodies in the induction of experimental autoimmune encephalomyelitis. *J Neuroimmunol*, **41**, 1-8.

Noseworthy, J.H., Lucchinetti, C., Rodriguez, M. and Weinshenker, B.G. (2000) Multiple sclerosis. *N Engl J Med*, **343**, 938-952.

O'Neill, S.K., Shlomchik, M.J., Glant, T.T., Cao, Y., Doodes, P.D. and Finnegan, A. (2005) Antigen-specific B cells are required as APCs and autoantibody-producing cells for induction of severe autoimmune arthritis. *J Immunol*, **174**, 3781-3788.

Oldstone, M.B. (2005) Molecular mimicry, microbial infection, and autoimmune disease: evolution of the concept. *Curr Top Microbiol Immunol*, **296**, 1-17.

Olerup, O. and Hillert, J. (1991) HLA class II-associated genetic susceptibility in multiple sclerosis: a critical evaluation. *Tissue Antigens*, **38**, 1-15.

Oleszak, E.L., Chang, J.R., Friedman, H., Katsetos, C.D. and Platsoucas, C.D. (2004) Theiler's virus infection: a model for multiple sclerosis. *Clin Microbiol Rev*, **17**, 174-207.

Olivares-Villagomez, D., Wang, Y. and Lafaille, J.J. (1998) Regulatory CD4(+) T cells expressing endogenous T cell receptor chains protect myelin basic protein-specific transgenic mice from spontaneous autoimmune encephalomyelitis. *J Exp Med*, **188**, 1883-1894.

Olson, J.K. and Miller, S.D. (2004) Microglia initiate central nervous system innate and adaptive immune responses through multiple TLRs. *J Immunol*, **173**, 3916-3924.

Papenfuss, T.L., Rogers, C.J., Gienapp, I., Yurrita, M., McClain, M., Damico, N., Valo, J., Song, F. and Whitacre, C.C. (2004) Sex differences in experimental autoimmune encephalomyelitis in multiple murine strains. *J Neuroimmunol*, **150**, 59-69.

Paterson, P.Y. (1960) Transfer of allergic encephalomyelitis in rats by means of lymph node cells. *J Exp Med*, **111**, 119-136.

Pearson, C.I., van Ewijk, W. and McDevitt, H.O. (1997) Induction of apoptosis and T helper 2 (Th2) responses correlates with peptide affinity for the major histocompatibility complex in self-reactive T cell receptor transgenic mice. *J Exp Med*, **185**, 583-599.

Perchellet, A., Stromnes, I., Pang, J.M. and Goverman, J. (2004) CD8+ T cells maintain tolerance to myelin basic protein by 'epitope theft'. *Nat Immunol*, **5**, 606-614.

Piddlesden, S.J., Lassmann, H., Zimprich, F., Morgan, B.P. and Linington, C. (1993) The demyelinating potential of antibodies to myelin oligodendrocyte glycoprotein is related to their ability to fix complement. *Am J Pathol*, **143**, 555-564.

Pozzilli, P., Signore, A., Williams, A.J. and Beales, P.E. (1993) NOD mouse colonies around the world--recent facts and figures. *Immunol Today*, **14**, 193-196.

Prinz, M., Garbe, F., Schmidt, H., Mildner, A., Gutcher, I., Wolter, K., Piesche, M., Schroers, R., Weiss, E., Kirschning, C.J., Rochford, C.D., Bruck, W. and Becher, B. (2006) Innate immunity mediated by TLR9 modulates pathogenicity in an animal model of multiple sclerosis. *J Clin Invest*, **116**, 456-464.

Purkerson, J.M. and Isakson, P.C. (1992) Interleukin 5 (IL-5) provides a signal that is required in addition to IL-4 for isotype switching to immunoglobulin (Ig) G1 and IgE. *J Exp Med*, **175**, 973-982.

Quezada, S.A., Jarvinen, L.Z., Lind, E.F. and Noelle, R.J. (2004) CD40/CD154 interactions at the interface of tolerance and immunity. *Annu Rev Immunol*, **22**, 307-328.

Racke, M.K., Hu, W. and Lovett-Racke, A.E. (2005) PTX cruiser: driving autoimmunity via TLR4. *Trends Immunol*, **26**, 289-291.

Reddy, J., Waldner, H., Zhang, X., Illes, Z., Wucherpfennig, K.W., Sobel, R.A. and Kuchroo, V.K. (2005) CD4+CD25+ regulatory T cells contribute to gender differences in susceptibility to experimental autoimmune encephalomyelitis. *J Immunol*, **175**, 5591-5595.

Rivers, T.M., Sprunt, D.H. and Berry, G.P. (1933) Observations on attempts to produce acute disseminated encephalomyelitis in monkeys. *J Exp Med*, **58**, 39–53.

Rock, K.L., Benacerraf, B. and Abbas, A.K. (1984) Antigen presentation by hapten-specific B lymphocytes. I. Role of surface immunoglobulin receptors. *J Exp Med*, **160**, 1102-1113.

Rottman, J.B., Smith, T., Tonra, J.R., Ganley, K., Bloom, T., Silva, R., Pierce, B., Gutierrez-Ramos, J.C., Ozkaynak, E. and Coyle, A.J. (2001) The costimulatory molecule ICOS plays an important role in the immunopathogenesis of EAE. *Nat Immunol*, **2**, 605-611.

Saadoun, S., Papadopoulos, M.C., Davies, D.C., Krishna, S. and Bell, B.A. (2002) Aquaporin-4 expression is increased in oedematous human brain tumours. *J Neurol Neurosurg Psychiatry*, **72**, 262-265.

Sakaguchi, S. (2004) Naturally arising CD4+ regulatory t cells for immunologic self-tolerance and negative control of immune responses. *Annu Rev Immunol*, **22**, 531-562.

Sawcer, S., Goodfellow, P.N. and Compston, A. (1997) The genetic analysis of multiple sclerosis. *Trends Genet*, **13**, 234-239.

Schluesener, H.J., Sobel, R.A., Linington, C. and Weiner, H.L. (1987) A monoclonal antibody against a myelin oligodendrocyte glycoprotein induces relapses and demyelination in central nervous system autoimmune disease. *J Immunol*, **139**, 4016-4021.

Seamons, A., Perchellet, A. and Goverman, J. (2003) Immune tolerance to myelin proteins. *Immunol Res*, **28**, 201-221.

Sharpe, A.H. and Freeman, G.J. (2002) The B7-CD28 superfamily. *Nat Rev Immunol*, **2**, 116-126.

Shlomchik, M.J., Craft, J.E. and Mamula, M.J. (2001) From T to B and back again: positive feedback in systemic autoimmune disease. *Nat Rev Immunol*, **1**, 147-153.

Singh, B. and Rabinovitch, A. (1993) Influence of microbial agents on the development and prevention of autoimmune diabetes. *Autoimmunity*, **15**, 209-213.

Slavin, A.J., Johns, T.G., Orian, J.M. and Bernard, C.C. (1997) Regulation of myelin oligodendrocyte glycoprotein in different species throughout development. *Dev Neurosci*, **19**, 69-78.

Soldan, S.S., Berti, R., Salem, N., Secchiero, P., Flamand, L., Calabresi, P.A., Brennan, M.B., Maloni, H.W., McFarland, H.F., Lin, H.C., Patnaik, M. and Jacobson, S. (1997) Association of human herpes virus 6 (HHV-6) with multiple sclerosis: increased IgM response to HHV-6 early antigen and detection of serum HHV-6 DNA. *Nat Med*, **3**, 1394-1397.

Sospedra, M. and Martin, R. (2005) Immunology of multiple sclerosis. *Annu Rev Immunol*, **23**, 683-747.

Stefferl, A., Brehm, U., Storch, M., Lambracht-Washington, D., Bourquin, C., Wonigeit, K., Lassmann, H. and Linington, C. (1999) Myelin oligodendrocyte

glycoprotein induces experimental autoimmune encephalomyelitis in the "resistant" Brown Norway rat: disease susceptibility is determined by MHC and MHC-linked effects on the B cell response. *J Immunol*, **163**, 40-49.

Steinman, L. (1999) Assessment of animal models for MS and demyelinating disease in the design of rational therapy. *Neuron*, **24**, 511-514.

Storch, M.K., Stefferl, A., Brehm, U., Weissert, R., Wallstrom, E., Kerschensteiner, M., Olsson, T., Linington, C. and Lassmann, H. (1998) Autoimmunity to myelin oligodendrocyte glycoprotein in rats mimics the spectrum of multiple sclerosis pathology. *Brain Pathol*, **8**, 681-694.

Sun, D., Whitaker, J.N., Huang, Z., Liu, D., Coleclough, C., Wekerle, H. and Raine, C.S. (2001) Myelin antigen-specific CD8+ T cells are encephalitogenic and produce severe disease in C57BL/6 mice. *J Immunol*, **166**, 7579-7587.

Swanborg, R.H. (1995) Experimental autoimmune encephalomyelitis in rodents as a model for human demyelinating disease. *Clin Immunol Immunopathol*, **77**, 4-13.

t Hart, B.A., Amor, S. and Jonker, M. (2004) Evaluating the validity of animal models for research into therapies for immune-based disorders. *Drug Discov Today*, **9**, 517-524.

Traugott, U., Reinherz, E.L. and Raine, C.S. (1983) Multiple sclerosis: distribution of T cell subsets within active chronic lesions. *Science*, **219**, 308-310.

Tsuchida, T., Parker, K.C., Turner, R.V., McFarland, H.F., Coligan, J.E. and Biddison, W.E. (1994) Autoreactive CD8+ T-cell responses to human myelin protein-derived peptides. *Proc Natl Acad Sci U S A*, **91**, 10859-10863.

Vajda, Z., Pedersen, M., Fuchtbauer, E.M., Wertz, K., Stodkilde-Jorgensen, H., Sulyok, E., Doczi, T., Neely, J.D., Agre, P., Frokiaer, J. and Nielsen, S. (2002) Delayed onset of brain edema and mislocalization of aquaporin-4 in dystrophin-null transgenic mice. *Proc Natl Acad Sci U S A*, **99**, 13131-13136.

von Budingen, H.C., Tanuma, N., Villoslada, P., Ouallet, J.C., Hauser, S.L. and Genain, C.P. (2001) Immune responses against the myelin/oligodendrocyte glycoprotein in experimental autoimmune demyelination. *J Clin Immunol*, **21**, 155-170.

Waldner, H., Collins, M. and Kuchroo, V.K. (2004) Activation of antigen-presenting cells by microbial products breaks self tolerance and induces autoimmune disease. *J Clin Invest*, **113**, 990-997.

Waldner, H., Whitters, M.J., Sobel, R.A., Collins, M. and Kuchroo, V.K. (2000) Fulminant spontaneous autoimmunity of the central nervous system in mice transgenic for the myelin proteolipid protein-specific T cell receptor. *Proc Natl Acad Sci U S A*, **97**, 3412-3417.

Walsh, M.J. and Tourtellotte, W.W. (1986) Temporal invariance and clonal uniformity of brain and cerebrospinal IgG, IgA, and IgM in multiple sclerosis. *J Exp Med*, **163**, 41-53.

Walsh, M.J., Tourtellotte, W.W., Roman, J. and Dreyer, W. (1985) Immunoglobulin G, A, and M--clonal restriction in multiple sclerosis cerebrospinal fluid and serum--analysis by two-dimensional electrophoresis. *Clin Immunol Immunopathol*, **35**, 313-327.

Wandinger, K., Jabs, W., Siekhaus, A., Bubel, S., Trillenberg, P., Wagner, H., Wessel, K., Kirchner, H. and Hennig, H. (2000) Association between clinical disease activity and Epstein-Barr virus reactivation in MS. *Neurology*, **55**, 178-184.

Wekerle, H., Kojima, K., Lannes-Vieira, J., Lassmann, H. and Linington, C. (1994) Animal models. *Ann Neurol*, **36 Suppl**, S47-53.

Whitacre, C.C., Reingold, S.C. and O'Looney, P.A. (1999) A gender gap in autoimmunity. *Science*, **283**, 1277-1278.

Wingerchuk, D.M., Hogancamp, W.F., O'Brien, P.C. and Weinshenker, B.G. (1999) The clinical course of neuromyelitis optica (Devic's syndrome). *Neurology*, **53**, 1107-1114.

Wolf, S.D., Dittel, B.N., Hardardottir, F. and Janeway, C.A., Jr. (1996) Experimental autoimmune encephalomyelitis induction in genetically B cell-deficient mice. *J Exp Med*, **184**, 2271-2278.

Wucherpfennig, K.W. and Strominger, J.L. (1995) Molecular mimicry in T cell-mediated autoimmunity: viral peptides activate human T cell clones specific for myelin basic protein. *Cell*, **80**, 695-705.

Xiao, B.G., Linington, C. and Link, H. (1991) Antibodies to myelin-oligodendrocyte glycoprotein in cerebrospinal fluid from patients with multiple sclerosis and controls. *J Neuroimmunol*, **31**, 91-96.

Zang, Y.C., Li, S., Rivera, V.M., Hong, J., Robinson, R.R., Breitbach, W.T., Killian, J. and Zhang, J.Z. (2004) Increased CD8+ cytotoxic T cell responses to myelin basic protein in multiple sclerosis. *J Immunol*, **172**, 5120-5127.

Zimecki, M., Kapp, J.A. and Pierce, C.W. (1988) Establishment of antigen-specific and MHC-restricted B cell hybridoma clones: a model for studying antigen presentation to T cell lines and clones. *Arch Immunol Ther Exp (Warsz)*, **36**, 395-408.

8. Appendices

8.1 Abbreviations

aa	Amino acid
ABTS	2, 2'-Azino-bis (3-ethyl-benzthiazoline-6-sulphonic acid)
APC	Antigen presenting cell
ASCs	Antibody secreting cells
BBB	Blood brain barrier
BCR	B cell receptor
BM	Bone marrow
CD	Cluster of differentiation
CFA	Complete Freund's adjuvant
CFSE	Carboxy-fluorescein diacetate succinimidyl ester
CNS	Central nervous system
cpm	Counts per minute
CSF	Cerebrospinal fluid
CTLA-4	Cytotoxic T-lymphocyte-associated protein 4
EAE	Experimental autoimmune encephalomyelitis
EBV	Epstein-Barr virus
ELISPOT	Enzyme-linked immunospot
FACS	Fluorescence activated cell sorting
FCS	Fetal calf serum
GITR	Glucocorticoid-induced tumor necrosis factor receptor family-related gene
H & E	Hematoxylin and eosin
h	Hour
HBV-P	Hepatitis B virus polymerase
HHV	Human herpes virus
HLA	Human leukocyte antigen
HSV	Hepes simplex virus
i.p	Intraperitoneal
i.v	Intravenous
ICOS	Inducible co-stimulator
ICOSL	Inducible co-stimulator ligand
Ig	Immunoglobulin
IgH^{MOG}	MOG-specific Ig heavy chain knock-in mice on C57BL/6 background
IPTG	Isopropyl thiogalactoside
KO	Knockout
LDAO	N, N-dimethyldodecylamine-N-oxide
LFB	Luxol fast blue
LPS	Lipopolysaccharide
MAG	Myelin-associated glycoprotein
MBP	Myelin basic protein
MHC	Major histocompatibility complex
Min	Minutes

MOBP	Myelin associated oligodendrocytic basic protein
MOG	Myelin oligodendrocyte glycoprotein
MS	Multiple sclerosis
NMO	Neuromyelitis optica
NOD	Non-obese diabetic
OSP	Oligodendrocyte specific protein
OT-II	Ovalbumin specific TCR transgenic mice on C57BL/6 background
PBMCs	Peripheral blood mononuclear cells
PBS	Phosphate buffered saline
PCR	Polymerase chain reaction
PD-1	Programmed death-1
PD-L	Programmed death-1 ligand
PLP	Proteolipid protein
PP-MS	Primary progressive MS
PR-MS	Progressive-relapsing MS
RAG	Recombinase activating gene
RBCs	Red blood cells
rMOG	Recombinant MOG
RR-MS	Relapsing-remitting MS
s.c	Subcutaneous
SD	Standard deviation
SEM	Standard error of the mean
SPF	Specific pathogen free
SP-MS	Secondary progressive MS
TCR	T cell receptor
TCR^{MOG}	MOG-specific TCR transgenic mice on C57BL/6 background
TLR	Toll-like receptor
WT	Wild-type

8.2 Curriculum vitae

Name: Gurumoorthy Krishnamoorthy

Date of birth: 05.06.1978

Place of birth: Pudupalayam

State: Tamilnadu

Nationality: Indian

Education:

Since September 2002	PhD student (Biology Faculty – LMU, Munich)
	Department of Neuroimmunology,
	Max-Planck Institute of Neurobiology, Martinsried,
	Germany.
	Supervisor: Dr. Andreas Holz
1999 - 2000	M.S (Pharm.)
	National Institute of Pharmaceutical Education and
	Research, Punjab, India.
1995 - 1999	B. Pharm
	Adhiparasakthi College of Pharmacy,
	Tamilnadu, India.

Publications:

1. Krishnamoorthy, G., Lassmann, H., Wekerle, H., and Holz, A. **(2006)** Spontaneous opticospinal encephalomyelitis in a double-transgenic mouse model of autoimmune T cell/B cell cooperation. *J. Clin. Invest.* **116**: 2385-2392.

2. Gullapalli, S., Gurumoorthy, K., Kaul, C.L. and Ramarao, P. **(2002)** Role of L-type Ca^{2+} channels in attenuated morphine antinociception in streptozotocin-diabetic rats. *Eur J Pharmacol.* **435**: 187-194.